Morphology of the Neurocentral Junction during Postnatal Growth of *Alligator* (Reptilia, Crocodylia)

by

Takehito Ikejiri

A dissertation submitted in partial fulfillment
of the requirements for the degree of
Doctor of Philosophy
(Geology)
in The University of Michigan
2010

Doctoral Committee:

Professor Jeffrey A. Wilson, Chair
Professor Tomasz K. Baumiller
Professor Ronald A. Nussbaum
Research Scientist Janice L. Pappas
Research Scientist William J. Sanders

ACKNOWLEDGMENTS

I owe a lot to my dissertation committee, especially, for their technical guidance and encouragement, without which I could not have completed this dissertation. My “muchas gracias” first goes to my adviser, Jeff Wilson, who invited me to his lab for a PhD and trained me well to carry on those projects. His love of natural sound (i.e., jazz) has been transmitted to me well, which really helped me to stay at my office for extra hours (of work, of course!). Tom Baumiller opened my eyes to look into various aspects of the biomechanics of vertebrae, axial skeleton, and Tae Kwon Do techniques. I had great advantages from endless discussions of vertebral morphology, evolution of axial locomotion, and the two rival baseball teams in NY (even we have ‘serious disagreement’) with Bill Sanders. My math master, Janice Pappas, generously guided me to deal with some questions in a new insight. Ron Nussbaum allowed me to stay with thousands of ‘dead’ reptiles and amphibians in the herpetology lab, which gave me truly amazing and important experiences for this work.

I was lucky to share an office space with John Whitlock and Mike D’Emic for four years of my PhD. They have intellectually influenced me a lot (although their musical tastes may not have been too impressive). I wish the best of luck to them. Two new officemates/lab-mates, Emile Moacdieh and Mike Cherney, made my life in the office more exciting (yes indeed, a bunch of ‘Sapporo’ to them!). Special thanks go to Greg Schneider (UM Museum of Zoology) for his encouragement and friendship. My work greatly benefited from his broad knowledge in herpetology and his ‘love’ of the herpetology collections.

Some specific individuals must be acknowledged for each project. For the histology project (Chapter 2), I got generous donations of fresh alligator specimens from Ruth Elsey (Louisiana Department of Wildlife and Fisheries, Rockefeller Wildlife Refuge, Grand Chenier) and Allan “Woody” Woodward (Fish and Wildlife Research laboratory in Gainesville, Florida). Kenny Krysko (Florida Museum of Natural History, Herpetology) let me sample very large specimens for this project, and he even caught the alligators and physically sectioned vertebrae for me. Chris Strayhorn (UM Dentistry School) kindly offered me his help for histological preparations; without his help, this project could not be done. The idea of using histology was originally from Greg Schneider (UMMZ) in the beginning of this project, who also allowed me to use a lab space for preparations. Moises Kaplan (UMMZ) also gave me some technical comments. I also thank endless encouragement for years from Greg Farley, Jack McIntosh, and Richard Zakrzewski.

I have debated some contents of Chapters 3 (suture complexity) in the earlier stage of this project. I thank the UM Museum of Paleontology Evo-Devo seminar, especially Miriam Zelditch and Aaron Wood. Adam Rountrey and Alex Janevski also gave me some comments, about the method and the basic concept of suture complexity. Furthermore, I have learned a lot — directly and indirectly — from people in UMMP, notably Catherine Badgley, Ryan Bebej, Devapriya Chattopadhyay, Thomas Eiting, Brady Foreman, Julia Fahlke, John Finarelli, Dan Fisher, Phil

Gingerich, Gregg Gunnell, Dan Miller, Ross Secord, Pieter Missiaen, Shanan Peters, Gerry Smith, Katy Smith, Valerie Syverson, Megan Tuura, and Iyad Zalmout ("shukran"!).

Data used in this work are largely based on museum research and I thank for hospitality of the following people during my visit to those areas: Gabe Bever and Amy Balanoff in NY, Paul Sereno and Gabrielle Lyon in Chicago, and Alex Hastings in Gainesville. Loans of specimens were made by Alan Reseter (Field Museum of Natural History, Amphibians and Reptiles), Kenny Krysko and Max Nickerson (Florida Museum of Natural History), Kevin de Queiroz, Jeremy Jacobs, Rob Wilson (Unite State National Museum), and University of Michigan Museum of Paleontology and Zoology. For access to collections, I also thank to staff at the following institutions: especially, in the States, Carl Mehling, Mike Norell (American Museum of Natural History, Vertebrate Paleontology), David Kizirian, (AMNH, Herpetology), Amy Henrici, Matt Lamanna, Allen Shaw (Carnegie Museum of Natural History in Pittsburg), Bill Sampson (Field Museum of Natural History, Vertebrate Paleontology), Yohannes Haile-Selassie, Lyman Jellema (Cleveland Museum of Natural History, Physical Anthropology), Wann Langston (Texas Memorial Museum in Austin), Dan Brinkman (Yale Peabody Museum, Vertebrate Paleontology, in New Haven), Ray Wilhite (Louisiana State University, Veterinary Medicine, in Baton Rouge); in overseas, Fernando Abdala, Bruce Rubidge, Adam Yates, Bernhard Zipfel (Bernard Palaeontological Institute in Johannesburg), Nicole Klein and Kristin Remes (Museum fűr Naturkunde Berlin), Nils Knőtschke (Freilichtmuseum Munchehagen, in Rehburg-Loccum, Germany), Sheena Kaal (Iziko Museums of Cape Town), Elize Butler (National Museum in Bloemfontein), and Kirby Siber (Sauriermuseum Aatahl, in Switzerland).

Aid from the Department of Geological Sciences and the Museum of Paleontology must be addressed. Becky Lange's help is certainly needed to finish a PhD. Anne Hudon's endless support made everything go easily. Also, technical help are from Cindy Stauch, Vlad Miskevich, Charlene Stachnik, and Chrissy Minor. Through my GSI jobs and others, I had great opportunities to work with some faculty members, who helped in perusing those projects, including Michela Arnaboldi, Eric Essene, Rod Ewing, Ingrid Hendy, Stephen Kesler, David Lund, Jeroen Ritsema, Larry Ruff, Peter van Keken, and Yoxue Zhang. "Domo arigato" also goes to my fellow students and other 'descendants' in- and off-campus, who made my grad school life smoothly, especially: Boris Avdeev, Pamela Bogart, Chris Dettore, Yuko Frazier, Dave and Kity Gray, Karen Gutierrez, Jinny Han, John Hawley, Dan Horton, Thaís Hyppolito, Yong Keun Hwang, Minako Kimura Edger, Yuehan Lu, John Naliboff, Chris and Cara Stefano, Meghan Wagner, Monica and Benicio Wilson, Wendy Whitlock, Ryo Yakushiji, Yang Zhang, Michal Zdziarski, and Jing Zhou.

Last but not least, many "thanks" go to endless support from the Ikejiri family in Japan: Takako Ikejiri (mother), Kotaro Ikejiri (brother), Michika Ikejiri (sister-in-law), Kaede Ikejiri (niece), and BuBu (Japanese saying: "Use even a cat's help when you are very busy"). This work was financially supported by the Turner Awards of the University of Michigan in 2007, 2008, and 2009.

TABLE OF CONTENTS

LIST OF FIGURES

LIST OF TABLES

LIST OF APPENDICES

ABSTRACT

The two main parts of a vertebra, the centrum and neural arch, form independently during early developmental stages in nearly all vertebrates, and they typically fuse together in later growth stages. Fusion between centrum and neural arch is the result of ossification of a thin cartilage layer (neurocentral synchondrosis) between them. The timing of neurocentral fusion varies considerably within the vertebral column and among species, especially in archosaurian reptiles, and may be related to changes in body size and/or locomotion. Despite the importance of neurocentral fusion to our understanding of archosaur evolution, basic information about this process and how it changed through time remains poorly understood.

In this dissertation, morphology of neurocentral sutures and vertebrae in crocodilians (Reptilia, Archosauria) is explored. In Chapter 2, the detailed cell- and tissue-level morphology of neurocentral sutures in the vertebrae of *Alligator mississippiensis* is documented. In chapter 3, complexity of neurocentral sutures are quantified, and changes related to differences in vertebral position, ontogenetic age, and phylogeny are examined. In Chapter 4, allometric changes in vertebrae of *Alligator* are quantified and investigated in relation to key ontogenetic events. As seen in some craniofacial bones in various vertebrates, neurocentral fusion may affect changes in relative size and shape of certain vertebral structures (e.g., centrum, neural spine, transverse processes, neural canal) during growth. In chapter 5, data examined in crocodilians (chapters 2–4) are applied to various fossil archosaurs from the Early Mesozoic to investigate the origin and evolutionary significance of two unique features of neurocentral sutures, delayed neurocentral fusion and complex neurocentral sutures.

Chapter 1

Introduction

This (morphology) is one of the most interesting departments of natural history, and may almost be said to be its very soul. (Charles Darwin, 1872: "The Origin of Species (6th edition)" in Ch 14)

Sutural growth may differ in rate, duration and with time. Sutures are not merely reactive and certainly not mere spandrels. (Brian Hall, 2005; "Bones and Cartilage")

I was moving toward what the critics later would call "fusion". I was just about trying a fresh, new approach. (Miles Davis and Quincy Troupe (1999): "Miles: The Autobiography")

In the summer of 1999, I was examining a number of skeletons of the Jurassic sauropod dinosaur, *Camarasaurus*, housed in a large dark fossil collection room (the "Big Bone Room") in the basement of the Yale Peabody Museum. I was particularly interested in some cervical and dorsal vertebrae of a few paratypes of *Camarasaurus grandis*, which were originally studied by Professor Othniel C. Marsh back in the late 19th century. I was gazing at those large centra (lower vertebral parts) of dorsal vertebrae. Those bones are much larger than my head and I needed both hands just to move them for photography and measurements. Some centra were missing their upper parts (neural arches). In fact, the neural arches were physically separated from the centra. Natural articular surfaces between two main vertebral parts were exposed, exhibiting well-ridged texture like an unworn mammoth tooth. In other vertebrates, we do not usually see this morphological feature.

In the museum, I was discussing this phenomenon with another visiting sauropod researcher. I asked, "Why aren't they fused together?" My colleague

said, “Perhaps, this dinosaur was not fully grown” (even though those vertebrae were so big!). The idea that unfused neural arches and centra (or visible neurocentral suture) could be used as indicators as relatively immature individuals of archosaurs came from the article of C. A. Brochu (1996): “Closure of neurocentral sutures during crocodilian ontogeny: implications for maturity assessment in fossil archosaurs”. In three extant crocodilians, he discovered that they typically have the back-to-front sequence of neurocentral fusion in the vertebral column and the cervical vertebrae often retain open sutures throughout postnatal ontogeny. Notably, Brochu suggested that the status of neurocentral fusion could be “a size-independent criterion for diagnosing its relative maturity”, but he was not certain if it is a reliable indicator of relative maturity in skeletal age (e.g., open suture = immature individual) (p. 56). He also posed two fundamental questions about the nature of neurocentral fusion: (1) what is the relationship between suture closure and suture fusion and (2) what interspecific variation exists in patterns of neurocentral fusion?

Although Brochu (1996) clearly stated some uncertainty and left open questions in the nature of neurocentral fusion, his findings and ideas seem to have been misused by some fossil archosaur researchers. A rule of thumb seemed to have emerged: open neurocentral sutures or unfused vertebral elements are indicative of juvenile or subadult status in non-avian dinosaurs and other fossil archosaurs (citations elsewhere). However, I suggest without understanding how much intra- and interspecific variations in timing of neurocentral fusion exists in those archosaurs, the status of vertebral sutures

may be questionable for estimating relative skeletal age.There is not much information about timing of neurocentral fusion in the vertebrate literature. One study in humans (Rajwani et al., 2002) reported that complete neurocentral fusion occurs at about age 14 (based on MRI data from males and females), but my data from dry skeletons show that at least 20% of 22 years old males still exhibit open sutures (pers. obs.). Based on quantitative comparisons with various extant and fossil reptiles, as well as amphibians, mammals and birds, I noticed that crocodilians and their close relatives, Mesozoic non-avian archosaurs, have late neurocentral fusion, relative to body size (Ikejiri, 2003; Ikejiri et al., 2005; Schwarz et al. 2007). In contrast, among non- archosaur terrestrial tetrapods, completely fused neurocentral arches and centra are very common. Unfused vertebral elements in mature and/or large individuals (relative to maximum or largest known individuals in taxon) are found in some aquatic animals, such as cetaceans and extinct aquatic reptiles, including basal choristoderan diapsids (e.g., *Champsosaurus*), sauropterygian ichthyosaurs and plesiosaurs (personal observations). Open neurocentral sutures in crocodilians and many non-avian Mesozoic archosaurs, which exhibit semi-aquatic to fully terrestrial life, are unique. Besides relatively late timing of neurocentral fusion, I also noticed that crocodilians and many non-avian dinosaurs, especially large species, exhibit wedged articular surfaces between centra and neural arches, characterized by finely ridged and pored texture. This feature is also unique in archosaurs. The primary question, which I have been investigating, is how have archosaurs gained delayed neurocentral fusion and wedged articulation between vertebral

parts during evolution? This also leads to an additional question: what other morphological changes in vertebrae and axial skeletons are involved in supporting the entire vertebral structures with unfused cartilaginous joints?

Another important question is how does neurocentral fusion exactly occurs? Humans are the best-studied taxon for gathering general anatomical information. Surprisingly, however, even in the medical literature, very little information is available about general morphology of the neurocentral sutures. The cartilaginous tissue that fills the space between centra and neural arches has been termed the “neurocentral synchondrosis” by Schmorl and Junghanns (1932). Morphologically similar synchondroid cartilage is also present in the cranial sutures of various vertebrates and the epiphyseal sutures of mammalian limb bones (e.g., Bick and Copel, 1950; Fawcett, 1994). Rajwani et al. (2005) stated that the neurocentral synchondrosis in human vertebrae is “secondary cartilage”, which has been known only in mammals, birds, and one species of bony fish (Benjamin 1989; Hall, 2005). So, what kind of cartilage is found in the neurocentral junctions of other vertebrates like non-avian archosaurs?

This dissertation is mainly based on data from vertebrae of the extant crocodilian, *Alligator mississippiensis* (Archosauria, Crocodylia). North American alligators are very abundant today, and a relatively large number of fresh and skeletal specimens are accessible for studies of morphological variation. Taxonomically, the species is also interesting for three primary reasons: (1) the presence of relatively late neurocentral fusion; (2) large body size among crocodilians; and (3) the existence of several extinct and extant species in the

genus, including dwarfs. Various fossil archosaurs, especially, basal forms from the Triassic period were also examined for comparisons of morphologies in vertebrae. Based on those extant and extinct archosaurs, I hypothesize that if patency of neurocentral fusion is linked to wedged neurocentral articular surfaces in archosaurs, suture complexity must keep increasing throughout postnatal ontogeny of *Alligator* and, possibly, during the archosaur evolution. Furthermore, fusion usually influences changes in size and shape of suturally connected bones, as seen in many craniofacial bones of various vertebrates, during ontogeny. Thus, if neurocentral fusion triggers changes in size and shape of some vertebral parts (e.g., stoppage of growth), shifting the timing of fusion relatively early and late must be reflected in allometric growth of overall vertebral proportions and size and, possibly, further linked phylogenetically to newly designed vertebral forms and structures during archosaur evolution.

Here I investigate morphologies of the neurocentral junctions in extant and extinct archosaurs, based on examples observed in various crocodilians. Chapter 2 shows, using histology, how neurocentral fusion occurs in cell- and tissue-level during ontogeny of *Alligator mississippiensis*. In Chapter 3, degrees of zigzagged neurocentral suture lines — suture complexity — are quantified and compared intracolumnally, ontogenetically, and interspecifically. Chapter 4 presents how timing of neurocentral fusion affects allometric growth of vertebrae in *A. mississippiensis*. In Chapter 5, the origin of delaying neurocentral fusion is explored, which further allows investigating its evolutionary significance of vertebral and axial skeletal modifications in the basal archosaurs. Hopefully, the

information and investigations presented here will provide some new insights for studies of neurocentral junctions and vertebrae across various extant and extinct vertebrates.

Chapter 2

Histology-based Morphology of the Neurocentral Synchondrosis in *Alligator mississippiensis* (Archosauria, Crocodylia)

ABSTRACT

Morphology and histology of the neurocentral synchondroses – thin cartilaginous layers between centra and neural arches – are documented in the extant crocodilian, *Alligator mississippiensis* (Archosauria, Crocodylia). Examination of dry skeletons demonstrates that neurocentral suture closure occurs in very late postnatal ontogeny. Before sexual maturity (body length $\geq$ ca. 1.80 m), completely fused centra and neural arches are restricted to the caudal vertebral series. In contrast, the presacral vertebrae often remain unfused throughout postnatal ontogeny, retaining open sutures in very mature individuals (body length $\geq$ 2.80 m). These unfused centra and neural arches are structurally supported by the relatively large surface area of the neurocentral junctions, which results from horizontal and vertical increases with strong positive allometry. Cleared and stained specimens show that the cartilaginous neurocentral synchondrosis starts to form after approximately 40 embryonic days. Histological examination of the neurocentral junction in dorsal and anterior caudal vertebrae of six individuals (body length = 0.28–3.12 m) shows that: (1) neurocentral fusion is the result of endochondral ossification of the neurocentral synchondrosis, (2) the neurocentral synchondrosis exhibits bipolar organization of three types of

cartilaginous cells, and (3) zigzagged neurocentral sutures come from clumping of bone cells of the neural arches and centra into the neurocentral synchondrosis. The last two morphological features can be advantageous for delaying neurocentral fusion, which seems to be unique in crocodilians and possibly their close relatives, including non-avian dinosaurs and other Mesozoic archosaurs.

INTRODUCTION

Vertebrae develop from multiple isolated regions of sclerotome cells (Christ et al., 2000) that eventually unite to form a single structural unit after the regions calcify and ossify (Williams, 1959). During this process, the two main vertebral components, the centrum and neural arch, fuse last. Up until their physical contact, the centrum and the neural arch can grow separately, due to different timings of chondrification and ossification (e.g., Christ et al., 2007). The immobile joint between centrum and neural arch is filled by a thin cartilaginous layer, the neurocentral synchondrosis. Despite its role of vertebral growth, cell-level growth of the neurocentral synchondrosis has not been understood well in vertebrates.

Fusion between centra and neural arches must occur after the result of ossification of the cartilaginous neurocentral synchondrosis. This ontogenetic event tends to appear at a specific ontogenetic stage in each vertebrate species (e.g., 16–20 years in humans; Rajwani et al., 2002). Correct timing of neurocentral fusion is important for vertebral growth. In fact, abnormal timing of

neurocentral fusion can produce vertebral malformations, such as asymmetrically sized left and right neural pedicles (Vital et al., 1989), which can contribute to severe axial growth disorders (e.g., scoliosis; Yamazaki et al., 1998).

Among vertebrates, timing of neurocentral fusion varies from the embryonic to the very late postnatal ontogenetic periods or even persists throughout life (= patency). Since Brochu (1996) pointed out relatively late timing of neurocentral fusion in fossil and extant crocodilians, the presence of unfused vertebral elements and/or open neurocentral sutures on the external vertebral surfaces has been routinely used to identify relatively immature individuals for various extinct archosaurs, especially dinosaurs (Fig. 2-1); e.g., sauropods (Ikejiri et al., 2005; Schwarz et al., 2007), non-avian theropods (Carpenter, 1997; Carrano et al., 2002), ornithischians (Horner and Currie, 1990). However, until intra- and inter-specific variation in timing of neurocentral fusion is understood, the nature of the neurocentral sutures as an indicator of relative skeletal maturity remains questionable.

Histology is a powerful way to observe cell- and tissue-level morphology in vertebrate skeletons, but it has been used only infrequently to examine neurocentral synchondroses in vertebrates. The main purpose of this study is to use histology to document cell-level morphology of the neurocentral synchondroses in vertebrae of *Alligator mississippiensis* (Archosauria, Crocodylia). Hatchling (body length = 0.28 m) to fully-grown individuals (= 3.12 m) show different patterns of postnatal ontogeny in the presacral and caudal vertebrae. Besides the neurocentral synchondroses, the surrounding

environments, the centra and neural arches along the sutural boundaries, are also examined. In addition, dry skeletons and cleared and stained specimens are studied to investigate general patterns of neurocentral fusion in the vertebral column.

Although various authors pointed out that crocodilians have late neurocentral fusion (e.g., Hoffstetter and Gasc, 1969; Brochu, 1996), timing of neurocentral fusion tends to be variable in the vertebral column. In fully-grown crocodilians, the neurocentral junctions are often closed in the caudal and the sacral vertebrae, but the sutures are still visible in the presacral vertebrae (Ikejiri, 2007). Therefore, data from histology of alligator vertebrae allow discussing key morphologies for fusion vs. patency in the neurocentral junctions, which may give some clues for further investigations of the evolutionary significance for delaying timing of neurocentral fusion in archosaurs.

MATERIALS AND METHODS

Dry Skeletons

Seventy-five dry skeletons of *Alligator mississippiensis*, including those from captive and wild populations, were examined (Table 2-1). Sutures are often visible on the external surface of vertebrae in dry skeletons, providing information about the pattern of neurocentral fusion and how it varies intracolumnarly and ontogenetically. Because dry skeletons of *A. mississippiensis* are readily available, data can be collected from a large number of specimens.

Two states of fusion, completely fused and partially fused neurocentral junction, were recorded for each vertebra in 75 skeletons. Completely fused external neurocentral sutures refer to no identical, open space along a line; partially fused neurocentral junctions have a combination of a visible suture lines and bony connections in any parts of sutures. In addition to fusion state, body length, femoral length, and sex were recorded for each specimen (Table 2-1).

Cleared and Stained Specimens

Neurocentral junctions were also examined in cleared and stained specimens of *Alligator* (Table 2-2). Twelve skeletons were prepared at the University of Michigan Museum of Zoology (UMMZ), including 20 embryonic days to hatchling (ca. 48 days after egg-laying) specimens. They were first cleared with enzyme and then stained by the solutions of alizarin red for bone tissues and alcian blue for cartilage tissues (Dingerku and Uhlers, 1977). Because the specimens are intact, the vertebral column is only visible in lateral view.

Histological Samples

Traditionally, three methods have been used in the medical sciences for examinations of the neurocentral junctions: Magnetic Resonance Imaging (MRI; Yamazaki et al., 1998; Rajwani et al., 2002, 2005); radiography (Matt et al., 1996); and Computed Tomography (CT; Vital et al., 1989).These methods are generally limited to identification of the presence or the absence of cartilaginous tissues in the neurocentral junctions, but they do not directly show the types of

cells and tissues present in the neurocentral synchondroses. Histology has been used occasionally only in humans and a few lab mammals (e.g., Rajwani et al., 2005), but this method is powerful for examining cell-level morphology of cartilage and bones in general.

Six individuals of the extant crocodilian *Alligator mississippiensis* were selected for this histological sectioning (vouchers catalogued at UMMZ). The six individuals are determined to include hatchling to fully-grown individuals based on the total body length (0.28–3.12 m; Table 2-3; Fig. 2-2). Body length was directly measured in the three smaller specimens, and the other three were estimated using the greatest length of the femur (Farlow et al., 2005). Chronological age was estimated based on growth increments in the transverse cross-section of the femora for the three large specimens. Histological preparations are also catalogued at the UMMZ. Sex determination, where known, is listed in Table 2-3.

Whole skeletons of the three smaller specimens were collected for this study from the Rockefeller Wildlife Refuge near Grand Chenier, Louisiana. The three larger specimens were captured near Gainesville, Florida (skulls, femora, and several vertebrae only). All six specimens were received freshly frozen, and only fresh vertebrae were used for the histological sampling. Vertebrae prepared by dermestid beetles provide information to identify cartilage and bone cells, but data from those dry skeletons, which can give inconsistent results (personal observation), are not shown in this study. Skeletons cleaned by bleaching and boiling may severely damage cartilage cells and were not histologically sampled.

A 10% EDTA solution was used to decalcify the vertebrae enough for slicing and thin-sectioning. Whole vertebrae of the three small individuals were soaked in the solution, but for the three large individuals, vertebrae were coronally sliced along the mid-points crossing the base of the transverse processes and the neural spine prior to decalcification (Fig. 2-3). A band saw was used to slice each section to about 2–3 mm. These slices were decalcified, and then the site of the neurocentral junction was cut to fit on standard microscopic slide (7.5 X 2.0 mm). All pieces of the vertebrae were further sliced by microtome to about 5–8 μm in thickness for staining. After mounting on a slide, hematoxylin and eosin (H&E) stain was used to dye bone and cartilaginous tissues. Histological samples were examined using light microscopy (Nikon E800). Magnifications of 2x–40x were used for digital photography. Images were saved as TIF files at 600 dpi resolution.

Measurements of Neurocentral Junctions

Transverse width and dorsoventral thickness of the neurocentral junctions were measured in the digital images using ImageJ Version 1.32 (Rasband, 2003; Abramoff et al., 2004). The transverse width is the straight distance between the lateral and medial margin of the cartilaginous synchondrosis. The thickness was measured at the thickest (maximum) and thinnest (minimum) spots, and then, the mean was calculated. All measurements were log-transformed. Growth rates were calculated using the log-log plots (total body length on the X-axis and the vertebral dimensions on the Y-axis). The slopes allow identifying either isometric

(i.e., the slope between 0.951 and 1.049) or allometric growth (slope outside of the above values).

RESULTS

Patterns of Neurocentral Fusion in Dry Skeletons

Seventy-five dry skeletons of *Alligator mississippiensis* across a postnatal ontogenetic range (Table 2-1) were examined to construct a sequence for closure of the external neurocentral sutures during postnatal ontogeny (Fig. 2-4). Among the 75 post-hatchling individuals, caudal 10 is the anterior-most vertebrae with open neurocentral sutures. At least in the ten anterior-most caudal vertebrae, neurocentral fusion progresses in a unidirectional posterior-to-anterior sequence, as observed by Brochu (1996). Neurocentral fusion is completed in the anterior-most caudal vertebrae after sexual maturity (body length = ca. 1.8 m; Fig. 2-2). The sutures disappear completely in the two sacral vertebrae by the time alligators reach 2.50 m total body length, which is nearly maximum size for females and ca. 70% maximum size for males. In contrast to the caudal vertebrae, neurocentral fusion tends to occur in the anterior-to-posterior sequence in the sacral region, where the anterior sacral vertebra exhibits slightly earlier fusion than the posterior sacral vertebra (Fig. 2-4).

In most individuals of *Alligator*, completely fused centra and neural arches are rarely found in presacral vertebrae. In the 75 specimens examined, only very large individuals (body length over 2.50 m) exhibited completely fused

neurocentral sutures in any presacral vertebrae. In three of these, only the posteriormost dorsal vertebra is fused. Four of these have partially fused neurocentral junctions in the mid- and anterior dorsal vertebrae. These patterns indicate that neurocentral suture closure in dorsal vertebrae occurs in a relatively short time among the fully-grown individuals. It is difficult to determine a "typical sequence" of fusion in the presacral vertebrae, as Brochu (1996) observed in the combination of *Alligator mississippiensis*, *Alligator sinensis*, *Crocodylus actus*, and *Osteolaemus tetraspis*. Even in the largest individual (body length = 4.2 m; ca. 40 years old), the sutures are fully open in all cervical vertebra (Figs. 2-2, 2-4).

Embryonic Vertebrae from Cleared and Stained Specimens

Cleared and stained specimens allow direct identification of bone and cartilage tissues in vertebrae, as used in embryonic to hatchling alligators (Rieppel, 1993). In specimens of 20 day-old embryos of *Alligator mississippiensis* (UMMZ 181276, 181277), all centra are largely cartilaginous, but the neural arches are not fully chondrified. No evidence of cartilaginous neurocentral junctions is found.

Cartilaginous neurocentral joints are visible in 40 day-old embryos (Fig. 2-5), which are about eight days from hatching (Ferguson, 1985). Cartilaginous layers, stained in blue, are identifiable in lateral view of the presacral to mid-caudal vertebrae. While ossified regions (stained in red) appear in the centra of all vertebrae, the neural arches are still largely cartilaginous. A gap in timing of chondrification and ossification exists between centra and neural arches.

Ossification has already started in the large portion of the centra and some portions of the neural arches.

The 40 day-old embryo (UMMZ 18192) shows a more advanced feature of the neurocentral junctions in the vertebral column. In the mid-dorsal vertebrae, a thick, cartilaginous neurocentral synchondrosis (0.248 mm; centrum height 2.31 mm) is present between the centra and the neural arch (Fig. 2-5). Notably, in the cervical and two anterior dorsal vertebrae, there is an open space between centra and neural arches (Fig. 2-5). This feature may indicate the neurocentral synchondrosis is formed as secondary cartilage (i.e., chondrification occurs after ossification of the centrum and neural arch) in *Alligator*, which has not been reported previously in non-avian archosaurs and other reptiles (Hall, 2005).

In posterior caudal vertebrae, the 40 day-old embryos have no cartilaginous boundaries in the neurocentral junctions (Fig. 2-5). The centra and neural arches in at least several posteriormost caudal vertebrae have highly ossified entire vertebral structure. Because these vertebrae lack neural canals, they may simply lack the neurocentral junction, but the entire vertebrae chondrify and ossify from a single piece.

Histology of Centrum and Neural Arch

In coronal cross-section, alligator vertebrae exhibit very similar topology among the centrum, neural arch, neural canal, and neural spine (Fig. 2-3). Although the shape and size of vertebrae vary in the vertebral column (Mook, 1921; Hoffstetter and Gasc, 1969), the neurocentral junction is always placed in

between the centra and the neural arch. In crocodilians, the junction is located near the lower portion of the neural canal, and left and right junctions never contact one another.

Transverse processes form differently in the presacral, sacral, and caudal vertebrae (Higgins, 1923). In the presacral vertebrae, the transverse processes develop as an outgrowth of the neural arch. In contrast, in the sacral and caudal vertebrae, the transverse processes have a separated ossification center. In crocodilians, these 'free caudal ribs' attach to the lateral surface of both centrum and neural arch across the neurocentral junction. An anterior caudal vertebra of the subadult *Alligator mississippiensis* (Fig. 2-3) has thin cartilaginous layers present in the junctions among the neural arch, centrum, and ribs.

Figure 2-6 shows coronal sections of the entire neurocentral junction of dorsal vertebra 14 and caudal vertebra 2 or 3 from five individuals of *Alligator mississippiensis*. In the hatchling (body length = 0.28 m), compact bone is already present in the external walls of the vertebra along the neurocentral junction, but cartilage is still the main component of the entire vertebra. Notably, a sharp gap in timing of endochondral ossification exists in between centra and neural arches: cartilaginous tissues largely occupy within the internal space of the neural arches, but osteoblast cells occur in large proportions of the centra. Moreover, a trabecular structure starts to appear in the entire vertebra of the hatchling. The differences in internal cell and tissue formation between the centrum and neural arch make the neurocentral junction identifiable under 2x–4x magnification.

In the juvenile (body length = 0.92 m), ossification is not yet complete in both centra and neural arches. The centrum exhibits a large cartilaginous space, which occupies about half of the cross-sectional area. However, compact bone structure appears in the external wall of both centrum and neural arch (Fig. 2-6). This dense compact bone occurs in parts of the neural spine, the transverse processes, and the inner wall along the neural canal. Relatively large marrow spaces are found near the bases of the centra and neural arches, forming a trabecular structure along the neurocentral junctions. Many bright red spots, representing osteoblasts and osteoclasts, indicate newly forming bone cells. These cells are dominant along the boundary between neurocentral junction and base of the centrum or neural arch.

The young adult (body length = 2.0 m) shows that further ossification in the dorsal and the caudal vertebrae (Fig. 2-6). The compact woven bone thickens in the external vertebral walls, and the degree of trabecular structure increases in both centra and neural arches. In the two large adults (body length = 2.5 m and 3.1 m), the internal structure of vertebrae is similar to those of the young adult. The external bone walls on lateral surfaces and along the neural canal tend to be thicker through ontogeny in *Alligator*.

Histology of Neurocentral Junction

Overall size and cross-sectional shape. Histology shows that the neurocentral synchondrosis is identical in all but the caudal vertebra of the largest individual (Fig. 2-6). Overall, the neurocentral synchondrosis is

transversely thin and sheet-like in coronal cross-section. The neurocentral synchondroses remain relatively the same dorsoventral thickness throughout the postnatal ontogeny. Maximum dorsoventral thickness ranges from 0.35–0.88 mm in the sutures, which exhibits strong negative allometry from the hatchling to large adult (Table 2-4). In contrast, the transverse width of the neurocentral junction indicates positive allometric change among the six individuals (allometric coefficient = 1.33; Table 2-4).

During postnatal growth, the caudal and the dorsal vertebrae show two main types of morphological changes in the neurocentral junctions, such as remodeling (tissue turnover) and modeling (shaping) of cells. In caudal vertebrae of the very large *Alligator* (body length = 3.12 m; Fig. 2-6), the cartilaginous boundary does not exist and only bony tissues are found spanning the neurocentral junction. This feature indicates a change from the synchondroid cartilage to endochondral bone tissue. Notably, a clear cartilaginous synchondroid layer still remains in the posterior dorsal vertebra of the same fully-grown alligator. The same pattern is found in some very large individuals of the dry skeletons (Fig. 2-4; Table 2-1).

The second type of ontogenetic change is observed in the overall cross-sectional shape of the neurocentral junctions. The hatchlings show much fewer numbers of directly connected sites (or smaller direct articular surface relative to the entire neurocentral junctions) between neurocentral synchondrosis and centrum or neural arch than the adults. Furthermore, in the three adult individuals (Fig. 2-6), a relatively straight shape forms in the caudal vertebrae, but vertically

wavy, zigzagged articulations exist in the dorsal vertebrae. Because the young individuals have straight neurocentral junctions, this vertical transformation of the neurocentral boundary is likely due to cell migrations.

Cell types of neurocentral synchondrosis. Detailed cellular morphology of the neurocentral synchondrosis can be observed under 4x–40x magnification. In *Alligator mississippiensis*, the neurocentral synchondrosis consists of three main types of cartilage cells: reserve cartilage (RC), proliferating cartilage (PC) and calcified cartilage (CC) cells (Fig. 2-7). Reserve cartilage cells are relatively small with identical nuclei. In the hatchling (Fig. 2-7, left column), those circular or angular cells are condensed and placed in the mid-zone of the neurocentral synchondrosis. Although the cells are crowded in the zone, no clear orientation of cell formation occurs in the hatchling stage. Proliferating cartilage cells are large and unnucleated. They are usually rounded and found in both upper and lower zones along the mid-zone with reserve cartilage, forming a ‘bipolar’ structure. Calcified cartilage cells, which appear light gray or blue under H&E stain, are formed in the outer-most layers of the neurocentral synchondroses. Structure of individual cells is usually not identical, but some cells still possess nuclei, indicating a relatively rapid rate of growth (calcification). The calcified cartilage tissues have denser structure and finer texture than the two other types of the synchondroid cartilaginous tissues. The calcified cartilage is also found in parts of the centrum and the neural arch along the suture. Cells stained dark red, which indicate osteoblasts, form a large proportion of the centrum and the neural arch,

but are absent in the neurocentral junction. Those newly formed bone cells occur along the calcified cartilage layers of the neurocentral junction.

The subadult alligator (Fig. 2-7, middle column) has the same three cartilaginous zones with bipolar structure in the neurocentral synchondrosis. Notably, reserve and proliferating cartilage cells start to be arranged vertically in long parallel columns, called lacunae. The reserve cartilage cells are still placed horizontally in the mid-level of the neurocentral synchondrosis with a relatively consistent thickness, but showing a weakly curved overall shape. The proliferating cartilage cells lack nuclei and are slightly larger than the reserve cartilage cells. These features indicate that hypertrophy occurs along the vertical axis towards the outer zones. This second outer layer(s) has a greater range of the vertical cell migration in the neurocentral synchondrosis. This inconsistency in vertical thickness forms curvature of the overall synchondroid layer and complex articular surfaces between neural arches and centra. As shown in areas of the calcified cartilage tissues, more extensive calcification occurs along the outer layers of the neurocentral synchondroses. Osteoblast cells continuously form along the calcified cartilage layer in the centrum and especially in the neural arch. Notably, a higher number of direct bony and/or calcified connections between the neurocentral synchondrosis and centra or neural arch are found in this individual than the hatchling. The increase in direct connection provides larger cross-sectional articular surface areas between centra and neural arches during postnatal ontogeny. Newly formed and ongoing-bridges between the

neurocentral synchondrosis and the two main vertebral parts can be also observed in the vertebra (arrows in Fig. 2-7).

The adult alligators have the same bipolar cell structure with some minor modification (Fig. 2-7, right column). The reserve cartilage zone is strongly curved relative to the horizontal axis. Importantly, the cartilage cells are regularly lined up to the vertical axis as shown in the subadult, indicating the shaping of the synchondroid layers does not affect polarity of those cartilaginous cells along the axis. In cross-section, the thickness of the synchondroid cartilage layer is highly variable, especially in adults. Some portions are thinner (and gently pinched) than others in the entire synchondrosis. The cross-sectional area of direct calcified and/or bony connections to centra or neural arches (arrows in Fig. 2-7) increases in this stage. Besides synchondroid cell migration into bone tissues of the centrum and neural arches, bone cells of the centra and neural arches also migrate to the neurocentral synchondroid layer. The combination of cell migration from both neurocentral synchondroses and centra or neural arches produces those highly irregular, zigzagged outlines of the sutural boundary.

Neurocentral suture in the external vertebral wall. The external margin of the neurocentral junction is covered with fibrous sheath (e.g., peristeum, perichondrium) (Fig. 2-8). This particular site is distinguishable from other portions of the vertebral walls, as observed sutures. Unlike the regular vertebral wall, which has homogeneous dense compact bone, the external margin of the neurocentral suture bears small nucleated osteoblast cells and newly formed calcified layers (avascular tissue). Many fine, overlapping layers are present,

indicating a relatively rapid rate of bone formation, as similarly found at sites of bone fracture during a healing period. Notably, the presence of the neurocentral synchondrosis (or any related cartilaginous cells) in the internal structure of vertebrae is directly linked to these unique external features. When the neurocentral synchondrosis is completely ossified, the external margin is no longer distinguishable as seen in the dorsal vertebrae of the fully-grown individual (Fig. 2-4).

DISCUSSION

Among tetrapods, *Alligator* and other crocodilians have drastically delayed neurocentral fusion in the presacral vertebrae (Fig. 2-4) (Brochu, 1996). Histology of vertebrae shows that *Alligator* has bipolar organization of the synchondroid cartilaginous layers and vertical cell migration of neurocentral synchondroses and bone cells of centra and neural arch along the neurocentral sutures. Possibly, the two features are related to each other and provide environments of delaying fusion between centra and neural arches in presacral vertebrae during growth. Relatively late timing of fusion commonly occurs in crocodilians and many non-avian archosaurs (Fig. 2-1), and this possibly synapomorphic character in the phylogenetic frame is also discussed.

Patency of Neurocentral Fusion during Crocodilian Postnatal Ontogeny

Bipolar structure of neurocentral synchondrosis. *Alligator* has bipolar structure of the neurocentral synchondrosis, consisting of the three types of the cartilaginous zones (Fig. 2-7). The cartilage cells grow from the mid-zone towards the dorsal and ventral zones of the neurocentral synchondroses (i.e., towards the neural arch and centrum, respectively). In contrast, newly formed bone cells (osteoblasts) occur along the outermost boundaries of the neurocentral junctions. Around the neurocentral junction, bone cells from the centra and neural arches and cartilage cells from the neurocentral sutures compete to occupy for space (Fig. 2-9).

This bipolar cell structure has not been studied extensively in vertebrae of other vertebrates, but very similar morphology has been reported in craniofacial bones of mammals that remain open into very late postnatal ontogenetic periods (Opperman et al., 2005). The bipolar organization of cranial synchondrosis structurally differs from the unipolar arrangement of the cartilage cells in epiphyseal growth plates (e.g., the ends of mammalian limb bones, vertebral bodies; Bick and Copel, 1950; Fawcett, 1994), which rarely retain patency throughout the life span. It is suggested here that bipolar organization of cartilage cells at the neurocentral junction is in some way related to sutural patency persisting into late ontogenetic stages.

Vertical cell migration. Besides positive allometric change in the articular surface area of the neurocentral junctions (Table 2-4), another evident ontogenetic change is the vertically zigzagged and/or interdigitated articulations.

This increase in the vertical dimension of articular surface area, which is more evident in the dorsal vertebrae than in caudal vertebrae (Fig. 2-6), results in a more complex topography of contact between centrum and neural arch. The increased 'toothiness' of contact at the neurocentral articular surfaces leads to a richer array of contacts between centrum and neural arch, which is predicted to be biomechanically more stable under a variable loading regime than a flat articulation of equal surface area.

The phenomenon of the increased complexity and interdigitation must be the result of migration or pushing of bone cells from both sides of the centra and neural arches along the neurocentral synchondrosis (Fig. 2-7). This forced movement of the bone cells is reported as the cause of interdigitation in various facial and cranial sutures. In rats, clumping of osteoblasts particularly occurs in the convex side of a synchondroid suture, but fewer (or none of) osteoblast cells appear in the concave side of sutures (Hall, 1972; Koskinen et al., 1976; Cohen, 2000). Seemingly, the same kind of cell migrations occur in the neurocentral junctions of *Alligator*, which provide environments for increasing suture complexity in the presacral vertebrae.

Relationship between suture morphology and fusion timing. Generally, the relationship between complex sutures and patency of fusion exist in craniofacial bones of mammals (Byron, 2006). While synchondroid sutures are growing (increasing complexity), neighboring bones remain unfused. Thus, complex zigzagged sutures generally indicate relatively late timing of fusion or patency through ontogeny. Cell-level morphology indicates this general pattern in

mammalian craniofacial sutures apply to the neurocentral synchondroid joints in the presacral vertebrae of crocodilians.

Controlling factors for the timing of endochondral ossification of the neurocentral synchondroses have not yet been studied extensively in vertebrates. In general, the mechanism of sutural fusion is complicated and various factors are involved. Combinations of intrinsic (e.g., vascular, genetic, hormonal), extrinsic (e.g., mechanical), and epigenetic factors have been suggested in some craniofacial sutures in various mammals (e.g., Herring, 1993). Some specific genes have been identified for the mechanism of both patent and fused sutures (Opperman, 2000; Hall, 2005). These findings are extremely important for the understanding of the mechanism of sutural growth because the patterns of fusion in those craniofacial sutures can be homologous across different groups of mammals and possibly other vertebrates. However, in vertebral sutures, such a study — detecting controlling factors of neurocentral fusion — has not yet been fully explored. Christ et al. (2000) reported that a series of *Pax* and *Msx* genes control endochondral ossification for large proportions of the centra and the base of neural arches in chickens and mice. Because neurocentral fusion is the result of ossification of the synchondrosis, *Pax*-1 and/or *Pax*-4 may be involved for the occurrence of this phenomenon, but further investigations are certainly needed.

Comments on Archosaur Synapomorphies

Fused centra and neural arches are known in mature individuals of most fishes, amphibians, mammals, and reptiles, and it may be hypothesized that this

is a vertebrate synapomorphy. However, some aspects of the neurocentral synchondrosis differ among vertebrates. The neurocentral synchondrosis in *Alligator* is likely secondary cartilage (Fig. 2-5), which has been suggested to be phylogenetically restricted in mammals and birds (and one species of teleosts; Benjamin 1989; Hall, 2005, chapter 5). Also, fused centra and neural arches in extant frogs and salamanders are suggested directly to develop from mesenchymal cells, meaning no synchondroid cartilage ever forms at the neurocentral junction during life, but, perhaps, only fully fused centra and neural arches appear (Smith, 1960, p.146; also personal interpretation in Pugener and Maglia, 1997, 2009). These differences in the neurocentral synchondrosis could be interpreted two ways: (1) they provide evidence for the independent origin of the neurocentral synchondrosis; or (2) they represent modifications of the basal vertebrate condition that occurred within vertebrate subgroups. Similarly, delayed timing of neurocentral fusion, associated with bipolar cell structure and complex sutural boundaries in the neurocentral junction, is present in archosaurs (Fig. 2-1) and mammals. To evaluate these hypotheses of homology, data of cell-level morphology of the neurocentral junctions from various vertebrates will be necessary.

CONCLUSIONS

1. Neurocentral fusion (neurocentral suture closure) is the result of endochondral ossification, which is a physical change of the synchondroid

cartilage into bone) (Fig. 2-6). Four stages of fusion are established primarily based on the relation of the timing of endochondral ossification among the centra, the neural arches, and the neurocentral synchondroses in *Alligator* (Fig. 2-9).

2. *Alligator* has considerably delayed timing of neurocentral fusion during postnatal ontogeny (Fig. 2-4). Fusion progresses from the posterior caudal to sacral vertebrae along a unidirectional posterior-to-anterior sequence, even after reaching sexual maturity. In the presacral vertebrae, complete fusion rarely occurs, indicating patency persisting throughout postnatal ontogeny. Fusion may occur in the dorsal vertebrae of very mature individuals, but this morphological change seems to occur in relatively short time during the postnatal growth. The cervical vertebrae fuses last in crocodilians.

3. The neurocentral synchondrosis in *Alligator* possibly belongs to secondary cartilage (Fig. 2-5). This type of cartilage has not been previously reported in any other non-avian reptiles, although it has been known in cranial bones of mammals and birds, as well as one fish species (Benjamin, 1989; Hall, 2005).

4. Bipolar cartilaginous cell structure is present in the neurocentral synchondrosis of *Alligator.* This cartilaginous cell organization seems to provide appropriate environments for increased complexity of sutural boundaries between centra and neural arches, which may link to delaying neurocentral fusion.

5. The wavy, zigzagged articulations between centra and neural arches and late neurocentral fusion in the presacral vertebrae commonly occur in

crocodilians. The two features are synapomorphies, possibly extended to their Mesozoic close relatives, such as non-avian dinosaurs and pseudosuchians.

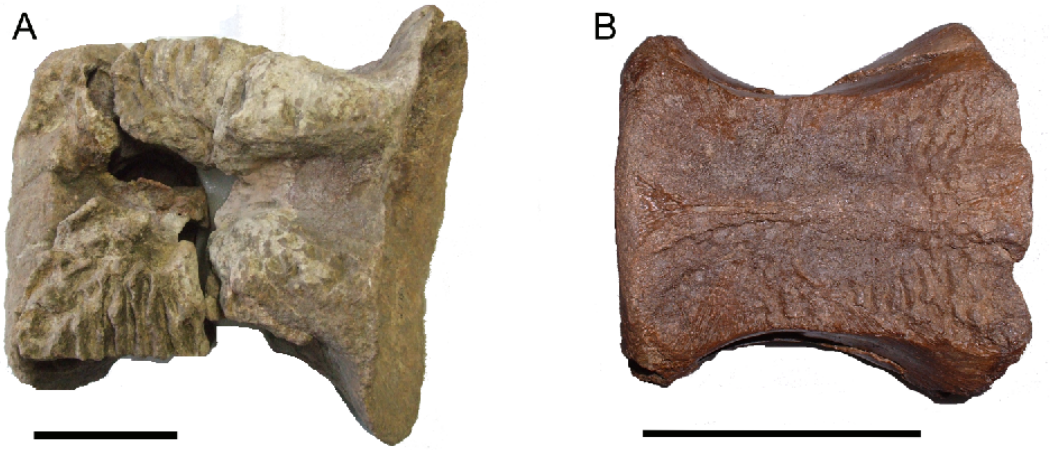

Figure 2-1. Centra of large dinosaurs with unfused neural arches. **A**: sauropod *Brachiosaurus* (Institut für Paläontologie, Museum für Naturkunde ‘dd 355’ in Berlin). **B**: Non-avian theropod *Tyrannosaurus rex* (Royal Tyrell Museum of Paleontology 82.16.122 in Alberta). Both centra show in dorsal view with anterior facing left. The rugose texture is the articular surface of the neurocentral junction. Scales equal 10 cm.

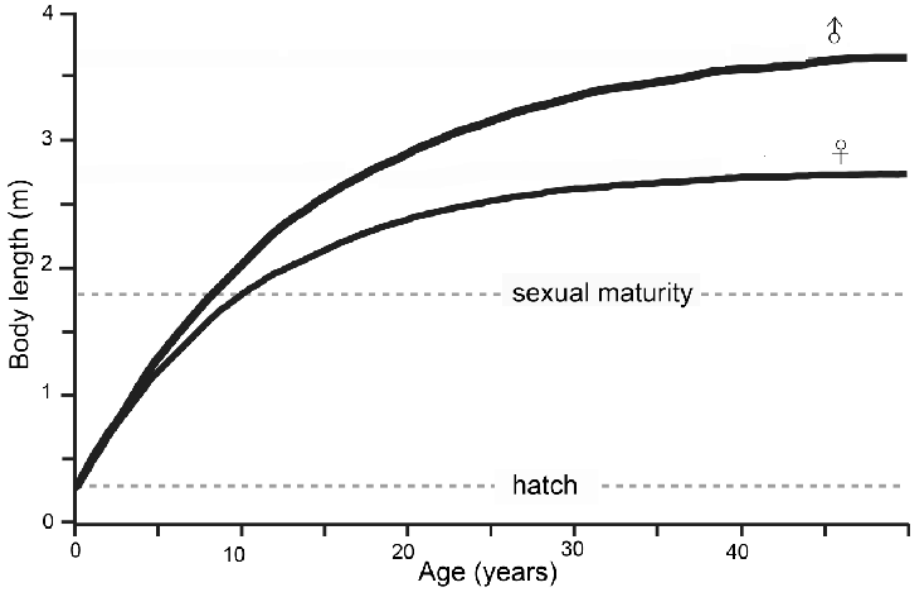

Figure 2-2. Growth curve of *Alligator mississippiensis*. Key ontogenetic events are marked. Skeletal ages based on timing of neurocentral fusion are established using data from Table 2-1. Growth curve is based on Wilkinson and Rhodes (1997).

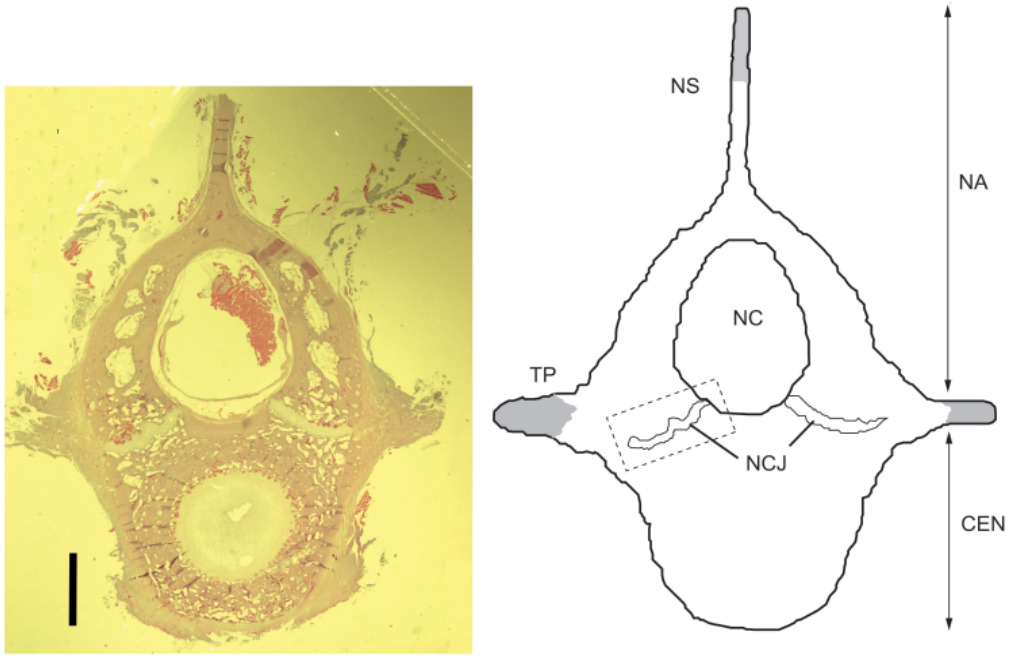

Figure 2-3. Histologic section of anterior caudal vertebra of *Alligator mississippiensis*. Caudal 3 (body length = 0.9 m: UMMZ 238965) was coronally sectioned and stained with hematoxylin and eosin (H&E). Light red color indicates bone; light pink and grey represents cartilage. Identification of key vertebral parts is shown in the illustration, including: **CEN**, centrum; **NA**, neural arch; **NC**, neural canal; **NCJ**, neurocentral junction; **NS**, neural spine; **TP**, transverse process. The dashed box indicates the area around the neurocentral junction (more details in Figure 2-6). Gray shaded areas are missing parts due to sectioning of the vertebra. Scale equals 1 mm.

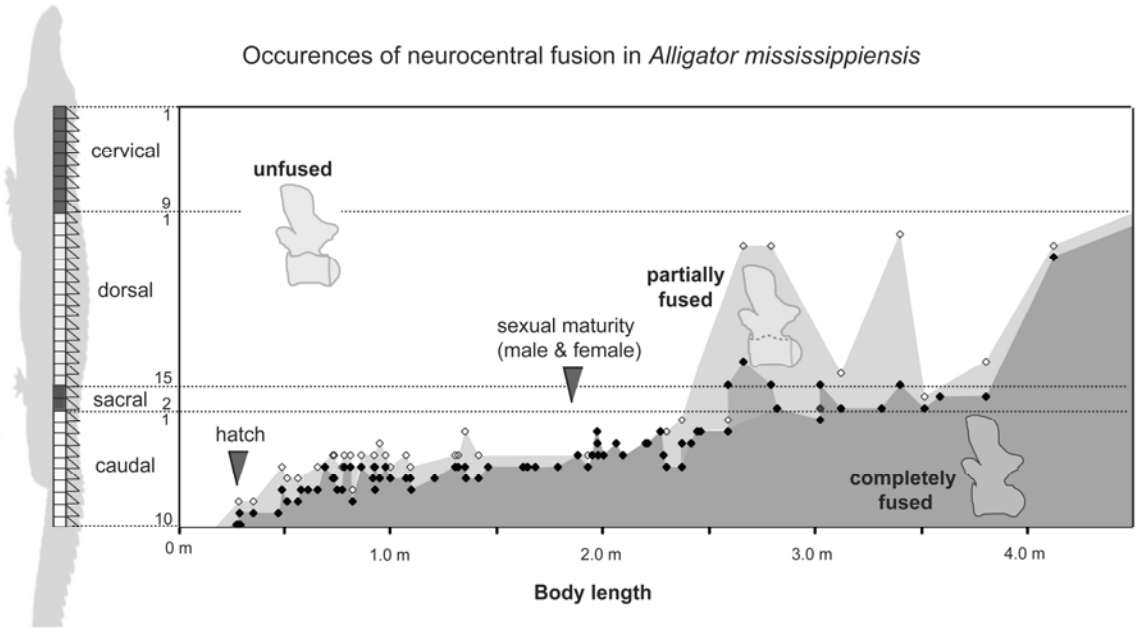

Figure 2-4. Occurrences of neurocentral fusion during postnatal ontogeny of *Alligator mississippiensis.* The dots indicate the positions of the anteriormost vertebra with completely and partially fused neurocentral sutures along the Y-axis for each individual (male and female are not separated). The gray area represents a 'fused' zone according to individuals with the highest number of vertebrae with fused vertebrae. The body length is estimated by the total femoral length (Farlow et al., 2004). Ontogenetic age is estimated by the total body length (Wilkinson and Rhodes, 1997). Timing of sexual maturity follows Ferguson (1985). Specimens are listed in Table 2-1.

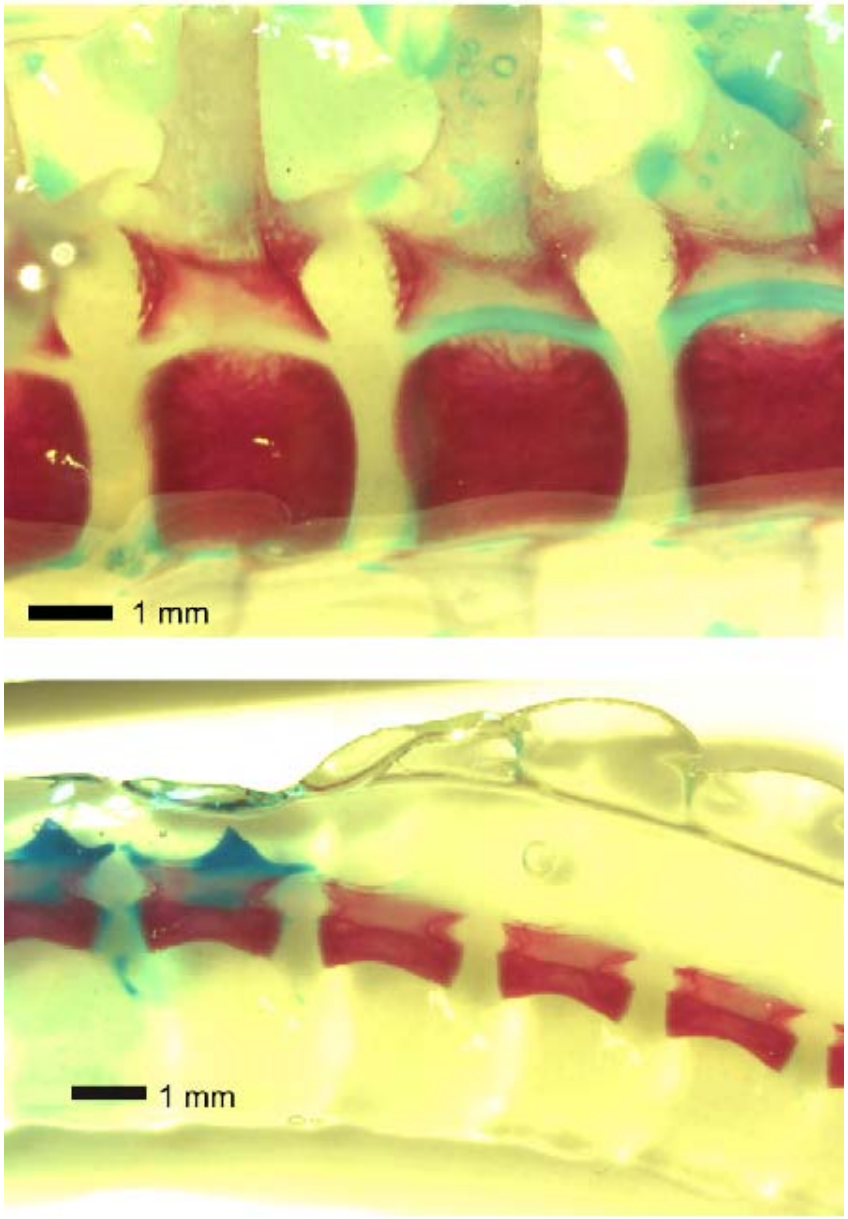

Figure 2-5. Vertebrae of 40 days-old embryonic *Alligator mississippiensis*. Cleared and stained specimen (UMMZ 18192) of **top**, the four anterior dorsal vertebrae and **bottom**, some posterior caudal vertebrae. Left lateral view.

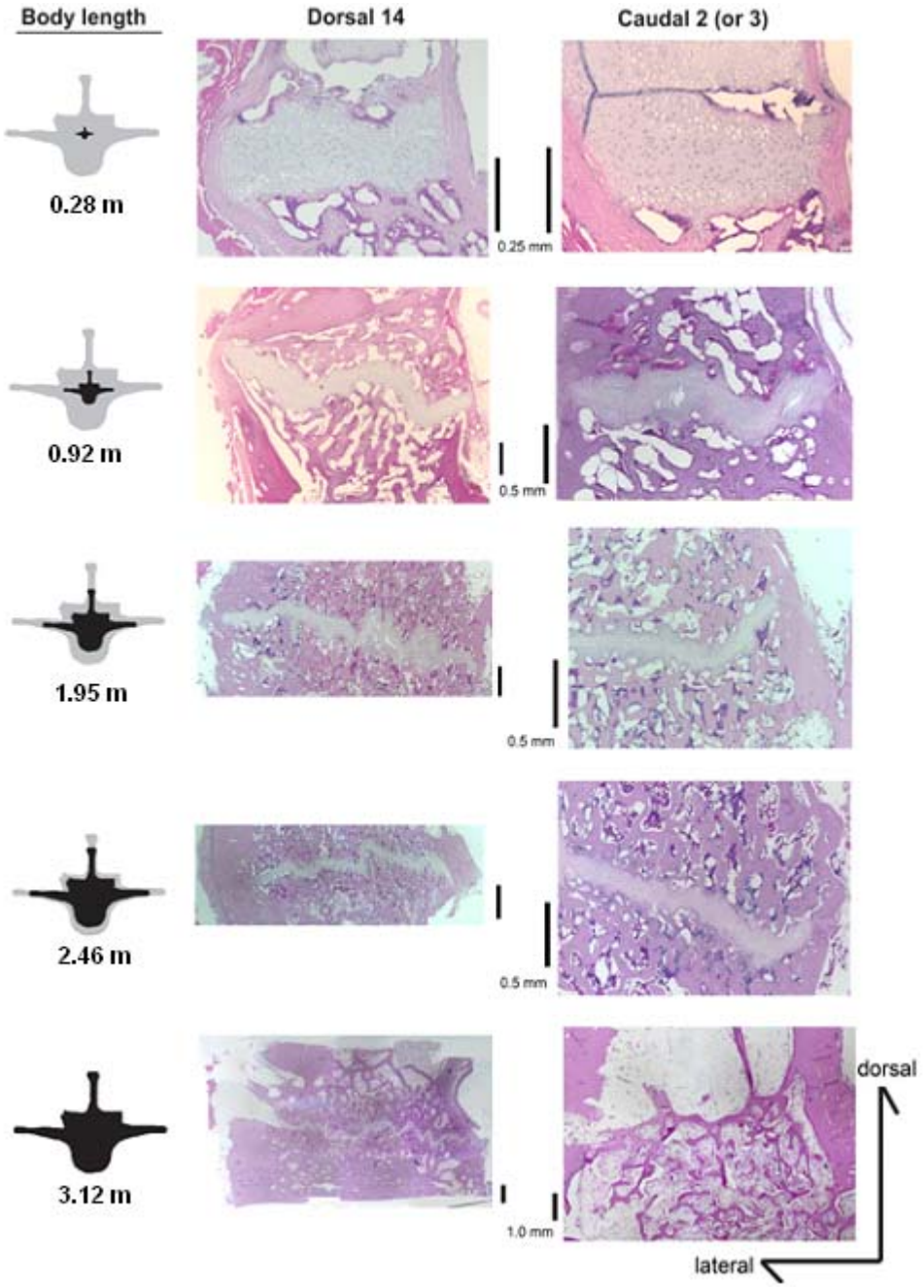

Figure 2-6. H&E stained histologic sections of neurocentral junction of *Alligator mississippiensis*. Dorsal 14 (**left column**) and caudal 2 or 3 (**right column**) were sectioned coronally. The five individuals represent hatchling (**upper row**) to fully-grown individuals (**lower row**): UMMZ 238965, 238959, 239623, 239624, and 239625, respectively. The vertebral silhouettes show a comparison of size based on the largest individual. Note: the large portion of the neural arch was accidentally removed during the process of thin-sectioning in the caudal vertebra of UMMZ 239625.

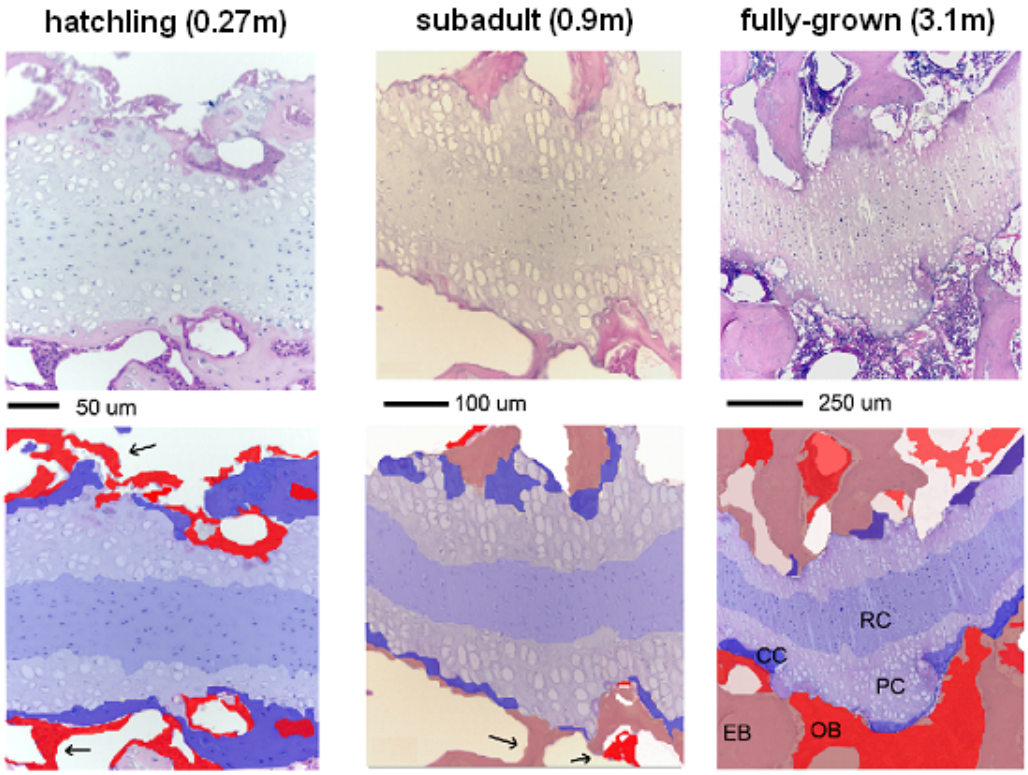

Figure. 2-7. Microscopic morphology of neurocentral junction in dorsal 14 of *Alligator mississippiensis*. **Left column**: hatchling (body length = 0.27 m; UMMZ 238961), **middle column**: subadult (body length = 0.9 m; UMMZ 238959), and **right column**: fully-grown (body length = 3.1 m; UMMZ 239625) individuals. Coronal cross-sectional view. **Upper row**: photomicrograph of H&E stained histologic section. **Lower row**: identification of key cells and tissues (interpreted based on the photo images). The neurocentral synchondrosis shows bipolar structure of cartilaginous cell layers along the mid-zone (reserve cartilage layer). Abbreviations for bone and cartilage: **CC**, calcified cartilage; **EB**, endochondral bone; **HC**, hypertrophic cartilage; **OB**, osteoblast; **OCL**, osteoclast; **PC**, proliferating cartilage; **RC**, reserve cartilage.

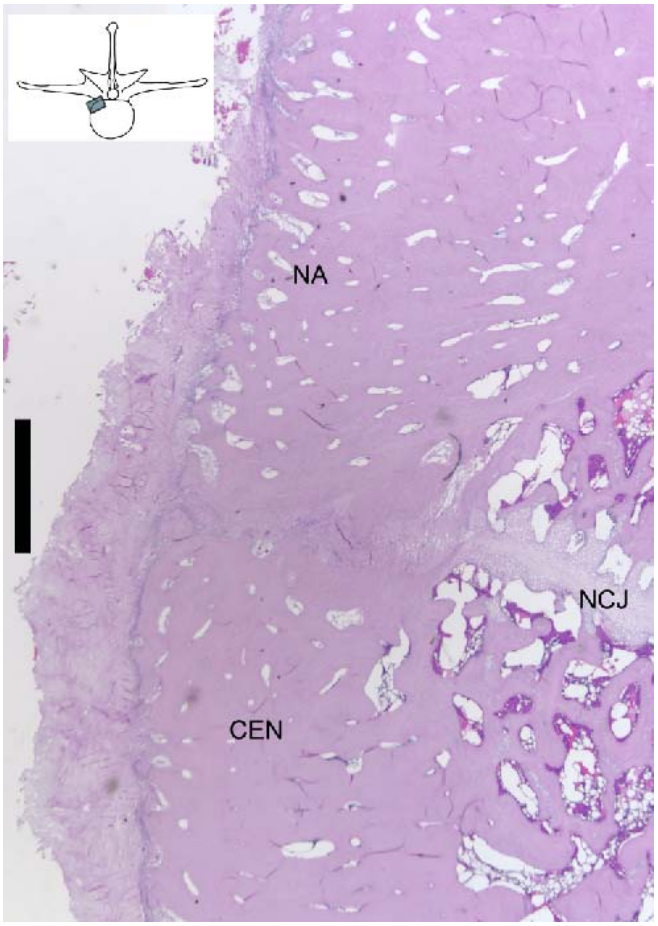

Figure 2-8. External wall of vertebrae along neurocentral junction in *Alligator mississippiensis*. Dorsal 14 of a fully-grown individual (UMMZ 239624). Coronal cross-sectional view shows a bony boundary in the external vertebral wall, which is directly connected to the cartilaginous suture in the internal vertebral structure. **CEN**, centrum; **NA**, neural arch; **NCJ**, neurocentral junction. Scale equals 1 mm.

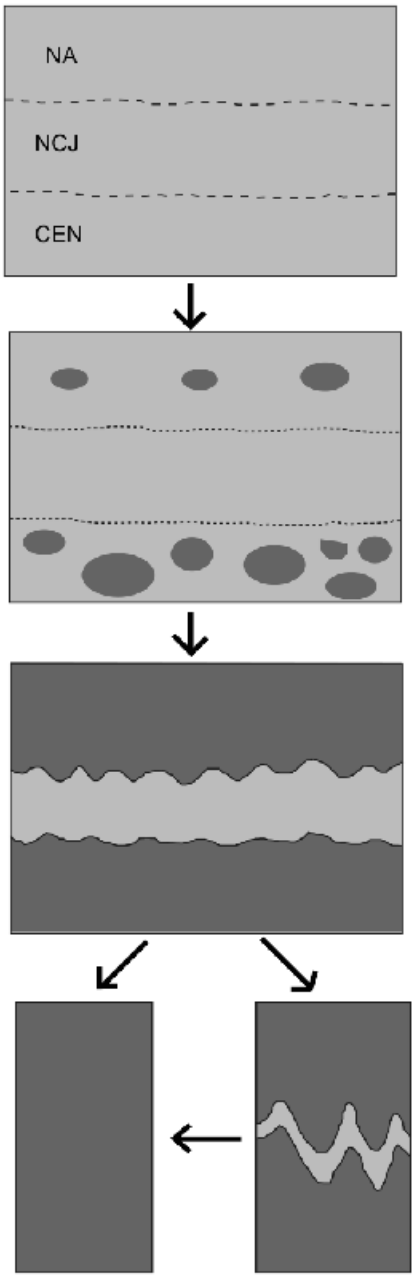

Figure 2-9. Diagramic representation of four stages of neurocentral fusion in caudal vertebrae of *Alligator mississippiensis*. The first stage represents the hatchling period. The bottom represents the very mature stage in caudal vertebrae (left) or presacral vertebrae (right). Dark gray indicates bone and light gray indicates cartilage cells. Abbreviations for vertebral parts: **CEN**, centrum; **NA**, neural arch; **NCJ**, neurocentral junction.

TABLE 2-1. Dry skeletons of Alligator mississippiensis *examined for patterns of fusion at neurocentral junction (NCJ). Positions of the anteriormost vertebrae with 'partially' fused (PF) and 'completely fused' (CF) neurocentral junctions are reported. The same data are used for Figure 2-4*.

Specimen	Femur length (mm)	Body length (mm)	Sex	PF	CF
UMMZ teaching ('03956')	18.0	277	?	Ca10	Ca10
USNM 313410	18.7	287	?	Ca8	Ca10
UMMZ 238961	19.0	291	?	Ca9	Ca9
TMM M7467	19.3	295	?	Ca10	Ca10
TMM M8664	23.5	356	?	Ca8	Ca9
AMNH 138124	31.6	473	?	Ca9	Ca9
UF 35145	32.8	490	M	Ca5	Ca7
UF 35146	34.5	515	M	Ca6	Ca8
UF 35144	38.0	566	M	Ca6	Ca8
UF 35149	39.0	580	F	Ca7	Ca7
UMMZ 155216	41.3	613	?	Ca7	Ca7
UF 37232	44.4	658	?	Ca5	Ca7
UF 40817	46.8	693	?	Ca5	Ca5
UF 11764	49.4	730	?	Ca4	Ca6
UF 42475	49.8	736	M	Ca4	Ca6
TMM M6998	50.8	751	?	Ca7	Ca7
UF 38973	52.4	774	?	Ca5	Ca7
UF 11127	53.1	784	?	Ca4	Ca5
UF 35152	55.1	813	?	Ca4	Ca5
USNM 313409	55.8	823	M	Ca7	Ca8
UF 109039	58.6	863	?	Ca4	Ca5
UF 115605	62.4	918	?	Ca6	ca6
UMMZ 238965	62.8	924	?	Ca4	Ca5
UF 42523	63.1	928	F	Ca5	Ca7
UF 40769	64.6	950	?	Ca3	Ca6
UF 40535	66.5	977	?	Ca4	Ca5
UF 39620	68.1	1000	?	ca5	Ca6
UF 38974	73.2	1074	?	Ca4	Ca6
UMMZ 238959	74.6	1094	M	Ca5	Ca6
UF 38972	74.9	1099	?	Ca5	Ca7
TMM M2433	82.5	1209	?	Ca6	Ca6
UF 39622	89.2	1305	?	Ca4	Ca5
UF 39621	90.2	1320	?	Ca4	Ca5
UF 39623	92.4	1352	?	Ca2	Ca5
LSUVM 15	92.7	1356	F	?	Ca6
UF 37230	96.8	1415	F	Ca4	Ca6
USNM 216198	99.9	1460	?	Ca5	Ca5
LSUVM 16	111.3	1625	M	Ca5	Ca5
TMM M4009	112.6	1644	?	Ca5	Ca5
LSUVM 21	112.8	1646	?	?	Ca5
LSUVM 17	115.3	1683	F	?	Ca5

LSUVM 19	122.6	1788	?	?	Ca5
TMM M7487	129.1	1882	?	Ca4	Ca4
USNM 312681	132.4	1930	?	Ca4	Ca5
UMMZ 239623	133.8	1950	?	?	Ca4
LSUVM 08	135.4	1973	?	?	Ca2
UF 87886	135.5	1974	F	Ca3	Ca3
LSUVM 12	135.7	1977	M	?	Ca4
UF 35153	137.5	2003	?	Ca4	Ca4
LSUVM 14	141.6	2063	M	?	Ca3
LSUVM 07	143.8	2094	?	?	Ca4
LSUVM 05	151.2	2201	?	?	Ca3
LSUVM 13	151.9	2211	M	?	Ca3
AMNH 43316	156.0	2271	?	Ca2	Ca2
LSUVM 11	157.0	2285	?	?	Ca4
USNM 321680	158.0	2300	F	Ca2	Ca5
LSUVM 22	163.0	2372	?	?	Ca5
USNM 312679	163.0	2372	F	Ca1	Ca3
TMM 2000-9-15	166.0	2415	?	Ca3	Ca3
LSUVM 18	168.0	2444	F	?	Ca2
UMMZ 239624	168.8	2460	?	?	Ca2(?)
UF 39106	178.0	2589	?	Ca1	Ca2
USNM 544377	178.0	2589	F	Ds15	Ds15
USNM 312673	183.0	2661	F	Ds3	Ds13
USNM 211235	192.0	2791	F?	Ds3	Ds15
AMNH R71621	194.0	2820	?	Sa2	Sa2
AMNH R31563	208.0	3022	?	Ds15	Ds15
UF 98341	208.0	3022	?	Sa2	Ca1
UMMZ 239625	214.1	3120	?	?	Ds14
TMM M8931	228.0	3311	?	Sa2	Sa2
UF109411	234.0	3398	?	Ds2	Ds15
TMM M4864	242.0	3513	?	Sa1	Sa2
TMM M4135	247.0	3586	?	Sa1	Sa2
UF 39618	262.0	3802	?	Ds13	Sa1
UF 134586	284.0	4120	?	Ds3	Ds4

Institutional abbreviations: **AMNH**, American Museum of Natural History, New York; **LSUVM**, Louisiana State University, School of Veterinary Medicine; **TMM**, Texas Memorial Museum University of Texas, Austin; **UF**, University of Florida Museum of Natural History; **UMMZ**, University of Michigan Museum of Zoology, Ann Arbor; **USNM**, United State National Museum, Washington DC.

TABLE 2-2. Cleared and stained skeletons of Alligator mississippiensis.

Specimen	Age (days after egg laying)	Femur length (mm)
UMMZ 181277	20 days	Not formed
UMMZ 181276	20 days	Not formed
UMMZ 181281	40 days	6.2
UMMZ 181282	40 days	5.8
UMMZ 181283	40 days	5.3
UMMZ 121284	40 days	4.9
UMMZ 181290	ca. 48 days (about hatching)	?
UMMZ 181291	ca. 48 days (about hatching)	13.7
UMMZ 181292	ca. 48 days (about hatching)	10.8
UMMZ 181293	ca. 48 days (about hatching)	13.5
UMMZ 181294	60 days (12 days after hatch)	15.1

*TABLE 2-3. Summary of specimens (*Alligator mississippiensis*) that were histologically sampled for this study. Neurocentral fusion (NCF) is based on the position of the anteriormost vertebrae with completely fused neurocentral junction (see also Figure 2-4).*

Body length	Femur length	Age	Sex	NCF	Specimens	Sampled
28 cm	19 mm	< 1 yr	n.a.	Ca 8–	UMMZ 238961	Cv 3, Ds 14, Ca 2
92 cm	62.8 mm	~5 yrs*	Male	Ca 5–	UMMZ 238965	Cv 3, Ds 14, Ca 3
110 cm	74.6 mm	~5 yrs*	Male	Ca 5–	UMMZ 238959	Ds 14, Ca 3
195 cm**	134 mm	20 yrs	?	?	UMMZ 239623	Ds 14, Ca 2
246 cm**	179 mm	30 yrs	?	?	UMMZ 239624	Ds 14, Ca 2
312 cm**	214 mm	25 yrs	Male?	Sa 1?–	UMMZ 239625	Ds 14, Ca 2

*Ontogenetic age is estimated based on the total body length (Wilkinson and Rhodes, 1997). Abbreviations for vertebrae: **Ca**: caudal; **Cv**, cervical; **Ds**: dorsal.
**Body length was estimated by the greatest length of the femur following Farlow et al. (2004).

TABLE 2-4. Measurements of neurocentral junctions (NCJ) in growth series of Alligator mississippiensis*. Transverse width is measured between the lateralmost and medialmost points in the coronal cross section of vertebrae (see Figure 2-4). The vertical thickness was measured at the minimum and the thickest point. All measurements (in mm) were log-transformed and slopes of the log-log plots are calculated separately in 'NCJ width' and 'NCJ thickness' (median) on the Y-axis relative to the total 'body length' on the X-axis as shown in the graph (below).*

Specimens	UMMZ 238961	UMMZ 238965	UMMZ 238959	UMMZ 239623	UMMZ 239624	UMMZ 239625
Body length	280	920	1100	1950	2460	3120
NCJ width	0.8	4.3	4.8	9.2	14.8	21.6
NCJ thickness (minimum)	0.24	0.25	0.25	0.45	0.50	0.66
NCJ thickness (maximum)	0.35	0.56	0.61	0.67	0.83	0.88
NCJ thickness (mean)	0.30	0.41	0.43	0.56	0.67	0.78

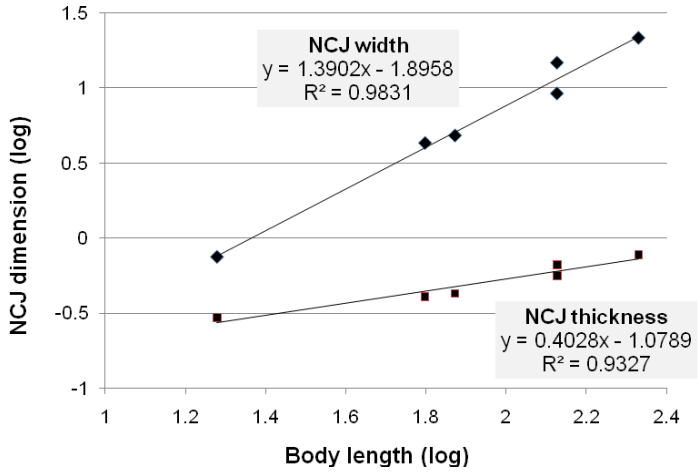

LITERATURE CITED

Abramoff MD, Magelhaes PJ, Ram SJ. 2004. Image processing with ImageJ. Biophotonics Int 11:36-42.

Benjamin M. 1989. The development of hyaline-cell cartilage in the head of the black molly, *Poecilia sphenops*. Evidence for secondary cartilage in a teleost. J Anat 164:145-154.

Bick EM, Copel JW. 1950. Longitudinal growth the human vertebra. J Bone Joint Surgery 32:803-814.

Brochu CA. 1996. Closure of neurocentral sutures during crocodilian ontogeny: implications for maturity assessment in fossil archosaurs. J Vert Paleontol 16:49-62.

Byron CD. 2006. Role of the osteoclast in cranial suture waveform patterning. Anat Rec:552-563.

Carrano MT, Sampson SD, Forster CA. 2002. The Osteology of *Masiakasaurus knopfleri*, a Small Abelisauroid (Dinosauria: Theropoda) from the Late Cretaceous of Madagascar. J Vert Paleontol 22:510-534.

Carpenter K. 1997. A giant coelophysoid (Ceratosauria) theropod from the Upper Triassic of New Mexico, USA. Neues Jahrb Geol Pal Abh 205:189-208.

Christ B, Huang R, Scaal M. 2007. Amniote somite derivatives. Devel Dynamics 236:2382-2396.

Christ, B, Huang R, Wilting J. 2000. The development of the avian vertebral column. Anat Embryol 202:179-194.

Cohen Jr MM. 2000. Chapter 2. Sutural biology. In: Cohen Jr MM, MacLean RE, editors. Craniosynostosis. Diagnosis, Evaluation, and Management. 2nd ed. New York: Oxford University Press. p 9-23.

Dingerku G, Uhlers LD. 1977. Enzyme clearing of alcian blue stained whole small vertebrates for demonstration of cartilage. Biotech Histochem 52: 229-232.

Farlow JO, Hurlburt GR, Elsey RM, Britton ARC, Langston Jr W. 2005. Femoral dimensions and body size of *Alligator mississippiensis*: estimating the size of extinct mesoeucrocodylians. J Vert Paleontol 25:354–369.

Fawcett DW. 1994. Bloom and Fawcett: A Textbook of Histology. 12th ed. New York: Chapman & Hall. Pp 964.

Ferguson MWJ. 1985. Reproductive biology and embryology of the crocodilians. In: Gans C, Billett F, Maderson PFA, editors. Biology of the Reptilia Volume 14, Development A. John Wiley & Son: New York. p 329-491.

Hall BA. 1972. Immobilization and cartilage transformation into bone in the embryonic chick. Anat Rec 173:391-403.

Hall BA. 2005. Bones and Cartilage: Developmental and Evolutionary Skeletal Biology. New York: Elsevier Academic Press. Pp 760.

Herring SE. 1993 Epigenetic and functional influences on skull growth. In: Hanken J, Hall BK, editors. The Skull. Volume 1 Development. Chicago: University of Chicago Press. p 153-206.
Higgins GM. 1923. Development of the primitive reptilian vertebral column, as shown by a study of *Alligator mississippiensis*. Am J Anat 31:373-406.
Hoffstetter R, Gasc JP. 1969. Vertebrae and ribs of modern reptiles. In: Gans C, Bellairs A, Persons TS, editors. Biology of the Reptilia. Vol. 1. New York: Academic Press. p 201-310.
Horner JR. Currie PJ. 1990. Embryonic and neonatal morphology and ontogeny of a new species of *Hypacrosaurus* (Ornithischia, Lambeosauridae) from Montana and Alberta. In: Carpenter K, Hirsch KF, Horner JR, editors. Dinosaur Eggs and Babies. New York: Cambridge University Press. p 312-336.
Ikejiri T. 2007. Ontogenetic and intracolumnar variation in the complexity of the neurocentral suture in dwarf and large crocodilian species. J Vert Paleontol 27 (Suppl 3):93-94A.
Ikejiri T, Tidwell V, Trexler DL. 2005. New adult specimens of *Camarasaurus lentus* highlights ontogenetic variation within the species. In: Tidwell V, Carpenter K, editors. Thunder-Lizards: the Sauropodomorph Dinosaurs. Bloomington: Indiana University Press. p 154-179.
Koskinen L, Isotupa K, Koski K. 1976. A note on craniofacial sutural growth. Am J Phys Anthropol 45:511-516.
Matt GJR, Matricali B, Meerten ELP. 1996. Postnatal development and structure of the neurocentral junction: its relevance for spinal surgery. Spine 21:661-666.
Mook CC. 1921. Notes on the postcranial skeleton in the Crocodilia. Bull Am Mus Nat Hist 44:67-100.
Opperman LA. 2000. Cranial sutures as intramembranous bone growth sites. Devel Dynamics 219:472-485.
Opperman LA, Gakunga PT, Carlson DS. 2005. Genetic factors influencing morphogenesis and growth of sutures and synchondroses in the craniofacial complex. Semin Orthod 11:199-208.
Pugener LA, Maglia AM. 1997. Osteology and skeletal development of *Discoglossus sardus* (Anura: Discoglossidae). J Morphol 233:267-286.
Pugener LA, Maglia AM. 2009. Skeletal morphogenesis of the vertebral column of the miniature hylid frog *Acris crepitans*, with comments on anomalies. J Morphol 270:52-69.
Rajwani T, Bagnall KM, Lambert R, Huang EM, Secretan C, Moreau M, Mahood J, Raso VJ, Bhargava R. 2005. Evaluating MRI as a technique for visualizing the neurocentral junction. Spine 30:807-812.

Rajwani T, Bhargava R, Moreau M, Mahood J, Raso JH, Jiang V, Bagnall KM. 2002. MRI characteristics of the neurocentral synchondrosis. Pediatric Radiol 32:811-816.

Rasband W. 2003. ImageJ version 1.31. National Institutes of Health. Maryland: Bethesda.

Rieppel, O. 1993. Studies on skeleton formation in reptiles. v. Patterns of ossification in the skeleton of *Alligator mississippiensis* Daudin (Reptilia, Crocodylia). Zool J Linn Soc 109: 301-325.

Smith, HM. 1960. Evolution of Chordate Structure. An Introductory to Comparative Anatomy. Holt, Rinehart and Winston: New York.

Vital JM, Beguiristain JL, Algara C, Villas C, Lavignolle B, Grenier N, Sénégas J. 1989. The neurocentral vertebral cartilage: Anatomy, physiology and physiopathology. Surgical Radiol Anat 11:323-328.

Wilkinson PM, Rhodes WE. 1997. Growth rates of American alligators in coastal South Carolina. J Wildlife Management 61:397-402.

Williams EE. 1959. Gadow's arcualia and the development of tetrapod vertebrae. Quart Rev 34:1-32.

Yamazaki A, Mason DE, Caro PA. 1998. Age of closure of the neurocentral cartilage in the thoracic spine. J Pediat Orthoped 18:168-172.

Chapter 3

Ontogenetic and Intracolumnar Variation of Neurocentral Suture Complexity in Large and Dwarf Species of *Alligator* (Archosauria, Crocodylia)

ABSTRACT

Among vertebrates, crocodilians are known to exhibit unique, highly zigzagged or even interdigitated neurocentral suture in vertebrae. These as well as morphological variation in the vertebral column during postnatal ontogeny are investigated among dwarf and large sister species. The large extant crocodilian, *Alligator mississippiensis* (Archosauria, Crocodylia), is preliminarily used to establish a model for identifying and quantifying those types of variations. The entire neurocentral suture is separable into the anterior and posterior neurocentral sutures by the mid-neurocentral peak in most presacral vertebrae. The anterior portion of the neurocentral suture exhibits a relatively smooth, straight line, but the posterior portion has a more complex contour. Here, suture complexity is quantified using the Length Ratio (LR) method, which compares the actual length of a suture to the straight distance between its endpoints. A young adult *A. mississippiensis* (body length = 1.90 m) shows relatively low complexity in the axis, sacral, and caudal vertebrae, but relatively high complexity between posterior cervical and mid-dorsal vertebrae. Suture complexity significantly increases (*t*-test: $P < 0.05$) in most presacral vertebrae during postnatal ontogeny

of *Alligator* (body length = 0.27–4.15 m). This *A. mississippiensis*-model allows comparisons with other crocodilian species. Dwarf species of both fossil and extant *Alligator* species also exhibit relatively complex neurocentral sutures in the presacral vertebrae, suggesting that this feature is not merely controlled by body size but it is a synapomorphy for crocodilians.

INTRODUCTION

Neurocentral sutures — sutures along the boundary between neural arches and centra — exhibit two main types of physical changes during growth of vertebrates. The most common ontogenetic change is fusion between centra and neural arches, which occurs as the result of ossification of the neurocentral synchondrosis (Chapter 2). Another ontogenetic change is the increases in rugosity of the articular surfaces between the neural arches and centra or in degrees of curvature and zigzagged lines as exposed on external vertebral surface. Among vertebrates, the latter type of change, as exemplified by the highly complex or interdigitated neurocentral sutures, is only known in crocodilians (Fig. 3-1) and some close relatives of Mesozoic archosaurs (and possibly, most turtles) (personal observation). However, growth pattern of complex neurocentral sutures in those animals and phylogenetic distribution of this character in vertebrates remain largely unstudied.

This study focuses on the types of intraspecific and interspecific variation in the neurocentral sutures of crocodilians. First, the terminology of the

neurocentral sutures and related vertebral morphologies is summarized. Second, key morphological features of the neurocentral sutures are documented in a young adult *Alligator mississippiensis*. Third, suture complexity is quantified, using the Length Ratio (LR), which is then used to examine intracolumnar and ontogenetic variation. Fourth, dwarf species of extant and fossil *Alligator* are compared with *A. mississippiensis*. These data allow a test of whether body size is linked to the occurrence of complex neurocentral sutures during postnatal ontogeny of alligators and among dwarf to large species.

MATERIALS AND METHODS

Taxonomic Scope and Samples

Skeletons of four species of *Alligator* were examined for this study (Table 3-1). Only two extant species, the North American alligator (*Alligator mississippiensis*) and the Chinese alligator (*Alligator sinensis*), are known in the genus. They are thought to have diverged in the Eocene (50.9 million years ago; Wu et al., 2003). Besides a number of morphological differences (Brochu, 1999), body size is the most evident feature distinguishing the two species. In *A. mississippiensis*, males can grow over 4.54 m in total body length (Woodward et al., 1995), but males of *A. sinensis* rarely exceed 1.6 m (Cong et al, 1998; Herbert et al., 2002). Hatchlings of *A. mississippiensis* are approximately 50% longer (body length = 0.25–0.30 m) and 67% higher (body mass = 50 g) than hatchlings of *A. sinensis* (Herbert et al., 2002).

Two Miocene species of *Alligator* were also examined. *Alligator olseni* from the early Miocene of Florida (Hulbert, 2001) has been suggested to be a dwarf species (maximum body length = ca. 2.50 m; Meylan et al., 2001). *Alligator mcgrewi* from the Miocene of Nebraska is also thought to be a small species based on the size of the holotypic skeleton (Schmidt, 1941). *A. olseni* has been suggested to be more closely related to *A. sinensis* than *A. mcgrewi* (Brochu, 2001).

Twenty-four dry skeletons of *Alligator mississippiensis* including hatchling to fully-grown individuals (body length = 0.29 m–4.12 m) were selected for this study (Table 3-1). The chronological age and sex are uncertain in most of the specimens, but measurements of the femur, skull, and some vertebrae allow estimating approximate body length (Farlow et al., 2005). Sexual maturity usually occurs at body length of about 1.80 m in both male and females (Wilkinson and Rhodes, 1997). Using that threshold, the 24 specimens consist of 14 juveniles and 11 adults.

The 24 skeletons have all presacral, sacral, and 10 anteriormost caudal vertebrae and include both articulated and disarticulated skeletons (Table 3-1). In all disarticulated skeletons, vertebra was first counted and then the exact vertebral positions were identified based on comparisons with articulated vertebral columns. Some skeletons were prepared by maceration, providing physically separated neural arches and centra (Table 3-1, skeleton status). Unfused vertebral elements were used to examine the morphology of the neurocentral articular surfaces.

Only vertebrae with completely open neurocentral sutures were measured in this study. In crocodilians, timing of fusion between neural arches and centra occurs relatively late during postnatal ontogeny (Hoffstetter and Gasc, 1969). Brochu (1996) reported that neurocentral suture closure gradually progresses from the posterior to anterior caudal vertebrae in various crocodilians. Centra and neural arches start to fuse in the anteriormost caudal vertebrae after sexual maturity (body length = ca. 1.80 m) in *Alligator mississippiensis*, but the neurocentral sutures are often open in the presacral vertebrae (especially cervical vertebrae) throughout the entire life of *A. mississippiensis* (Chapter 2). In contrast to the caudal vertebrae with a unidirectional back-to-front sequence, the dorsal vertebrae may not have a typical pattern of neurocentral fusion (Brochu 1996). In addition, since neurocentral fusion occurs in a very short time in a very late ontogenetic stage, and a typical sequence is difficult to determine in the dorsal vertebrae (Chapter 2).

Institutional abbreviations: American Museum of Natural History (AMNH), NY; Field Museum of Natural History (FMNH), Chicago; University of Florida Museum of Natural History, divisions of Herpetology and Vertebrate Paleontology (UF), Gainesville; University of Michigan Museum of Zoology (UMMZ), Ann Arbor.

Length Ratio Method

The Length Ratio (LR) method has been used to quantify the degree of complexity of skeletal sutures in various animals (Jaslow, 1989; Anton et al.,

1992). In contrast to the Fractal Dimension (FD) method[1] which is an indicator of relative suture complexity using a certain scale for complex lines, the LR method is based on direct measurements of actual distance of complex lines (Nicholay and Vaders, 2006). In this study, the LR method was used with some modification. Two landmarks, such as two end points of an entire suture line (Fig. 3-2), were traced for measurements (i.e., with 100–150 dots which physically covers an entire suture; see a detailed procedure below). Those dots are usually sufficient to describe all curvatures and/or concavo-convex outlines in a sutural line. This method avoids some of the difficulties with choice of computer-based software. Further, this method proves practical for measuring vertebrae of hatchlings to fully-grown alligators.

Landmarks. Three landmarks were used for measuring neurocentral sutures, including the anteriormost endpoint, posteriormost endpoint, and the mid-neurocentral peak (MNCP) (Table 3-2, Fig. 3-2). The anteriormost and posteriormost endpoints represent in the two furthermost points along the

[1]In the FD method, a certain size of scale, either a ruler or a box, is used to count a total number of fillings in the space to measure complex lines. A perfect straight line requires the least number of boxes or rulers and provide 1.0 FD (lowest), and a solid plane is ideally the most complex line, which refers to 2.0 FD (Mandelbrot, 1977). This technique seems to have been used preferably for extremely complex lines like some ammonite sutures (Lutz and Boyajian, 1995; Pérez-Claros et al., 2002) and mammalian cranial sutures (Byron et al., 2004), which are generally unable physically to measure all curvatures and concavo-convex indentations. In the FD method, different sizes of scale produce different FD values (e.g., smaller scales generally provide higher fractal dimensions than larger scales; Mandelbrot, 1967). Also, a primary problem to get consistent results in using this method is due to the choice of computer-based software (personal observation). While they automatically calculate a number of either rulers or boxes, the results can be slightly variable due to thickness of lines, resolution of photo images, and image size relative to actual size of an object (personal observation). To avoid these potential problems, direct measurements of the actual distance, which is the principal idea in the LR method, are more advantageous than relative sutural distances calculated by a certain scale. In Addition, Nicholay and Vaders (2006) pointed out the FD and LR methods produce statistically similar results. Thus, I suggest the LR method is practical when all curvatures and/or concavo-convex outlines are physically measurable, such as crocodilian neurocentral sutures.

neurocentral suture. The mid-neurocentral peak is characterized by a dorsally pointed sharp convexity in the centrum, which is the highest point in neurocentral sutures. This mid-neurocentral peak is present only in the presacral vertebrae (except of the atlas) and sacral 1, but it is absent in sacral 2 and all caudal vertebrae (see Descriptive Morphology below). Using these three landmarks, the entire neurocentral suture (ENCS) can be separated into the anterior neurocentral suture (ANCS) and posterior neurocentral suture (PNCS) (i.e., ENCS = ANCS + PNCS; Fig. 3-2). Actual and straight distances were separately measured in the anterior and posterior neurocentral sutures in all vertebrae except sacral 2 and caudal vertebrae.

Photography. Digital photographs of vertebrae were taken in both left and right lateral views with a scale bar. Color images were saved in JPEG format. When specimens were too small to photograph using standard techniques (i.e., body length $\leq$ 0.30 m or vertebral length $\leq$ 5 mm), digital photographs were taken using a microscope (Nikon E800).

Measurement protocol. Vertebral sutures were measured on JPEG or TIF digital images using the freely-downloadable program ImageJ Version 1.32 (Rasband, 2003; Abramoff et al., 2004). To measure the straight distance between end points, the “Straight Distance” tool was used. To measure actual suture length, the “Segmented Lines” tool was used. Under the tool, each suture was measured by 100–150 dots, which generally cover the entire line of a suture, for the actual distance. Two dots were set at the end points of a suture for a

straight distance. All measurements were recorded in millimeters to three decimal places.

All measurements were log-transformed to normalize the distributions of data (e.g., Gingerich, 2000), which allows comparison among hatchling to fully-grown alligators. To calculate the LR of each suture, the log-transformed actual length was divided by the log-transformed straight length. These log-log ratios have been used for comparisons of related anatomical structures (e.g., teeth in jaws) and various specimens (e.g., individuals, taxa) as Simpson (1941, p. 23–24) first proposed in his 'Ratio Diagram'. Higher LR values indicate more complex neurocentral sutures.

Statistics. All statistical tests were conducted with SPSS 17.0 for Windows (SPSS, Inc., Chicago, Illinois). First, a Shapiro-Wilk test ($P < 0.05$) was used for the LR values to check whether those measurements were normally distributed for each vertebra (cervical 2–caudal 3) and each suture dimension (entire, anterior, and posterior neurocentral sutures). Second, 95% CIs were used to determine intracolumnar variation of LR values. "High" and "low" suture complexity was defined for values outside the 95% CI. Third, the paired *t*-test (i.e., Independent Sample *t*-test in SPSS) was used to identify which vertebrae had significantly different LR values between juveniles and adults. When values were significantly different ($P < 0.05$), suture complexity changes significantly during ontogeny. Fourth, a Post Hoc test in a One-way ANOVA was used to compare means and variances of LR values between *Alligator mississippiensis* and *Alligator sinensis*. A Dunnett's T3 test, which has been suggested to be useful for

comparing one individual with others (Motulsky, 1996), was used to test the significance level ($P < 0.05$) of the 24 individuals of the large species with a fully-grown individual of the dwarf species.

Vertebral Counts and Regions in *Alligator*

Terminology of Romer (1956) is used for vertebral regions in this study. I will refer to cervical, dorsal, sacral, and caudal vertebrae rather than alternatives such as trunk and lumbar which were used by, for example, Hoffstetter and Gasc (1969). The vertebral count for crocodilians is nine cervical, 15 dorsal, 2 sacral, and about 30 caudal vertebrae (Hoffstetter and Gasc, 1969; Chiasson, 1969). Within the presacral vertebrae, sub-regions can be recognized: the atlas-axis (presacral or cervical 1–2), anterior cervical (presacral or cervical 3–5), mid-cervical (presacral or cervical 6–8), cervico-dorsal transition (presacral 9–11; cervical 9, dorsal 1 and 2), anterior dorsal (presacral 12–15; dorsal 3–6), mid-dorsal (presacral 16–19; dorsal 7–10), and posterior dorsal (presacral 20–24; dorsal 11–15) vertebrae, based on morphological features of vertebrae (see Chapter 4) and neurocentral sutures (see Descriptive Morphology below; Table 3-3). The identification of vertebral position is based on a combination of overall proportion, size, and key features in a specific dimension shown in Appendix 3-1 (see also Mook 1921; Hoffstetter and Gasc, 1969).

RESULTS

Neurocentral sutures of the cervical to anterior caudal vertebrae were examined in a young adult *Alligator mississippiensis* (body length = 1.90 m) in two ways (Fig. 3-4). First, the articular surfaces of the neurocentral sutures were treated as a two-dimensional objects (i.e., generally shown in unfused centra in dorsal view or neural arches in ventral view). Second, the neurocentral sutures, exposed on the external surface of vertebrae, were described as one-dimensional objects. Morphological information of both two-dimensional articular surfaces and one-dimensional sutural lines are important to determinate if they were morphologically linked. Then, LR values of the neurocentral sutures are quantified in the vertebral column of a young adult individual of *A. mississippiensis*, between the juveniles and adults of *A. mississippiensis*, and among four species of *Alligator*.

Descriptive Morphology of Neurocentral Sutures

Neurocentral sutures in dorsal view (articular surface). In the atlas, the overall outline of the articular surface is nearly circular, but slightly widened transversely. The surface is smooth, without any rugosity (e.g., ridges) in the young adult alligator.

The axis has an anteroposteriorly elongate, rectangular shaped neurocentral articular surface (Fig. 3-4). The articular surfaces can be separated into anterior and posterior portions based on surface texture. The anterior portion

of the articular surface is smooth and bears some small, low rounded bumps. These bumps are separated from each other and lack a particular orientation. In contrast, the posterior portion of the articular surface has fine ridges that connect the lateral (vertebral wall) and medial (neural canal) margins transversely. The posterior margin of the articular surface is pinched out posterolaterally. The separation between the anterior and posterior neurocentral articular surfaces is marked by the mid-neurocentral ridge, which forms the mid-neurocentral peak (Fig. 3-2).

Anterior cervical vertebrae (cervical 3–5) also exhibit rectangular shaped neurocentral articular surfaces (Fig. 3-4). The lateral margin is slightly concave near the mid-point. The medial margin near the mid-neurocentral ridge is extended towards the neural canal. The anterior portion of the articular surface has thin wavy ridges, forming a bumpy surface. Those ridges radiate from the center of the centrum to the anterior and lateral margins of the centrum. The posterior portion of the articular surface has thin straight transverse ridges, on a triangular space (Fig. 3-4).

The articular surface of the mid-cervical vertebrae (cervical 6–8) is similar to those of the anterior cervical vertebrae, but the centrum is slightly shorter anteroposteriorly and wider transversely. The lateral margin of the articular surface is nearly straight in dorsal view, but the medial margin is gently convex medially near the mid-point. In the centra, the posterior portion of the articular surface is highly ridged and slightly depressed ventrally. These fine transverse

ridges are found on triangular space, which is widened posterolaterally from the mid-point of the centrum.

The vertebrae of the cervico–dorsal transition (cervical 9–dorsal 2) have a short, stout centrum with anteroposteriorly short and transversely wide neurocentral articular surfaces. The parapophysis is directly incorporated as a part of the articular surface in these vertebrae. The anterolateral margin of the articular surface is greatly expanded (Fig. 3-4). The mid-neurocentral ridge is tall and weakly curved, directed anterolaterally from the center of the centrum. The anterior portion of the neurocentral articular surface exhibits many coarse bumps and broad, wavy ridges. The posterior portion of the articular surface, placed nearly along a flat horizontal plane, is triangular with very fine sharp ridges that run transversely.

The anterior portion of the articular surface is larger than the posterior portion of the articular surface in the mid-dorsal vertebrae. The lateral and medial margins are nearly parallel to each other. A few tall transverse ridges lay anterolaterally from the mid-neurocentral ridges. The posterior neurocentral surface is slightly depressed and exhibits very fine ridges.

In the posterior dorsal vertebrae, anteroposterior length of the centrum decreases, but the diameter increases posteriorly. This overall morphology of the centrum reflects that of the articular surfaces, which are anteroposteriorly short and transversely wide (Fig. 3-4). The anterior neurocentral articular surface is much longer than the posterior portion of the articular surface, and the lateral margin of the anterior neurocentral articular surface is slightly expanded. The

mid-neurocentral ridge is lower in the posterior dorsal vertebrae than it is in more anterior dorsal vertebrae. The ridge runs posterolaterally from the mid-point of the centrum. Many thin, low ridges also occur in the posterior portion of the articular surface. The centra of the two last dorsal vertebrae are much shorter and transversely wider than those of other posterior dorsal vertebrae. In these vertebrae, the posterior portion of the articular surface is smaller.

The mid-neurocentral ridge is present in sacral 1, but is absent in sacral 2 (Fig. 3-4). In sacral 1, the mid-neurocentral ridge is very low, connecting the medial wall and lateral surfaces of the vertebra. The posterior margin of the rib articular surface also merges into the mid-neurocentral ridge. The anterior and posterior neurocentral articular surfaces are morphologically distinguishable in sacral 1. The anterior portion of the neurocentral articular surface is roughly rectangular, but the posterior articular surface has a triangular outline with fine transverse ridges. The posterior end of the articular surface is pinched out and curved posterolaterally. The neurocentral articular surface is weakly rugose with a shallow transverse depression, instead of a dorsally convex ridge, on the centrum.

In sacral 2 (Fig. 3-4, sacral 2), the mid-section of the articular surface of the neurocentral junction is depressed instead of ridged. The anterior portion has many wavy bumps or weak ridges, oriented in no particular direction. The surface is nearly horizontal. The posterior articular surface has a very smooth texture, which is gently convex dorsally in the centrum. The posterior end is strongly

pinched out. The medial margins of the articular surfaces are much closer to each other in sacral 2 than they are sacral 1.

The young adult alligator has unfused centra and neural arches up to caudal 3. The articular surfaces of the anterior caudal vertebrae are similar to those of sacral 2 (Fig. 3-4, caudal 1). The mid-neurocentral ridge is absent, and the entire articular surfaces of the neurocentral sutures are very narrow transversely. The neurocentral articular surfaces have no transverse ridges, but bumpy, wavy textures. The anterior margin of the articular surface is slightly widened transversely, but the posterior portion is strongly narrowed with a sharply pointed end. In the posterior articular surface, the medial margin is strongly curved out laterally.

Neurocentral sutures in lateral view (sutural line). Below, morphology of the neurocentral sutures in the external surface of vertebrae is described in the same young adult individual (body length = 1.90 m). As the articular surfaces of the neurocentral sutures are morphologically variable in the vertebral column, the sutures in the external surface of vertebrae also exhibit different forms (summary in Table 3-3).

In the atlas, the neurocentral sutures are very short and straight without any interdigitation. In the axis, the anterior and posterior neurocentral sutures are identifiable. The anterior neurocentral suture exhibits a smooth, straight line (Fig. 3-4, axis). The anterior neurocentral suture is slightly inclined upward to the mid-neurocentral peak, occurring nearly at the mid-point along the anteroposterior axis of the centrum. The mid-neurocentral peak is very low, compared to other

presacral vertebrae. The posterior neurocentral sutures are weakly curved (convex ventrally) with very finely zigzagged articulations. In the young adult alligator, the odontoid process is unfused, but it is fused to the axial centrum in fully-grown crocodilians (Brochu, 1996, fig. 7). The neurocentral suture does not have a direct contact with the suture between the axial centrum and the odontoid process.

In anterior cervical vertebrae (cervical 3–5), the anterior neurocentral sutures consist of a part of the transverse process and/or the diapophysis (Fig. 3-4). Around the parapophysis, the anterior neurocentral suture is ventrally concaved and extended laterally. A sharply pointed low mid-neurocentral peak is found just behind the base of the transverse process. Overall, the posterior neurocentral sutures show corrugated articulations. The posterior sutures are nearly straight and parallel to the neural canal.

Overall, the entire neurocentral suture is relatively straight, but the degree of interdigitated articulation is greater in cervical 6–8 than the anterior cervical vertebrae. The anterior neurocentral suture runs underneath the base of the transverse process like the other posterior presacral vertebrae. The anterior neurocentral suture is nearly straight and runs parallel to the neural canal. The anterior neurocentral suture has weakly corrugated articulations. In contrast, the posterior neurocentral suture has much more zigzagged (i.e., weakly interdigitated) articulations than the anterior neurocentral sutures. The straight distance of the posterior neurocentral sutures (i.e., between mid-neurocentral peak and posterior neurocentral end) is about equal to that of the anterior

neurocentral suture. The whole posterior neurocentral suture is inclined to the posterior neurocentral end (ca. 25°). The mid-neurocentral peak is better developed in the mid-cervical vertebrae than in the anterior cervical vertebrae.

The neurocentral sutures cross the parapophyses only in vertebrae of cervico-dorsal transition (Fig. 3-4). The anterior neurocentral sutures are extended laterally, especially in dorsal 2. The anterior neurocentral sutures are straight and slightly inclined from the mid-neurocentral peak to the anterior neurocentral end. The slope tends to decrease in dorsal 2 and more posterior dorsal vertebrae. Straight distance of the anterior neurocentral suture is longer (150–160%) than that of the posterior suture in vertebrae of the cervico-dorsal transition. Straight anterior neurocentral sutures are weakly interdigitated.

The mid-neurocentral peak is tall, pointed dorsally, and placed slightly more posteriorly than the mid-point of the centrum. The posterior neurocentral suture is highly interdigitated in the three mid-neurocentral vertebrae. At least, 10 to 15 sharp concavo-convex blocks exist in each posterior neurocentral suture. The posterior neurocentral sutures exhibit a steep down slope from the mid-portion to the posterior neurocentral end overall. Cervical 9 and dorsal 1 have a nearly straight line, but dorsal 2 has a slightly curved outline.

Dorsal 3 and other posterior dorsal vertebrae have a pair of parapophyses placed above the neurocentral sutures (i.e., either on the base of the neural arch in dorsal 3 or on the transverse process in others). As a result, the anterior neurocentral suture is nearly straight in dorsal 3–6, unlike dorsal 1 and 2. In the anterior dorsal vertebrae, the lateral margins of the anterior neurocentral sutures

have a low ridge (which also occurs in the other posterior dorsal vertebrae). The anterior neurocentral sutures are longer (127–155% in dorsal 3–6, respectively) than the posterior sutures in the four vertebrae. This feature is more evident in dorsal 6 and the mid-dorsal vertebrae.

Compared to the condition of other dorsal vertebrae, the mid-neurocentral peak in the anterior dorsal vertebrae is large and tall (especially, dorsal 3). Besides the mid-central ridges, several other lower transverse ridges form dorsally pointed peaks on the centra around the mid-neurocentral peak in lateral view of the centra. The mid-neurocentral peak is placed more posteriorly along the anteroposterior axis of the centrum, due to very elongate anterior neurocentral sutures. The whole posterior neurocentral suture is strongly curved (concave down), forming nearly a crescent or a half moon-shape in dorsal 3–5, but those tend to be straighter in dorsal 6.The posterior neurocentral suture is highly zigzagged, as in dorsal 2.

The anterior neurocentral suture is longer than the posterior neurocentral suture in dorsal 7 and 8 (122–130 %), but nearly equal in dorsal 9 and 10 (Fig. 3-4). The anterior sutures are nearly straight with very low wedges, forming a corrugate outline. The mid-neurocentral peak is present, but lower in the mid-dorsal than in the anterior dorsal vertebrae. Dorsoventral height of the mid-neurocentral peak in the centra gradually decreases to more posterior dorsal vertebrae. The posterior neurocentral sutures exhibit a weak S-shaped outline, characterized by a dorsally convex half front and ventrally concave half back portions of the posterior neurocentral sutures.

Overall, the neurocentral suture in posterior dorsal vertebrae is intermediate between mid- and posterior dorsal vertebrae. As shown in the centra (Fig. 3-4), anteroposterior length gradually decreases from dorsal 12 to the last dorsal vertebra. The anterior neurocentral suture is nearly straight in all posterior dorsal vertebrae. Straight distance between anterior neurocentral end and mid-neurocentral peak is nearly equal to that of the posterior neurocentral sutures (98–104 %) in dorsal 11–13. The mid-neurocentral peak is lower in more posterior dorsal vertebrae. The posterior neurocentral sutures exhibit a weakly corrugated outline, but are not interdigitated. The entire posterior suture tends to be straighter, instead of curved, in dorsal 11–13.

The two last dorsal vertebrae differ from other posterior dorsal vertebrae in their anteroposteriorly shortened and transversely widened centra. In those robust centra, straight distance of the anterior neurocentral suture is much shorter (27% and 35 % in dorsal 14 and 15, respectively), but longer than that of the posterior neurocentral suture (Fig. 3-4). The anterior neurocentral suture is nearly straight, inclined from the mid-neurocentral peak to the anterior neurocentral end. The lateral margin of the anterior neurocentral sutures exhibits a weakly flared ridge. The mid-neurocentral peak is relatively low in dorsal 13–15. The posterior neurocentral suture tends to be more interdigitated in the last dorsal vertebra than other mid- and posterior dorsal vertebrae.

The two sacral vertebrae have large rib facets on the lateral surface that are divided by the neurocentral sutures (Fig. 3-4). The neurocentral suture is

straighter than that of the presacral vertebrae. No interdigitated articulations appear in the entire neurocentral suture of the sacral vertebrae.

The neurocentral sutures differ between sacral 1 and sacral 2. Overall, sacral 1 is similar to the dorsal vertebrae (e.g., the presence of the mid-neurocentral peak), and this morphology can make the anterior and posterior neurocentral sutures distinguishable (Fig. 3-4). The mid-neurocentral peak of sacral 1 is occurs, approximately anteriorly at the two-fifths of the centrum. In sacral 1, the mid-neurocentral peak is low and the entire suture is nearly straight. Sacral 2 has no mid-neurocentral peak (as in the caudal vertebrae; see below). As the articular surfaces of the centra or neural arches are relatively smooth and flat, the neurocentral sutures on the external vertebral surface are nearly straight without any interdigitation.

The neurocentral suture is similar in caudal 1–3 and sacral 2 (Fig. 3-4). The sutures are nearly straight, with no interdigitated articulations. Instead, a number of low, bumpy surfaces can be seen in the lateral view of the vertebrae. The posterior base of the neural arch does not merge to the dorso-posterior margin of the centrum. Thus, the anteroposterior length of the neurocentral sutures is shorter than that of the centrum.

Variation in Neurocentral Suture Complexity

Using the LR method, degrees of neurocentral suture complexity are compared in three ways. First, suture complexity is compared along the vertebral column of a young adult individual of *Alligator mississippiensis* (intracolumnar

variation). Second, the 24 skeletons of *A. mississippiensis*, which include hatchlings to fully grown individual, are examined (ontogenetic variation). Then, the changes in suture complexity are compared among extant and fossil species of *Alligator*, which exhibit a relatively large range of maximum body sizes in crocodilians (size variation).

Intracolumnar variation. LR values are compared in the axis to caudal 3 of the young adult individual (body length = 1.90 m) (Table 3-4; Fig. 3-5). Three measurements, the entire, anterior, and posterior neurocentral sutures (Fig. 3-2), are separately quantified. Because the anterior and posterior sutures are not morphologically distinguishable in sacral 2 and caudal vertebrae (see Descriptive Morphology above), only the entire neurocentral suture is shown in these vertebrae.

The distribution of LR values is relatively similar between the entire neurocentral and posterior neurocentral sutures (Fig. 3-5). Among the three values of neurocentral sutures, the posterior neurocentral sutures have the highest mean of the LR values (1.068) and the widest range (1.004–1.200) (Table 3-4). The anterior neurocentral sutures have the lowest mean (1.040) with the smallest range. The LR values of the entire neurocentral sutures fall between the anterior and posterior neurocentral sutures in cervical 2–sacral 1.

LR values for the entire neurocentral sutures are relatively high in cervical 6–dorsal 6 (> the upper limit of a 95% CI: 1.058; Table 3-4). The cervico-dorsal transitional and the anterior dorsal vertebrae have higher values than other vertebrae, and the highest value (1.085) appears in dorsal 4 (Fig. 3-5). The axis

has the lowest LR value (= 1.020) among the presacral vertebrae, and relatively low values (LR < the lower limit of a 95 % CI: 1.040) also occur in dorsal 7 and other posterior dorsal vertebrae, except for the last dorsal vertebra which fits in a 95% CI (1.042). Sacral 1 (LR = 1.030) has lower complexity than all presacral vertebrae, except for the axis. Sacral 2 and all anterior caudal vertebrae have lower values than the presacral vertebrae.

The anterior neurocentral sutures have the smallest range of the LR values: 1.001 in dorsal 15 to 1.039 in cervical 9 (Table 3-4; Fig. 3-3). The occurrences of high–low LR values in the vertebral column show a different pattern in anterior and posterior (or entire) neurocentral sutures. Relatively low LR values (< 1.015) occur in the axis, most posterior dorsal vertebrae, and sacral 1. Relatively high LR values (> 1.023) are found in the anterior cervical vertebrae and cervical 9–dorsal 7.

In the posterior neurocentral sutures, very high LR values (< 1.095) are found in cervical 6 and dorsal 7, whereas the highest value is found in dorsal 1 (1.177) (Fig. 3-5). The LR values gradually decrease from the anterior to the posterior dorsal vertebrae. Very low LR (> 1.095) is found in dorsal 9–14. The lowest LR value appears in the axis (1.027) among the presacral vertebrae among the vertebrae. Sacral 1 has the second lowest value (1.068). Only dorsal 7 and the last dorsal vertebra have very high values among the mid- and posterior dorsal vertebrae in the young adult. The data from the three sutural measurements in the vertebrae suggest that high suture complexity occurs primarily in posterior neurocentral sutures in presacral vertebrae of *Alligator*.

Ontogenetic variation. Box-plots show comparisons of the means, medians and variances of the LR values between juveniles and adults of *Alligator mississippiensis* (Figs. 3-6, 3-7). The two ontogenetic categories were defined by the mean body length at sexual maturity (ca. 1.8 m; Wilkinson and Rhodes, 1997). Thirteen individuals fall in the juvenile group, and 11 alligators in the adult group. The 13 juveniles have visible neurocentral sutures in vertebrae up to the anteriormost caudal vertebrae, but the centra and neural arches are completely fused in all caudal vertebrae in most adults. Only a few very mature individuals (i.e., body length $\geq$ 3.40 m in the samples) show partially and/or completely closed neurocentral sutures in the dorsal vertebrae (Table 3-1).

Caudal vertebrae and sacral 2 do not have a mid-neurocentral peak (see Descriptive Morphology above), so LR values for the entire suture were quantified (Figs. 3-6, 3-7). For presacral vertebrae, LR values were calculated separately for the anterior, posterior, and entire neurocentral sutures (Fig. 3-7).

LR values increase in the entire, anterior, and posterior neurocentral sutures during postnatal ontogeny. The posterior neurocentral sutures have the higher LR values than the two other sutural measurements (maximum = 1.398; mean = 1.131) (Table 3-5A). The anterior sutures have the lowest values (maximum = 1.148; mean = 1.040). The LR values for the entire neurocentral suture are intermediate between the anterior and posterior neurocentral sutures.

The entire neurocentral suture shows that the LR values significantly increase in cervical 3–dorsal 15 (Paired *t*-test; $P < 0.05$) from the juvenile to adult stage (Table 3-5B). The intracolumnar occurrence of low-high LR values of the

adults is similar to that of the young adult individual (Fig. 3-5; Table 3-4), but the adults have much higher values (means of cervical 2–dorsal 15 = 1.095; Table 3-5A). Relatively large ontogenetic changes occur in the cervico-dorsal transitional and anterior dorsal vertebrae in the adults (Fig. 3-6). Among the adults, relatively low values are found in cervical 2 (mean of LR = 1.041), posterior dorsal (mean of LR in dorsal 13 = 1.065), sacral 1–2 (means of LR = 1.028 and 1.022), and caudal vertebrae (mean of LR in caudal 1–3 = 1.040–1.012), except for the last dorsal vertebra (mean of LR = 1.085).

The three hatchlings (body length $\leq$ 0.32 m) have considerably low LR values in the entire neurocentral suture of all vertebrae (mean of LR in cervical 2–dorsal 15 = 1.050; Table 3-5A). In the juveniles, cervical 9, which exhibits the highest mean in the adults, has a very low value (i.e., lower than the axis) in the column (Fig. 3-6). Vertebrae of the cervico-dorsal transition show relatively high upper limits of the LR values along the vertebral column.

LR values of posterior neurocentral sutures significantly increase in cervical 3–dorsal 15 during postnatal ontogeny (Paired *t*-test; $P < 0.05$; Table 3-5B; Fig. 3-7). The highest value occurs in dorsal 1 in the adults (mean of LR = 1.248), and several neighboring vertebrae have relatively high values (> 1.900 in cervical 6–dorsal 4). The posterior neurocentral sutures have much higher values in all presacral vertebrae than the entire neurocentral sutures in the adults, except for the axis. The three hatchlings share the lowest LR values in the vertebrae. Among the juveniles, the LR values are slightly higher in the vertebrae of the cervico-dorsal transition than other vertebrae.

The anterior neurocentral sutures tend to have low LR throughout postnatal ontogeny. The means of the LR values do not exceed 1.10 in all vertebrae in the adult stage (Fig. 3-7). Only seven vertebrae show significant increases in the LR values, including cervical 8, dorsal 1–2, dorsal 4, dorsal 6–7, and dorsal 14 (Paired *t*-test; $P < 0.05$) (Table 3-5B). Among the adults, the highest LR value occurs in dorsal 3 (mean = 1.072), but relatively high values appear from the mid-cervical to mid-dorsal vertebrae. In the juveniles, most vertebrae exhibit very low LR values in all presacral vertebrae (Fig. 3-7, Table 3-5A).

Size variation. Comparisons of the means and variances of the LR values among 24 individuals of *Alligator mississippiensis* and one individual of *Alligator sinensis* are shown in Table 3-6. The individual of *A. sinensis* (body length = ca. 1.44 m) was determined to be fully grown based on the average of total body length at sexual maturity in the species (ca. 0.8 m; Fairbairn et al., 2007). In the entire neurocentral sutures of the axis–dorsal 15, five individuals (body length = 0.29, 0.29, 0.88, 1.59, and 3.80 m) of *A. mississippiensis* have significantly different LR values, based on a One-way ANOVA (the Dunnett's T3 test: $P < 0.005$) (Table 3-6).

Intracolumnar distributions of the LR values of *Alligator mississippiensis* are compared with those of *Alligator sinensis* (Figure 3-8A). Three individuals of *A. mississippiensis* — hatchling (body length = 0.29 m), young adult (body length = 1.90 m), and fully-grown (body length = 3.18 m) individuals — are used to establish the adult and juvenile categories. The fully-grown individual of *A.*

sinensis is superimposed on this *A. mississippiensis* model. The individual of *A. sinensis* fits in the adult category of *A. mississippiensis*. The LR values are higher in the dwarf individual (body length = 1.44 m) than in the young adult *A. mississippiensis* (body length = 1.90 m) in all presacral vertebrae, except for cervical 4. As shown in the young adult *A. mississippiensis* (Fig. 3-5), the dwarf specimen shows the similar intracolumnar occurrence of low-high LR values. Relatively high LR values are dominant around cervical 5–dorsal 7, with the highest LR value in dorsal 3 (1.159) (Fig. 3-8A).

Mean differences of LR values between the two species of *Alligator* are further compared for the entire neurocentral suture of cervical 5–dorsal 7. Figure 3-9 shows that, relative to body size, the mean of the fully-grown individual of *Alligator sinensis* (1.44 m) is close to the means of the 24 individuals of *Alligator mississippiensis* (body length = 0.29–4.12 m). Generally, larger individuals (i.e., body length > 1.44 m) of *A. mississippiensis* exhibit closer LR values to the dwarf than smaller individuals. Among the 24 individuals of *A. mississippiensis*, the closest mean value to that of the dwarf is found in the adult individual with 2.00 m in body length, and two other adults (body length = ca. 3.04 m and 2.82 m) also have close mean values. Besides the three individuals, only two others individuals of *A. mississippiensis* with about the same body size have relatively close LR values (i.e., a mean difference $\leq$ 0.019; Fig. 3-9). The juveniles tend to have smaller LR values than the dwarf. In particular, the two hatchlings and one juvenile show significantly lower means than the fully-grown dwarf individual. The

young adult of North American alligator (body length = 1.59 m) also exhibit a significantly different mean compared to the dwarf.

DISCUSSION

Ontogenetic and evolutionary significances of highly complex neurocentral sutures in crocodilians have been largely uncertain. Based on general morphology of the neurocentral sutures described above, general mechanical factors of complex sutures in vertebrae are first interpreted. Those ideas of general functional roles allow discussing how complex sutures may relate to body size of alligators in the growth series of individuals (i.e., during ontogeny) and in mature individuals of small to large species of *Alligator* (i.e., during evolution).

Function of Complex Neurocentral Sutures

Immobile synchondroid sutures are thought to play an important role in adjusting the movement of bones and resisting various types of stresses (Cohen, 2000). While actual strains between neural arch and centrum have not been measured in crocodilians, it seems probable that more complex sutural boundaries generally have greater absorption of mechanical stress (Jaslow, 1989; Anton et al., 1992; Nicolay and Vaders, 2006). Crocodilian trunk generally have four main types of mechanical loads in the axial column: transverse shearing along the horizontal plane, torsion along the colonal plane, dorsoventral shear along the sagittal or horizontal plane due to gravity, and anteroposterior

compression among vertebrae (e.g., Salisbury and Frey, 2000, fig. 9). Among dorsal vertebrae, while the centra are connected by fibrous cartilage, the intervertebral disk, to the bonny parts of the anterior and posterior articular surfaces, the neural arches provide the main insertion sites of various epaxial muscles and the articulations of elongate dorsal ribs, which insert various hypaxial muscles (Organ, 2006). Presumably, those epaxial and hypaxial muscles are the main generator of those mechanical loads, and the functional difference between the centrum and neural arch can create various types of repetitive stresses in the neurocentral suture.

Herring (2008) summarized the relationship between two main types of stress (i.e., compressive and tensile) and suture morphologies (i.e., smooth and interdigitated) in mammalian craniofacial bones. According to her interpretation, smooth sutural boundaries are better for resisting tensile stress, and interdigitated sutures are better for resisting compressive stress. Hypothetically, this general rule may apply to neurocentral sutures in the presacral vertebrae of crocodilians, such as relatively smoother anterior and more complex posterior sutures. Also, articular surfaces of the neurocentral suture exhibit transversely oriented, fine ridges (Fig. 3-4). Those transverse ridges, which are oriented perpendicular to the axial column, may be responded to transverse sharing stress, which can occurs when the neural arch is twisted either clockwise or counterclockwise along the horizontal plane by those axial muscles.

Relationships between Body Size and Neurocentral Suture Complexity during Ontogeny and Evolution

Based on those general functions of neurocentral sutures, highly complex sutures may be strictly controlled by size (i.e., interdigitated neurocentral sutures are advantageous for supporting structures of larger vertebrae). Increases in size of vertebrae are generally seen during growth and/or evolution of crocodilians, which provide two main hypotheses discussed below. First, crocodilians are unique for considerably delayed timing of neurocentral fusion during the postnatal ontogeny (Hoffstetter and Gans, 1969; Brochu 1996). In particular, the presacral vertebrae tend to have patency of fusion throughout the life span (Chapter 2). Thus, the relationship between timing of fusion and increases in suture complexity may exist in crocodilian vertebrae. If neurocentral suture complexity keeps increasing throughout the entire life span, this morphological feature must be advantageous for delayed neurocentral fusion.

Second, based on the nature of a relatively wide range in maximum body size of crocodilians (e.g., *Alligator mississippiensis* and *Alligator sinensis*), highly complex neurocentral sutures can be hypothesized to evolve primarily in large crocodilian species. In contrast, if complex neurocentral sutures appear in both dwarf and large crocodilian species, this feature must be driven by evolutionary force (i.e., various factors of natural selection) across crocodilians.

Increasing complexity during ontogeny. During ontogeny of *Alligator*, highly complex neurocentral sutures appear mainly in the presacral vertebrae (Figs. 3-5, 3-6, 3-7). Notably, the means of the LR values of the entire and

posterior neurocentral sutures are higher in the adults than in juveniles (Table 3-5). Also, in posterior neurocentral sutures of presacral vertebrae, the LR values are significantly correlated to body size in cervical 2–dorsal 15 (Pearson's correlation: $P < 0.05$; Table 3-7). The data indicate that suture complexity keep increasing (and even accelerating in the later ontogenetic period; personal observation). This general pattern suggests degrees of suture complexity of presacral vertebrae — in particular, posterior neurocentral sutures in cervical 3 – dorsal 15 — can be useful to estimate relative skeletal maturity in *Alligator* (further discussion below).

Highly complex sutures in dwarf and large species. Comparisons of suture complexity between fully-grown individuals of *Alligator mississippiensis* and *Alligator sinensis* indicate that both dwarf and large species have considerably high LR values in the presacral vertebrae. Notably, the entire neurocentral sutures in all presacral vertebrae are more complex in the fully-matured individual of the dwarf species (body length = 1.44 m; mean of LR = 1.798) than the young adult individual of the large species (body length = 1.90 m; mean of LR = 1.055) (Tables 3-4, 3-6, Fig. 3-8A). This individual of *A. mississippiensis* is determined to have just reached sexual maturity based on the body size criterion (the average body size = ca. 1.80 m; Wilkinson and Rhodes, 1997), and the LR values of this individual suggest relatively mature skeletal age (Figs. 3-8A, 3-9).

Based on this young adult of *Alligator mississippiensis*, two individuals of *Alligator mcgrewi* and *Alligator olseni* are also likely to be fully-grown, in spite of

their smaller total body length (Fig. 3-8B). *A. olseni* has been suggested to be a dwarf species, based on multiple isolated and fragmentary skeletons (Hulbert, 2001). The mid-cervical and mid-dorsal vertebrae of one of the largest specimens (body length: ca. 2.60 m estimated by vertebral size) exhibit relatively high complexity, which fits in the adult zone of *A. mississippiensis* (Fig. 3-8B). In addition, larger individuals (vertebrae) of *A. olseni* often have completely fused neurocentral sutures (personal observation). Those data indicate *A. olseni* is a considerably smaller species than *A. mississippiensis*. The holotype of *A. mcgrewi* was originally thought to be 'a half-grown' individual (Schmidt, 1941, p.27) based on size (body length = ca. 1.60; based on vertebral and skull sizes). However, this individual also shows relatively high neurocentral complexity in cervical 8–dorsal 1 (Fig. 3-8B). Thus, *A. mcgrewi* is liked to be a smaller species than *A. mississippiensis*.

The high LR values in the vertebrae of the cervico-dorsal transition to the anterior dorsal vertebrae are not just characteristic of the four species of *Alligator*, but also in other crocodilians (e.g., *Paleosuchus palpebrosus*, very large species, C*rocodylus niloticus*, C*rocodylus porosus*; personal observation). Therefore, this character — complex neurocentral sutures in presacral vertebrae — is most likely a synapomorphy for crocodilians. The evolutionary significance of complex neurocentral suture remains largely unexplored. Various extant crocodilians and other fossil close relatives may provide important information for further investigations.

CONCLUSIONS

1. Adult *Alligator mississippiensis* have highly complex neurocentral sutures in the presacral vertebrae, especially, cervical 5–dorsal 6. The axis, all sacral, and caudal vertebrae have relatively low complexity (Figs., 3-4, 3-5).

2. Complexity primarily comes from the posterior neurocentral sutures (Figs., 3-5, 3-6, 3-7). The anterior sutures generally exhibit a smoother articulation with gentle curvature.

3. Suture complexity significantly increases from the juvenile to adult stages in all presacral vertebrae (except for atlas and axis) in *Alligator mississippiensis* (Figs., 3-6, 3-7; Table 3-4). Sacral and caudal vertebrae remain of low in complexity until neurocentral sutures disappear (i.e., fuse).

4. Suture complexity continuously increases in the presacral vertebrae during postnatal ontogeny of *Alligator mississippiensis* (Tables 3-5, 3-7).

5. Both dwarf and large species of *Alligator* exhibit relatively high LR values in the posterior to anterior dorsal vertebrae during the adult stage (Figs. 3-8, 3-9), indicating highly complex neurocentral sutures are a synapomorphy for crocodilians.

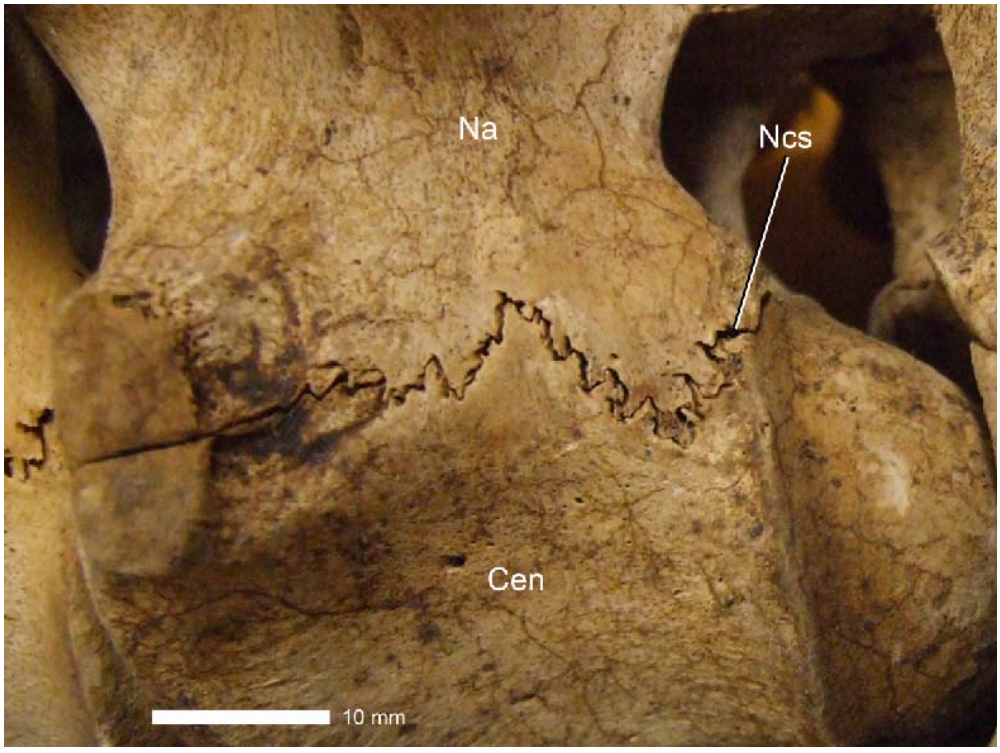

Figure 3-1. Highly interdigitated neurocentral suture in anterior dorsal vertebra of very mature *Alligator mississippiensis* (body length = ca. 4.12 m). Abbreviations: **Cen**, centrum; **Na**, neural arch; **Ncs**, neurocentral suture. Left lateral view.

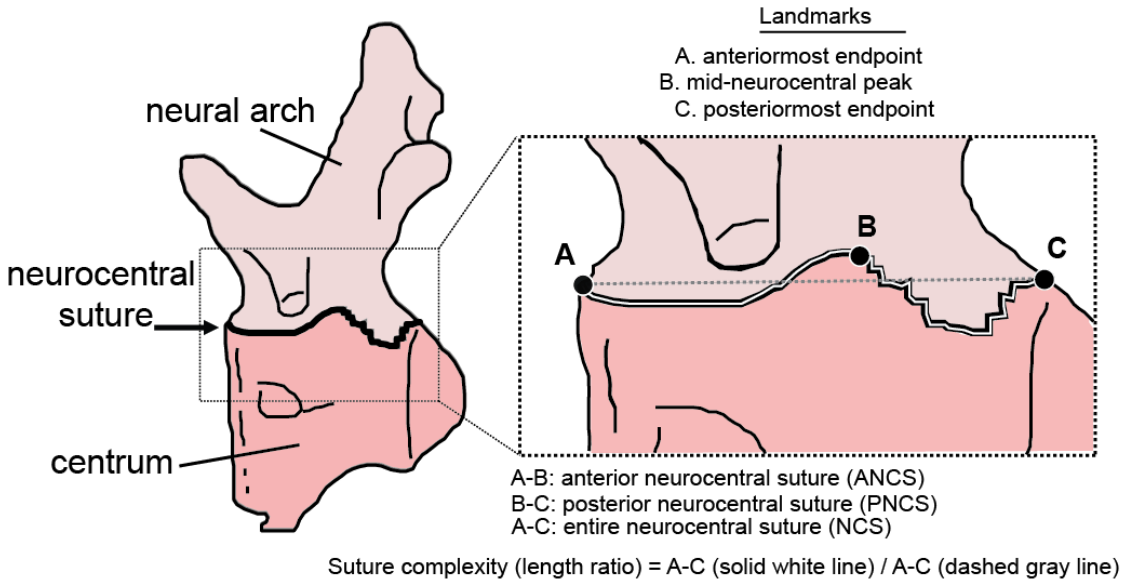

Figure 3-2. Terminology for vertebrae and neurocentral sutures in crocodilians. Length Ratio (LR) is calculated by a ratio of the actual (white solid line)-to-straight (gray dashed) distances of log-transformed measurements between the landmarks A and C (entire neurocentral suture). LR values are also calculated between A and B (anterior neurocentral suture) and B and C (posterior neurocentral suture), separately.

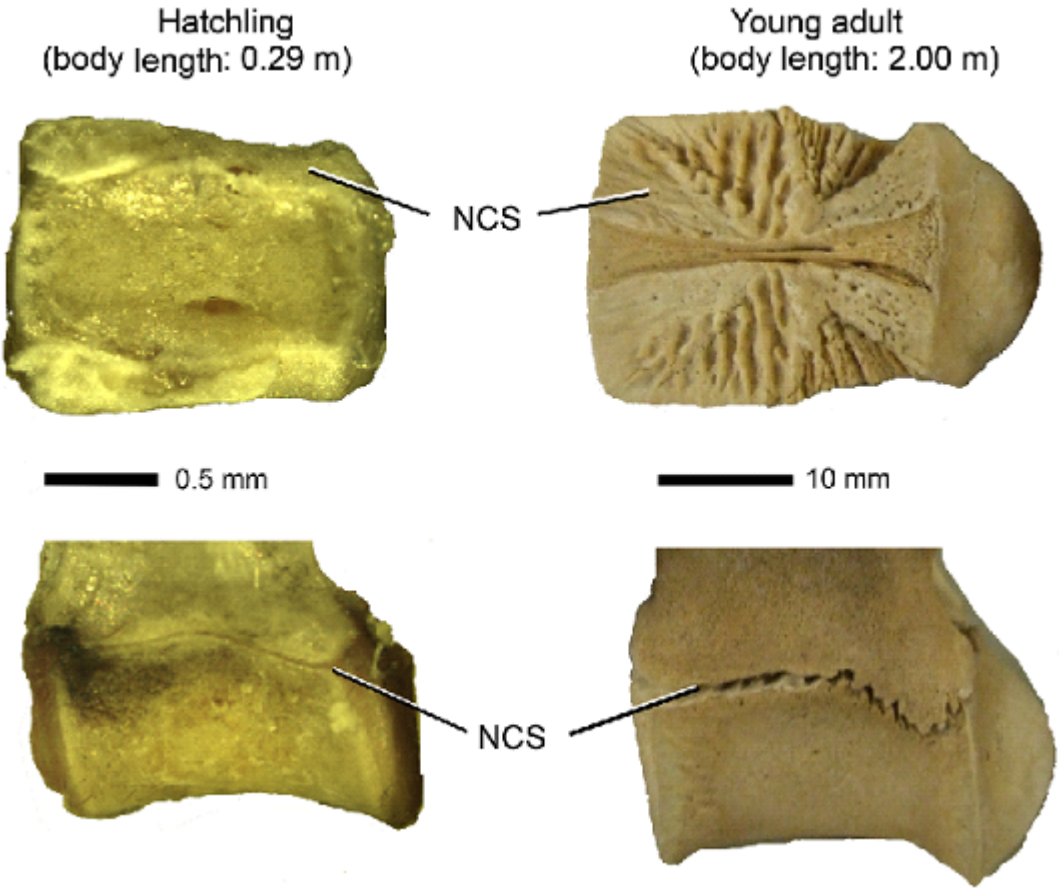

Figure 3-3. Neurocentral sutures (NCS) of mid-dorsal vertebrae in hatchling and young adult *Alligator mississippiensis*. **Top**: Dorsal view of the centrum shows the neurocentral articular surface. **Bottom**: Left lateral view of the vertebrae shows the lateral exposure of the suture between centrum and neural arch. **Left column**, hatchling (body length = 0.29 m); **right column**, young adult (body length = 2.00 m).

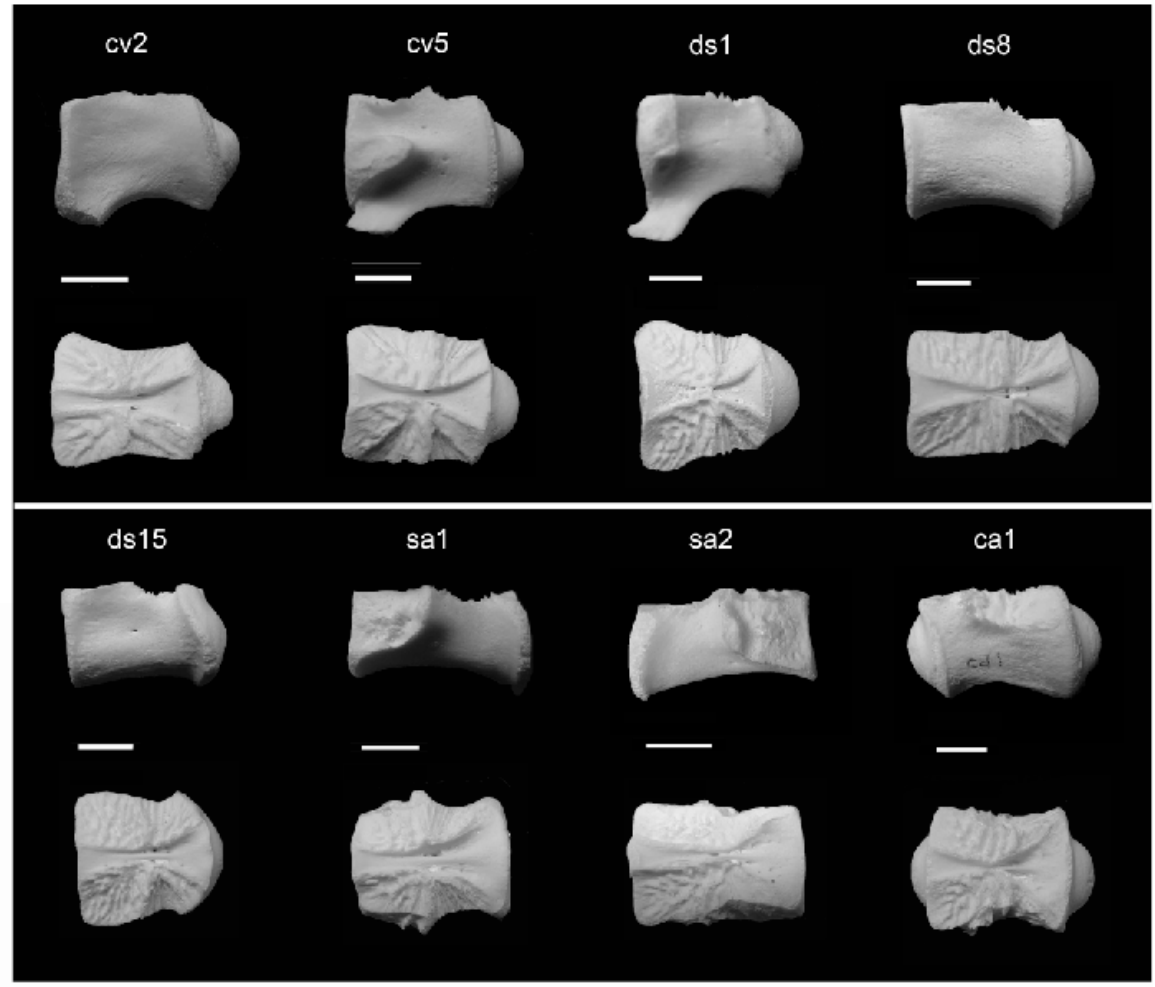

Figure 3-4. Neurocentral sutures and neurocentral articular surfaces of young adult *Alligator mississippiensis* (body length = ca. 1.90 m). Upper row, left lateral view; lower row, dorsal view of centrum. Scale equals 1 cm. Abbreviations: **ca**, caudal; **cv**, cervical; **ds**, dorsal; **sa**, sacral.

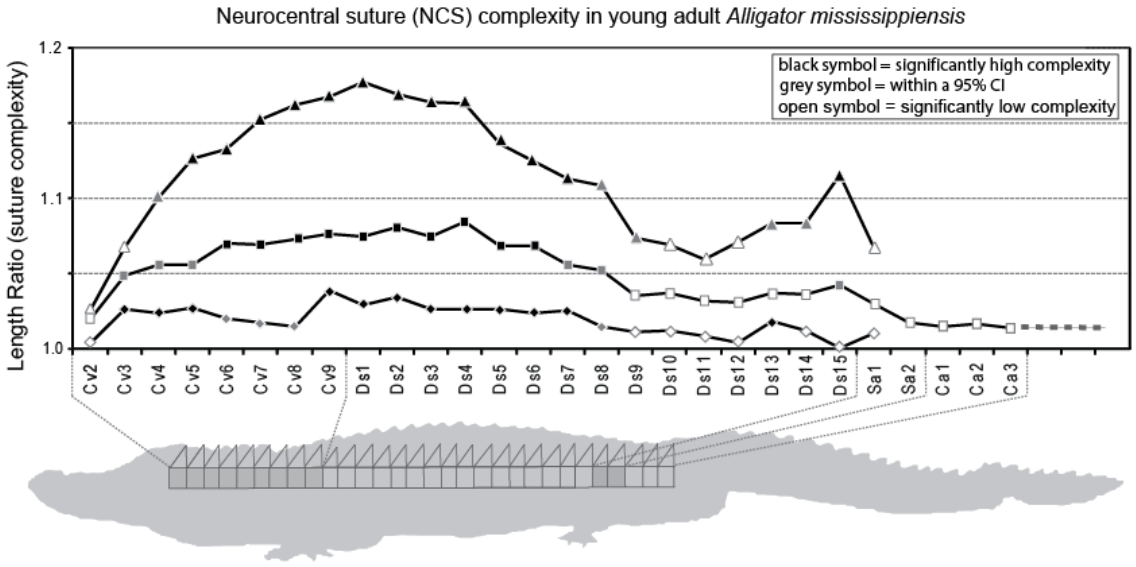

Figure 3-5. Neurocentral suture complexity in the vertebral column of young adult *Alligator mississippiensis* (body length = ca. 1.90 m). Length Ratio values of the entire, anterior, and posterior neurocentral sutures are shown. Open symbols indicate relatively low (< lower limit of a 95% CI) or high (> upper limit of a 95% CI) Length Ratio values; filled symbols represent values that fit within a 95% CI. Abbreviation for vertebrae: **Ca**, caudal vertebra; **Cv**, cervical vertebra; **Ds**, dorsal vertebra.

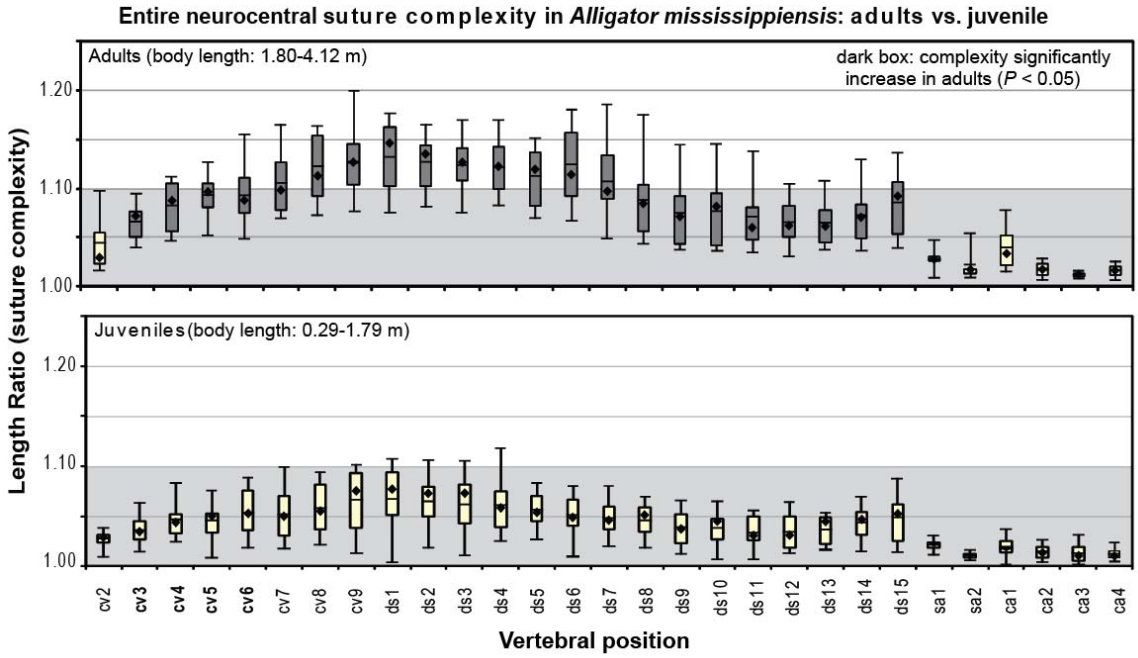

Figure 3-6. Ontogenetic variation in entire neurocentral suture complexity in *Alligator mississippiensis*. Box plots show a statistic summary of the Length Ratio values, including the means, medians, and variances, in: **juveniles** smaller than 1.8 m in body length (sexual maturity) and **adults** larger than 1.8 m in body length. The dark gray boxes indicate that suture complexity significantly increases in the adult stage ($P < 0.05$; *t*-test).

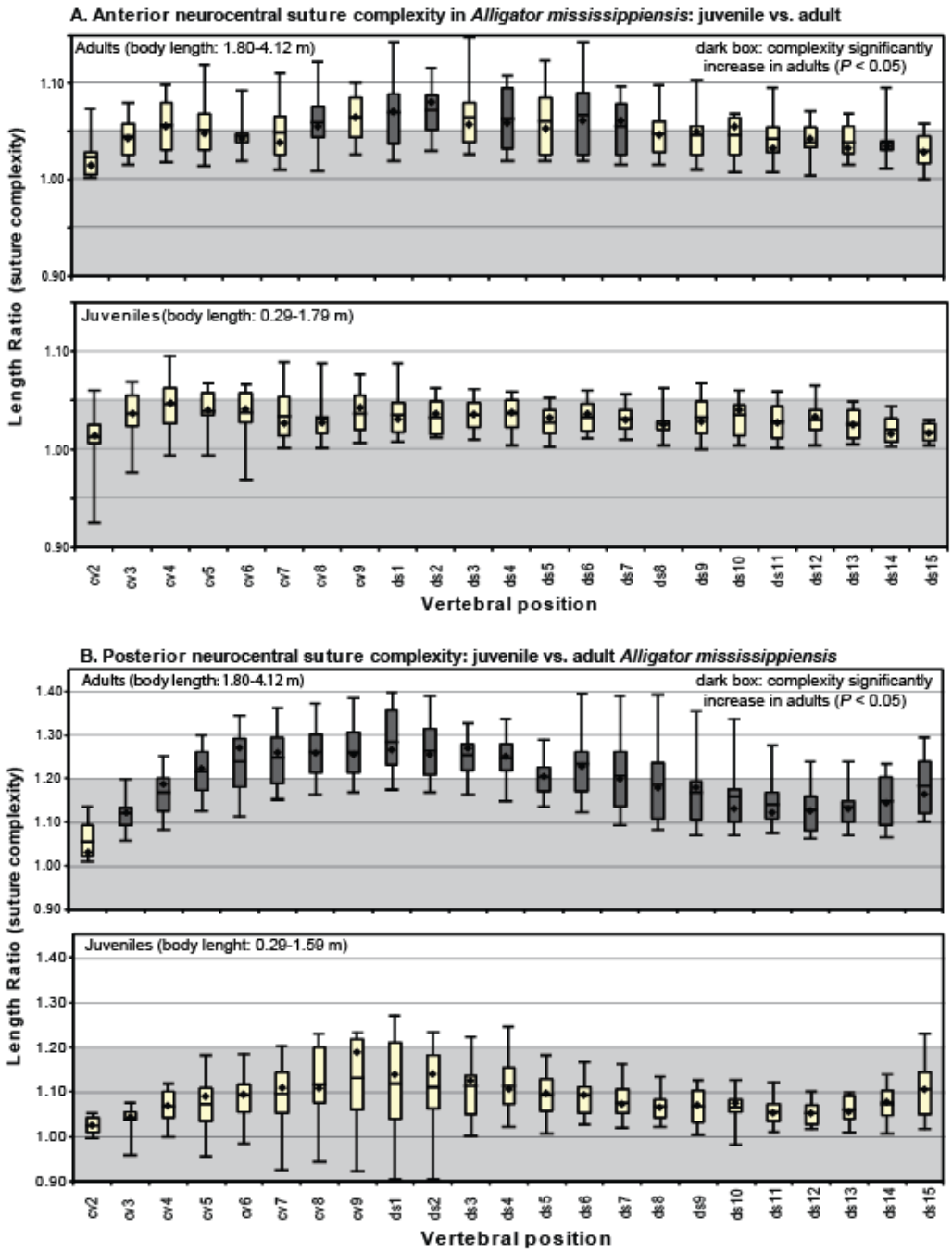

Figure 3-7. Ontogenetic variation in anterior and posterior neurocentral suture complexity in *Alligator mississippiensis*. Box plots show a statistic summary of the Length Ratio values, including the mean, median, and variances, in **juveniles** representing individual smaller than 1.80 m in body length (= sexual maturity) and **adults** larger than 1.80 m in body length. The dark gray boxes indicate that suture complexity significantly increases in the adult stage ($P < 0.05$; *t*-test).

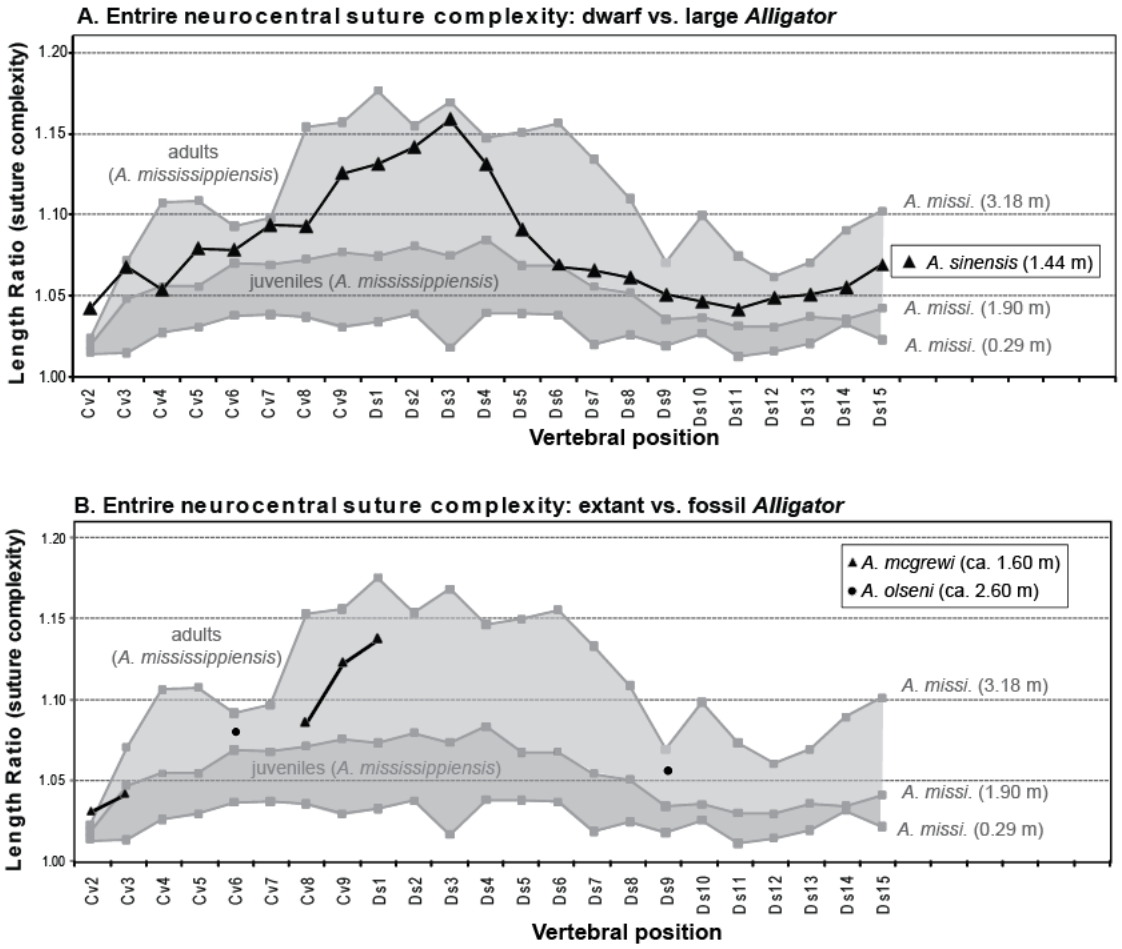

Figure 3-8. Interspecific variation of neurocentral suture complexity in dwarf and large species of *Alligator*. The Length Ratio values of the entire neurocentral suture of the hatchling (body length = 0.29 m), young adult (1.90 m), and very large adult (3.18 m) are shown. **A**, fully-grown individual of extant dwarf *Alligator sinensis* (1.44 m) and **B**, Miocene *Alligator olseni* (ca. 2.60 m) and *Alligator mcgrewi* (ca. 1.60 m) are superimposed.

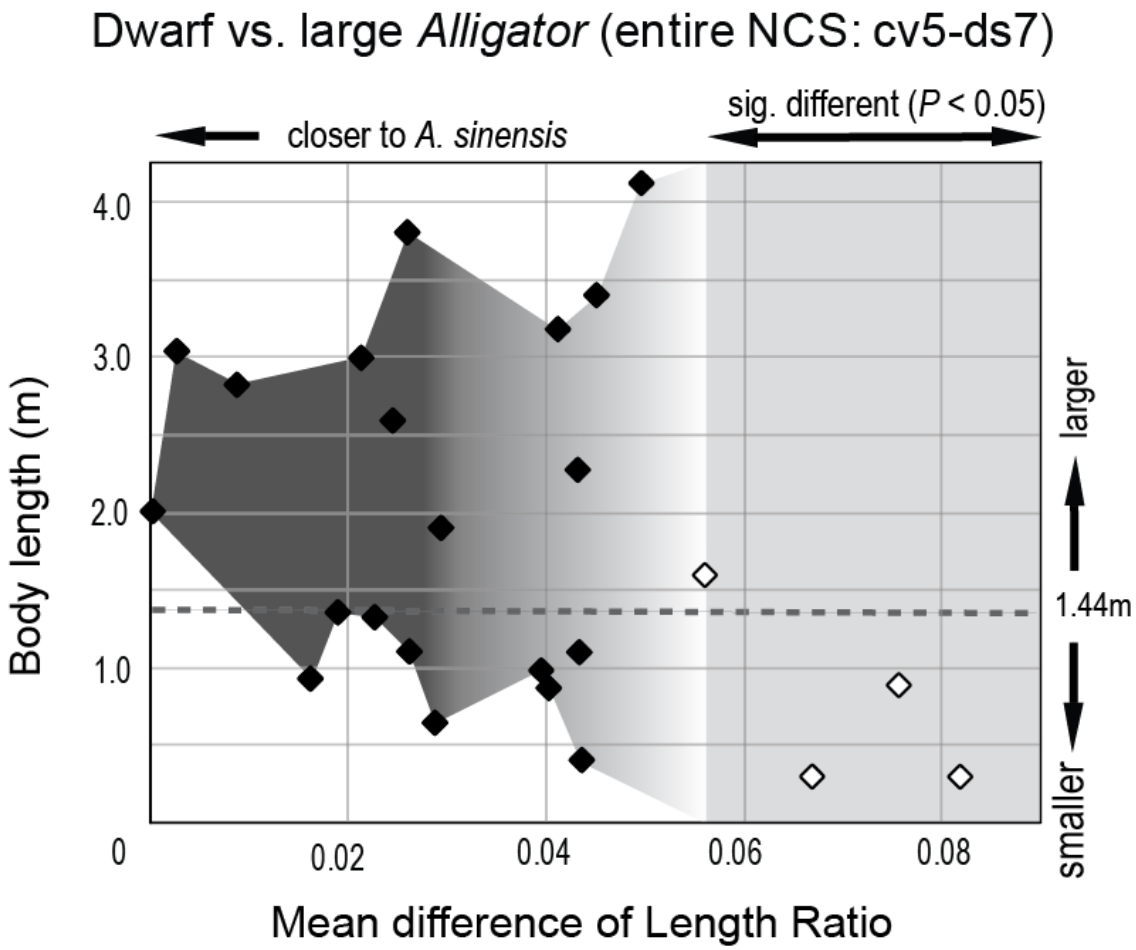

Figure 3-9. Neurocentral suture complexity in dwarf vs. large species of *Alligator***.** A fully-grown dwarf individual (*Alligator sinensis*; body length = 1.44 m) is compared with various size of individuals of *Alligator mississippiensis* (body length = 0.29–4.12 m, shown in the Y-axis). The Length Ratio values of cervical 5–dorsal 7 are selected (highly complex neurocentral sutures in adults; see Figure 3-5). The X-axis shows mean differences from the dwarf species to each individual of the large species (towards left, the length ratios are closer). Four individuals (with open symbol in the right gray zone) have significantly different Length Ratio values (One-way ANOVA, Dunnett's T3 test; $P < 0.05$).

TABLE 3-*1. Skeletons of Alligator examined for this study. The anteriormost vertebrae with completely fused neurocentral junctions (NCS) are recorded.*

Specimen	Femur length (mm)	Estimated body length (m)	Anteriormost vertebra w/ fused NCS	Skeleton status
Alligator mississippiensis				
UMMZ 6A*	18.3	0.28	Ca8	com, art,
UMMZ 238961	18.9	0.29	Ca9	com, art
UMMZ no #*	26.5	0.40	Ca6	inc, art
UF 39620	43.1	0.64	Ca6	com, dis
UF 109039	58.6	0.86	Ca4	com, dis
UF 115605	62.4	0.918	Ca6	com, dis
UMMZ 238965	62.8	0.924	Ca4	com, dis
UF 40535	66.5	0.978	Ca4	com, dis
UMMZ 238959	74.6	1.09	Ca5	com, art
UF 38972	74.9	1.01	Ca5	com, dis
UF 39621	90.2	1.32	Ca4	com, dis
UF 39623	92.4	1.35	Ca2	com, dis
Ike_R006**	130.1	1.90	Ca3	com; dis
UMMZ 239623	133.8	1.95	Ca4	com, art
UF 35153	137.5	2.00	Ca4	com, dis
AMNH 43316	156.0	2.27	Ca2	com, art
UF 39106	178.0	2.59	Ca1	com, dis
AMNH R71621	194.0	2.82	Sa2	com, art
AMNH R31563	208.0	3.02	Ds15	com, art
UF 42548	218.8	3.18	Sa1	com, dis
UF 98341	208.0	3.02	Sa2	com, dis
UF109411	234.0	3.40	Ds2	com, dis
UF 39618	262.0	3.80	Ds13	com, dis
UF 134586	284.0	4.12	Ds3	com, dis
Alligator sinensis				
AMNH 7303	130.0	1.896	Ds15	com, art
Alligator olseni				
UF 59100	?	2.59	?	inc, aso
Alligator mcgrewi				
AMNH 7303	?	1.60	?	inc, art

*Uncatalogued UMMZ teaching collections.

** Personal collection.

Abbreviations for skeletal status in (1) completeness: **com**, nearly complete; **inc**, largely incomplete; **(2) in articulation**: **art**, articulated; **aso**, associated; **dis**, disarticulated.

TABLE 3-2. Terminology for neurocentral sutures in crocodilians. Some terms are illustrated in Figure 3-1.

Terms	Abbreviation	Category	Remarks
Anterior neurocentral end	ANCE	Sutural landmark	Anteriormost point along suture
Mid-neurocentral peak	MNCP	Sutural landmark	Dorsally convex point on suture
Posterior neurocentral end	PNCE	Sutural landmark	Posteriormost point along suture
Neurocentral suture (or junction)	NCS (NCJ)	Sutural topology	One dimensional sutural boundary between centrum and neural arch
Anterior neurocentral suture	ANCS	Sutural topology	Between ANCE and MNCP
Posterior neurocentral suture	PNCS	Sutural topology	Between MNCP and PNCE
Neural arch	NA	Vertebral part	Spinous upper part of vertebra
Centrum	CEN	Vertebral part	aka. vertebral body

TABLE 3-3. Key morphological features of vertebrae and neurocentral sutures (NCS) in adult Alligator.

Vertebral region	Vertebral position	Keys
Atlas-Axis	Cv 1–2 (Psa 1–2)	Very small circular NCJ; very smooth surface (atlas); straighter; no interdigitation; elongate NCJ (axis)
Anterior cervical	Cv 3–5 (Psa 3–5)	ANC weakly curved; straight NCS; ANC≈PNC; low MNCP; low ridged NCJ; narrow NCJ
Mid-cervical	Cv 6–8 (Psa 6–8)	Low but pointed MNCP; weakly curved PNCS; ANCS≈PNC in length; down-sloped PNC
Cervico-dorsal transition	Cv 9, Ds 1–2 (Psa 9–11)	Tall MNCP; short NCS; ANCS > PNCS (ca. 150–160%); highly interdigitated, curved PNCS; square-shaped NCJ (short ANCS)
Anterior dorsal	Ds 3–6 (Psa 12–15)	Elongate, straight ANCS (> more anterior dorsals); interdigitated PNCS; tall MNCP
Mid-dorsal	Ds 7–10 (Psa 16–19)	Oval-shaped NCJ; very elongate ENCS; ANCS > PNCS (ca. 120–150%); gently curved PNCS; overall smoother articulation in ENC; low but large MNCP
Posterior dorsal	Ds 11–15 (Psa 20–24)	Short NCS; ANCS = PNCS in length (dorsal 11–13); ANCS > PNCS (dorsal 14–15): highly interdigitated PNC (in dorsal 15), transversely broaden NCJ
Sacral	Sa 1–2	Low MNCP present in sacral 1, but absent in sacral 2; weakly ridged NCJ (sacral 1) or lacking transverse ridges (sacral 2) ; transversely narrowed NCJ; posterior end of NCJ, pinched out
Anterior caudal	Ca 1–10	Overall similar to sacral 2; no MNCP; no transverse ridges in NCJ; transversely narrow; posterior end of NCJ, pinched out
Mid-caudal	Ca 11–20	NA (fused before hatching)
Posterior caudal	Ca 21–	NA (fused before hatching or NCS never formed)

Abbreviations for vertebrae: **Ca**, caudal; **Cv**, cervical; **Ds**, dorsal; **Psa**, presacral; **Sa**, sacral. Other anatomical abbreviations are listed in Table 3-2.

TABLE 3-4. Summary of Length Ratio values of neurocentral sutures (NCS) in young adult Alligator mississippiensis (body length = 1.90 m). Data plots are shown in Figure 3-5. The normality test (Shapiro-Wilk: P > 0.05) indicates normal distributions of Length Ratio values in the three suture dimensions. Abbreviations for vertebrae are listed in Figure 3-5.

	Entire NCS	**Entire NCS**	**Anterior NCS**	**Posterior NCS**
Vertebrae	Cv2–Ca3	Cv2–Ds15	Cv2–Sa1	Cv2–Sa1
Mean	1.049	1.055	1.019	1.113
SD	0.022	0.019	0.010	0.043
SEM	0.004	0.004	0.002	0.009
95% CI (lower)	1.040	1.047	1.015	1.095
95% CI (upper)	1.058	1.063	1.023	1.131
Shapiro-Wilk (*P*)	0.62	0.104	0.699	0.184

TABLE 3-5. Statistic summary of Length Ratio values of neurocentral sutures (NCS) in 24 individuals of Alligator mississippiensis. Data are sorted separately in the entire, anterior, and posterior neurocentral sutures. Abbreviations for vertebrae are listed in Figure 3-5.

A. Basic statistics of all individuals, juveniles, and adults are listed separately.

Age **NCS** **Vertebrae**	**All** **Entire** **Cv2–Ca4**	**All** **Entire** **Cv2–Ca4**	**Juveniles** **Entire** **Cv2–Ds15**	**Adults** **Entire** **Cv2–Ds15**
N (vertebra)	620	515	297	219
Mean	1.060	1.068	1.050	1.095
Median	1.052	1.060	1.049	1.091
Minimum	1.001	1.004	1.004	1.014
Maximum	1.200	1.200	1.118	1.200
SD	0.041	0.039	0.024	0.040
SE	0.002	0.002	0.001	0.003

Age **NCS** **Vertebrae**	**All** **Anterior** **Cv2–Ds15**	**Juveniles** **Anterior** **Cv2–Ds15**	**Adults** **Anterior** **Cv2–Ds15**	**All** **Posterior** **Cv2–Ds15**	**Juveniles** **Posterior** **Cv2–Ds15**	**Adults** **Posterior** **Cv2–Ds15**
N (vertebra)	523	295	219	523	295	219
Mean	1.040	1.032	1.052	1.131	1.082	1.199
Median	1.035	1.029	1.048	1.111	1.075	1.189
Minimum	0.925	0.925	1.001	0.904	0.904	1.011
Maximum	1.148	1.095	1.148	1.398	1.272	1.398
SD	0.027	0.021	0.030	0.095	0.066	0.088
SE	0.001	0.001	0.002	0.004	0.004	0.006

(Table 3-5: cont.)

B. Comparisons of means of Length Ratio values between juveniles and adults in cervical 2–caudal 3. Bold numbers indicate Length Ratio values significantly increase from the juvenile to adult stages, based on Individual Sample *t*-test and Mann Whitney *U*-test ($P < 0.05$).

	Entire NCS		**Anterior NCS**		**Posterior NCS**	
Vertebra	***T*-test**	***U*-test**	***T*-test**	***U*-test**	***T*-test**	***U*-test**
Cv2	0.1573	0.5767	0.3625	0.6641	0.0771	0.1724
Cv3	**0.0003**	**0.0007**	0.4163	0.5429	**0.0001**	**0.0001**
Cv4	**0.0018**	**0.0016**	0.4506	0.5430	**0.0001**	**0.0004**
Cv5	**0.0001**	**0.0002**	0.2604	0.4341	**0.0001**	**0.0001**
Cv6	**0.0022**	**0.0050**	0.4262	0.7065	**0.0001**	**0.0004**
Cv7	**0.0002**	**0.0011**	0.2289	0.2350	**0.0001**	**0.0004**
Cv8	**0.0001**	**0.0005**	**0.0317**	**0.0257**	**0.0003**	**0.0009**
Cv9	**0.0003**	**0.0008**	0.0507	**0.0407**	**0.0024**	**0.0043**
Ds1	**0.0002**	**0.0009**	**0.0143**	**0.0298**	**0.0006**	**0.0019**
Ds2	**0.0001**	**0.0003**	**0.0048**	**0.0110**	**0.0004**	**0.0008**
Ds3	**0.0002**	**0.0012**	0.0209	**0.0300**	**0.0000**	**0.0004**
Ds4	**0.0001**	**0.0009**	**0.0833**	0.1475	**0.0002**	**0.0011**
Ds5	**0.0013**	**0.0014**	0.0520	0.0505	**0.0001**	**0.0004**
Ds6	**0.0026**	**0.0005**	**0.0474**	**0.0300**	**0.0001**	**0.0003**
Ds7	**0.0037**	**0.0014**	**0.0400**	0.0570	**0.0034**	**0.0007**
Ds8	**0.0029**	**0.0056**	0.0911	0.1018	**0.0059**	**0.0007**
Ds9	**0.0049**	**0.0101**	0.1998	0.2705	**0.0012**	**0.0024**
Ds10	**0.0028**	**0.0123**	0.3037	0.1511	**0.0115**	**0.0068**
Ds11	**0.0027**	**0.0045**	0.1559	0.2167	**0.0004**	**0.0007**
Ds12	**0.0034**	**0.0083**	0.3521	0.2705	**0.0041**	**0.0012**
Ds13	**0.0028**	**0.0123**	0.1139	0.1330	**0.0003**	**0.0015**
Ds14	**0.0287**	**0.0333**	**0.0450**	0.0634	**0.0106**	**0.0333**
Ds15	**0.0181**	**0.0357**	0.0718	0.1604	**0.0386**	0.0634
Sa1	0.6691	0.2733	0.8504	0.6056	0.2876	0.1416
Sa2	0.1876	0.0679	Na	Na	Na	Na
Ca1	0.2299	0.1410	Na	Na	Na	Na
Ca2	0.6266	0.7728	Na	Na	Na	Na
Ca3	0.8119	1.000	Na	Na	Na	Na

TABLE 3-6. Comparisons of entire neurocentral suture complexity in presacral vertebrae of Alligator sinensis with Alligator mississippiensis. Based on the fully-grown individual of A. sinensis (mean of Length Ratio values = 1.0797; body length = 1.44 m), various sizes of A. mississippiensis are. Means of Length Ratio values are analyzed by one-way ANOVA (Dunnett's T3 test). Significantly different degree of neurocentral suture complexity is determined between the two species (P < 0.05) under Remarks.

Body size (m)	Mean Difference	Std. Error	*P*	Remarks
0.291	0.060	0.008	0.001	Different
0.292	0.052	0.008	0.001	Different
0.399	0.028	0.008	0.282	Not different
0.639	0.025	0.009	0.743	Not different
0.863	0.032	0.008	0.104	Not different
0.882	0.058	0.008	0.001	Different
0.924	0.011	0.009	1.000	Not different
0.977	0.025	0.008	0.548	Not different
1.094	0.028	0.008	0.246	Not different
1.099	0.017	0.009	0.999	Not different
1.320	0.016	0.009	1.000	Not different
1.352	0.008	0.008	1.000	Not different
1.592	0.043	0.008	0.002	Different
1.896	0.023	0.008	0.783	Not different
2.003	0.006	0.010	1.000	Not different
2.271	-0.040	0.011	0.173	Not different
2.589	-0.018	0.011	1.000	Not different
2.820	-0.013	0.010	1.000	Not different
2.993	0.017	0.009	0.999	Not different
3.037	-0.005	0.010	1.000	Not different
3.178	-0.032	0.011	0.718	Not different
3.398	-0.055	0.013	0.078	Not different
3.802	-0.044	0.010	0.024	Different
4.120	-0.051	0.013	0.152	Not different

TABLE 3-7. Correlation between suture complexity and body size during postnatal ontogeny of *Alligator mississippiensis*. Body size (log-transferred) and Length Ratio values in the posterior neurocentral sutures are analyzed by the Person's correlation test ($P < 0.05$). *Abbreviations for vertebrae are listed in Figure 3-5.*

vertebra	r	*P*	N
cv2	0.50	0.02	23
cv3	0.73	0.01	24
cv4	0.76	0.01	24
cv5	0.81	0.01	24
cv6	0.79	0.01	24
cv7	0.78	0.01	24
cv8	0.76	0.01	24
cv9	0.76	0.01	23
ds1	0.74	0.01	24
ds2	0.73	0.01	24
ds3	0.73	0.01	23
ds4	0.70	0.01	21
ds5	0.73	0.01	21
ds6	0.69	0.01	22
ds7	0.67	0.01	22
ds8	0.66	0.01	22
ds9	0.59	0.01	22
ds10	0.64	0.01	22
ds11	0.63	0.01	22
ds12	0.60	0.01	22
ds13	0.58	0.01	22
ds14	0.57	0.01	18
ds15	0.60	0.01	18

LITERATURE CITED

Abramoff MD, Magelhaes PJ, Ram SJ. 2004. Image processing with ImageJ. Biophotonics Int 11:36–42.

Anton SC, Jaslow CR, Swartz SM. 1992. Sutural complexity in artificially deformed human (*Homo sapiens*) crania. J Morphol 214:321-332.

Brochu CA. 1996. Closure of neurocentral sutures during crocodilian ontogeny: implications for maturity assessment in fossil archosaurs. J Vert Paleontol 16:49–62.

Brochu CA. 1999. Phylogeny, systematics, and historical biogeography of Alligatoroidea. Soc Vert Paleontol Supp Mem 6:9–100.

Brochu CA. 2001. Congruence between physiology, phylogenetics and the fossil record on phylogenetics and the fossil record on crocodilian historical biogeography. In: Griggs GC, Seebacher F, Franklin C, editors. Crocodilian Biology and Evolution. Sydney: Surrey Beatty & Sons. p 9–28.

Byron CD. 2006. Role of the osteoclast in cranial suture waveform patterning. Anat Rec 288:552-563.

Chiasson RB. 1969. Laboratory Anatomy of the *Alligator*. Dubuque, Iowa: WM. C. Brown Company Publishers. Pp 56.

Cohen MM. 2000. Sutural biology. In Cohen M, MacLean RE, editors. Craniosynostosis: Diagnosis, Evaluation, and Management 2nd edition. New York: Oxford University Press. p 11–23.

Cong L, Hou L, Wu X, Hou J. 1998. The gross anatomy of *Alligator sinensis* Fauvel. Beijing: Science Press. Pp 388.

Farlow A, Hurlburt GR, Elsey RM, Britton ARC, Langston Jr W. 2005. Femoral dimensions and body size of *Alligator mississippiensis*: estimating the size of extinct mesoeucrocodylians. J Vert Paleontol 25:354–369.

Gingerich PJ. 2000. Arithmetic or geometric normality of biological variation:and emprical test of theory. J Theor Biol 204:201–221.

Herbert JD, Coulson TD, Coluson RA. 2002. Growth rates of Chinese and American alligators. Comp Biochem Physiol 131:909–916.

Herring SE. 2008. Mechanical Influences on Suture Development and Patency. In: Rice DR, editor. Craniofacial Sutures. Development, Disease and Treatment (Frontiers of Oral Biology Vol. 12). Bassel: Karger: p 41–56.

Hoffstetter R, Gasc JP. 1969. Vertebrae and ribs of modern reptiles. In Gans C. editor. Biology of the Reptilia, v. 1: Morphology A. New York: Academic Press. p 201–310.

Hulbert Jr RC. 2001. The Fossil Vertebrates of Florida. Gainesville: University Press of Florida. Pp 350.

Jaslow CR. 1989. Sexual dimorphism of cranial suture complexity in wild sheep (*Ovis orientalis*). Zool J Linn Soc 95:273-284.

Lutz TM, Boyajian GE. 1995. Fractal geometry of ammonoid sutures. Paleobiology 21:329–342

Mandelbrot BB. 1967. How long is the coast of Britain? Statistical self-similarity and fractional dimension. Science 156:636–638.

Mandelbrot, BB.1977. The fractal geometry of nature. New York: W.H. Freeman and Company. Pp 468.
Meylan PA, Auffenberg WA, Hulbert RC. 2001. Reptilia 2: Lizards, Snakes, and Crocodilians. In: Hulbert RC, editor. The Fossil Vertebrates of Florida. Gainesville: University of Florida Press. p 137–151.
Mook CC. 1921. Notes on the postcranial skeleton in the Crocodilia. Bull Am Mus Nat Hist 44:67–100.
Motulsky H. 1996. Intuitive Biostatistics. New York: Oxford University Press. Pp 386.
Nicolay CW, Vaders MJ. 2006. Cranial suture complexity in White-Tailed Deer (*Odocoileus virginianus*). J Morphol 267:841–849.
Organ CL. 2006. Thoracic epaxial muscles in living archosaurs and ornithopod dinosaurs. Anat Rec 288:782-793.
Pérez-Claros JA, Palmqvist P, Olóriz F. 2002. First and second orders of suture complexity in ammonites: a new methodological approach using fractal analysis. Math Geol 34:323–343.
Rasband W. 2003. ImageJ version 1.31. National Institutes of Health. Bethesda, Maryland, USA.
Romer AS. 1956. Osteology of the Reptiles. Chicago: University of Chicago Press. Pp 772.
Salisbury SW, Frey E. 2000. A biomechanical transformation model for the evolution of semi-spherodial articulations between adjoining vertebral bodies in crocodilians. In: Grigg GC, Seebacher F, Franklin CE, editors. Crocodilian Biology and Evolution. Sydney: Surrey Beatty & Sons. p 85–134.
Schmidt KP.1941. A new fossil alligator from Nebraska. Geol Ser Field Mus Nat Hist 8:27–32.
Simpson GG. 1941. Large Pleistocene felines of North America. Am Mus Novit 1136:1–27.
SPSS 17.0 for Windows. Statistical Package for Social Science (SPSS). Release Version 17.0.1. 2008. Chicago: SPSS Incorporation.
Wilkinson PM, Rhodes WE. 1997. Growth rates of American alligators in coastal South Carolina. J Wildlife Manage 61:397–402.
Woodward AR, White JH, Linda SB. 1995. Maximum size of the alligator (*Alligator mississippiensis*). J Herpetol 29:507–513.
Wu X, Wang Y, Zhou K, Zhu W, Nie J Wang C. 2003. Complete mitochondrial DNA sequence of Chinese alligator, *Alligator sinensis*, and phylogeny of crocodiles. Chinese Sci Bull 48:2050–2054.

Chapter 4

Allometric Change in Vertebrae during Postnatal Ontogeny of *Alligator mississippiensis* (Archosauria, Crocodylia)

ABSTRACT

Allometric changes in 10 selected vertebrae from axis–caudal 2 were examined during postnatal ontogeny of *Alligator mississippiensis* (Archosauria, Crocodylia). Allometric coefficients were calculated in 12 measurements of the centrum, neural spine, transverse process, zygapophysis, and neural canal, relative to femoral length. In the 10 vertebrae, most measurements show strong positive allometry (especially, the length of centrum, the height of neural spine, and the length of transverse process), but the diameter of neural canal has negative allometry during postnatal ontogeny. Allometric coefficients were also compared separately between before and after four ontogenetic events: (1) complete vertebral ossification; (2) sexual maturity; (3) the stoppage of growth; and (4) neurocentral fusion. The degrees of allometric change in vertebral structure shift during the life span. In the relatively early ontogenetic period (before complete vertebral ossification), the strongest positive allometry occurs, but most vertebral measurements exhibit negative allometric change in the relatively late ontogenetic period (after the stoppage of growth). After neurocentral fusion, neural canals and zygapophyses tend to retain about the same size, but the

posterior ball of the centrum, the transverse process, and the neural spine may keep increasing in size.

INTRODUCTION

Allometric changes in vertebrae during postnatal growth have not been documented well in most vertebrates, but detailed patterns of vertebral allometry may provide important information to understand the meanings of complex vertebral structures and the evolutionary significance of vertebrae in various species. In this study, detailed patterns of allometric changes in vertebrae are documented in the postnatal ontogenetic series of the extant crocodilian, *Alligator mississippiensis* (Archosauria, Crocodylia). Based on quantitative comparisons between hatchlings (body length = ca. 0.28 m) and very mature individuals (body length < ca. 3.8 m) (Fig. 4-1), overall vertebral shape changes drastically during postnatal ontogeny of *Alligator*. Complex overall vertebral shape, which is expressed by various key structures like the centrum, neural spine, transverse process, neural canal, and zygapophyses (Fig. 4-2), tends to be more exaggerative in mature than immature individuals. The relationship of allometric change in those vertebral structures and different positions of the vertebrae are primarily scoped.

To understand relative growth of complex vertebral structures, two approaches of allometry are highlighted in this study. First, the allometric relationship between the life history and relative size of vertebral structures in

Alligator mississippiensis is investigated. The life history of *A. mississippiensis* has been studied well in details (e.g., McIlhenny, 1987). As shown In the growth curve (Fig. 4-3), growth rates change through postnatal ontogeny of *Alligator*: the fastest and slowest rates occur in the earliest and latest ontogenetic periods, respectively, and moderate rates are observed in between. Because the growth curve is based on total axial body length, which is a sum of the lengths of vertebral segments, allometric changes in vertebrae (especially, the length of centrum) may be linked to those of growth rates. To test this hypothesis, the degrees of allometric change are compared in three ontogenetic periods: (1) the "cartilage vertebra" period (the earliest period: before complete vertebral ossification); (2) an "intermediate" period around sexual maturity; and (3) the "slower growth" period (the latest representative: after the stoppage of growth) (Fig. 4-3). If allometric change of vertebrae follows the growth curve, the largest degree of allometric change in vertebrae must occur in the earliest period, and the least degree of change must occur in the latest ontogenetic period.

Second, the allometric relationship between vertebral structure and the developmental origin is explored. A whole piece of vertebra generally forms in three main locations of sclerotome cells during the early developmental stage (Christ et al., 2000). The three main parts, which are expressed as the lower part (centrum), mid-part (zygapophysis-neural pedicle and neural canal), and upper part (neural spine-transverse process) in the later life, may grow independently during postnatal ontogeny. To investigate the allometric relationship of the three vertebral parts, neurocentral fusion is of interest. This fusion between the

centrum and the neural arch, which occurs after the result of ossification of the connective cartilaginous layer, the neurocentral synchondrosis, may characterize an important mechanism for allometric change in the three main vertebral parts. In particular, neurocentral fusion may limit allometric change in the dimensions of centrum and zygapophysis-neural canal, which are placed topologically closer to neurocentral fusion, more so than structures associated with the neural spine-transverse process (Fig. 4-2). To test this hypothesis for the developmental origin of the vertebral structure, the degrees of shift in allometric change are compared in before and after neurocentral fusion. In addition, among vertebrates, crocodilians have drastically late neurocentral fusion in the presacral vertebrae during postnatal ontogeny (Hoffstetter and Gasc, 1969; Brochu, 1996; Chapter 2), and thus *Alligator* may provide some important information about the significance of neurocentral fusion in vertebral growth.

MATERIAL AND METHODS

Samples

Specimens. Thirty-one dry skeletons of *Alligator mississippiensis* were examined (Table 4-1). The skeletons are either articulated or disarticulated. Some are incomplete, but only specimens exhibiting all presacral–anterior caudal vertebrae and a femur were selected. The 31 specimens include hatchlings to fully-grown individuals (body length = 0.28–4.12 m). Body size was estimated by the greatest length of femur using the equation of Farlow et al. (2005) when

actual measurement was not recorded. Sex is unknown in most specimens, but individuals of *Alligator* longer than 2.9 m in body length are typically male (Wilkinson and Rhodes, 1997).

Total body length was used to determine whether each specimen had passed each of the four ontogenetic events (Fig. 4-3). Histology shows that endochondral ossification of centra and neural arches is nearly complete in posterior dorsal and anterior caudal vertebrae when specimens of *Alligator* reach 0.9 m (Chapter 2). Sexual maturity occurs when both males and females reach at 1.80 m in *Alligator mississippiensis* (based on the average from 140 individuals; Wilkinson and Rhodes, 1997). Based on the growth curve of postnatal ontogeny in *A. mississippiensis* (Wilkinson and Rhodes, 1997), body size usually stops increasing after reaching at approximately 2.80 m in females and 3.3 m in males. The sizes of these three events are primarily used as references to separate into the three relative ontogenetic periods (early, intermediate, and late), even exact timing of the occurrences of the three ontogenetic events must slightly varies among individuals.

The fourth ontogenetic event, neurocentral fusion, does not occur simultaneously throughout the vertebral column. Instead, there is a sequence of neurocentral fusion during ontogeny (Brochu, 1996) (Chapter 2). Generally, neurocentral fusion starts to appear from the posterior caudal to the mid-caudal vertebrae before sexual maturity (Fig. 4-3), but the anterior caudal-to-sacral vertebrae usually fuse after reaching 2.4 m in body length. The presacral vertebrae often retain unfused neurocentral sutures throughout ontogeny. Thus,

the status of neurocentral fusion was used to separate vertebrae, instead of individuals, into unfused and fused groups. The fused status includes the presence of partial bony bridges between the centrum and neural arch (i.e., the beginning of neurocentral fusion), and the unfused status refers to only completely open neurocentral sutures in this study.

Vertebrae. Among 24 presacral, two sacral, and 20–30 caudal vertebrae of *Alligator* (Chiasson, 1969; Hoffstetter and Gasc, 1969), ten vertebrae were selected for measurements. Those vertebrae include the axis (cervical 2), cervical 3, cervical 8, dorsal 1, dorsal 4, dorsal 10, dorsal 15, sacral 1, caudal 1, and caudal 2. Those vertebrae represent nine major vertebral regions in crocodilians based on some key morphologies (e.g., overall shape, size; Mook, 1921) (Appendix 4-1) and the topological relationships with other skeletal parts (e.g., ribs, girdle bones) (Table 4-2).

Three main vertebral parts, “centrum”, “neural spine–transverse process”, and “zygapophysis-neural canal” (Fig. 4-2) are here suggested to group the overall vertebral structure. The three vertebral parts are primarily defined by their independent sclerotomal origin during the early developmental stage and their expression genes, which were reported by Christ et al. (2000). In the entire vertebral structure, the centrum consists of the main lower vertebral body, which is connected by fibrous cartilage (intervertebral disk) to other centra. The neural arch, placed above the centrum, consists of the two parts. The neural spine-transverse process is generally characterized by rod, process, and/or blade like structures, directed horizontally or vertically relative to the vertebral axis. In

tetrapods, those vertebral structures provide muscle insertion sites, and transverse processes of dorsal vertebrae are attached to elongate dorsal ribs. The zygapophysis-neural canal mainly consists of the surroundings of the base of the neural arch, located just above the neurocentral junctions. The neural canals primarily enclose the spinal cord, spinal nerve roots, and blood vessels (Smith, 1960). The prezygapophyses and postzygapophyses form direct articulations between vertebrae, connected by fibrous cartilage (Gál, 1993). These parts also serve as attachment sites of some epaxial muscles in crocodilians and other reptiles (Organ, 2006). The internal structure of a vertebra differs between the centrum or the base of the neural arch (i.e., zygapophysis, near the neural canal) and the neural spine-transverse process. The former mainly consists of trabecular structure, whereas transverse processes and neural spines mainly have dense compact bone (Chapter 2) in the adult stage.

Four measurements were chosen for each vertebral part (a total of 12 measurements; Fig. 4-4; Table 4-3). The 12 measurements represent overall proportion of vertebra by lengths and width or breadth, of each vertebral part. Because overall vertebral shape is considerably variable in the vertebral column of crocodilians, some measurements in specific vertebrae cannot be recorded. Those include the length and breadth of the transverse processes in cervicals 2 and 3, the breadth of the transverse processes in sacral vertebrae, and the total length (with a posterior ball) of sacral centra (see Descriptive Morphology below).

Allometric Coefficients

Calculation. Allometric coefficients of the 12 vertebral measurements were calculated by the following way: (1) measurements of the 12 vertebral dimensions and the greatest length of femora were taken in mm to the 1st decimal place; (2) all measured values were log-transformed; and (3) all data were plotted on log-log diagrams. The femoral length is used as a scale (i.e., plotted on the X-axis) in this study because this dimension exhibits a linear relation with overall body length in crocodilians and other archosaurs (Houck et al., 1990; Currie, 2003; Farlow et al., 2005). All vertebral dimensions are plotted on the Y-axis. Using a least-squares method, regression lines are defined as $\mathrm{Log}(y) = b + k\mathrm{Log}(x)$ or $y = bx^k$. Isometric and allometric changes were identified based on a 95% CI of the allometric coefficient (k). When the allometric coefficient is greater than 1.05, positive allometry is determined. When it falls in 0.95–1.05, isometry is identified. Negative allometry is referred to as lower than 0.95. Intercepts (b) and coefficient of determination (r^2) were also recorded for each slope.

The allometric coefficients were first calculated in the 31 individuals, which represent allometric changes during the entire postnatal ontogeny. The allometric coefficients were also calculated separately before and after the four ontogenetic events in each vertebra.

Statistics. Basic statistical tests were conducted with SPSS 17.0 for Windows (SPSS, Inc., Chicago, Illinois). The Shapiro-Wilk test ($p < 0.05$) was used for checking whether or not measurements of vertebrae exhibit a normal

distribution for each vertebra and each vertebral measurement. One-sampled *t*-test ($p < 0.05$) was used for comparisons of the means of all allometric coefficients for each vertebral measurement and for each vertebra. In addition, the differences of the means from the later to earlier ontogenetic periods were calculated.

A compositional data analysis (Aichison, 1990; Aichison and Egozcue, 2005; Pawlowsky-Glahn et al., 2006) was used to examine relationships of allometric change among the three vertebral parts after neurocentral fusion. In the six vertebrae (dorsals 4, 10, 15, sacral 1, caudal 1, and caudal 2), the specimens were grouped into before and after neurocentral fusion. Then, differences of the allometric coefficients from after to before neurocentral fusion were compared. Relative to the total (sum) of the differences (= 100%), a proportion of changes in allometric coefficients was calculated as a percentage for each vertebral part and plotted in a ternary diagram.

RESULTS

General morphological differences in vertebrae between hatchling and fully-grown alligators are described first. This quantitative comparison provides general ideas of main ontogenetic changes in *Alligator* vertebrae. The allometric coefficients from the 12 vertebral dimensions from the 10 vertebrae are first shown in all 31 individuals (representing postnatal ontogeny), and then, before

and after the four key ontogenetic events (vertebral ossification, sexual maturity, stoppage of growth, and neurocentral fusion).

Descriptive Morphology

Key morphological features in major vertebral regions from the atlas-axis to posterior caudal vertebrae are summarized in Table 4-2 (also Appendix 4-1). The main morphological differences include the relative size and shape of centrum (e.g., anteroposteriorly short or elongate, transversely narrow or wide), zygapophysis (e.g., transversely wide or anteroposteriorly long articular surface), neural spine (e.g., rod-like or blade-like, short or tall), and transverse process (e.g., elongate or short) (Fig. 4-2).

Some unique features in specific vertebrae are also worth noting. In the axis and cervical 3, the transverse processes are drastically shorter (or nearly absent) than in more posterior vertebrae. The centra of the two sacral vertebrae have nearly flattened articular surfaces between them and a convex ball-like structure is absent, which differs from the procoelous articulations (i.e., concave front and convex back) in other vertebrae.

Sacral 1 has considerably large prezygapophyses (ca. 145% larger than dorsal 15; 480% larger than sacral 2) in fully-grown alligators. Because the sacral vertebrae have very stout, elongate ribs (= transverse processes) which possess morphologically more complex structure, the anteroposterior breadth at the mid-point of the transverse process is not included in this analysis. Caudal 1 has biconvex articular surfaces of the centrum in most crocodilians (Hoffstetter and

Gasc, 1969), but measurements of both anterior and posterior balls were included for the total length of the centrum in the vertebra.

All vertebrae show some typical features of postnatal ontogenetic changes. Based on quantitative comparisons of anterior dorsal vertebrae (Fig. 4-1), the diameter of the neural canal is proportionally large, relative to overall size of the centrum or overall vertebral height in hatchlings, but relative size of the neural canal is drastically reduced in fully-grown alligators. Hatchlings also exhibit a relatively short neural spine and transverse processes, which contrast with the elongate ones in adults. In hatchlings, the articular surface area of the prezygapophysis is relatively small. Centra of adults have a greatly extended posterior ball, which is contrast to a nearly flattened posterior surface in hatchlings.

Variation in Allometric Changes

The allometric coefficients are sorted by the 10 selected vertebrae and the 12 vertebral dimensions, separately. The two entries are examined in all 31 individuals first, which provide information about general patterns of allometric change during the entire postnatal ontogeny. Then, the allometric coefficients are compared in the four ontogenetic events. Only summarized results of the allometric coefficients are shown below, and more detailed results of the allometric coefficients, intercepts, and coefficient of determinations are listed in Appendices 4-2 to 4-6.

Postnatal ontogeny (body size: 0.28–4.12 m). The 10 vertebrae show that the means of the allometric coefficients from all vertebral dimensions of the 31 individuals are not significantly different (*t*-test: $p > 0.05$) (Table 4-3A). The highest mean of the allometric coefficients is found in dorsal 4 (1.179). Sacral 1 (1.172) also has a relatively high mean of the allometric coefficients (> 95% CI). Other dorsal vertebrae also have relatively high means of the allometric coefficients, except for dorsal 15. Cervical 3 has the lowest degree of allometric change (1.084). Only cervical 3 and the axis exhibit mean values that are below the 95% CI (1.100).

Among the 12 vertebral dimensions, positive allometric change is the most common type of relative growth (Table 4-3B). All dimensions, except for the height and width of the neural canal, show positive allometry ($k > 1.05$). Significantly high positive allometric changes (*t*-test: $p < 0.05$) appear in the lengths (with and without a posterior ball) of centrum, the transverse length of transverse processes, the dorsoventral height of neural spines, and the two measurements of the prezygapophyses. The largest mean of the allometric coefficients (1.353) appears in the dorsoventral height of neural spine. The transverse process also exhibits a high mean value (1.330) in the 10 vertebrae. The strongest positive allometry is found in the transverse length of transverse process in dorsal 10 (slope = 1.527) (Appendix 4-3). In neural spines and transverse processes, the anteroposterior breadths have much lower allometric coefficients than the transverse lengths (mean of all vertebrae = 1.069 and 1.070, respectively). The anteroposterior length of the centrum without a posterior ball

also changes with positive allometry (mean of all vertebrae = 1.091), but the total length of centrum has a much higher allometric coefficient (mean of all vertebrae = 1.1670; Table 4-3B).

Only the height and width of the neural canal have negative allometry (k < 0.95) (Table 4-3B). The height increases slightly more than does the width in neural canal. The allometric coefficients range between 0.745 (dorsal 10) and 0.891 (sacral 1) for the anteroposterior height and between 0.736 (dorsal 15) and 0.921 (caudal 2) for the transverse width (Appendix 4-3).

Isometry (k = 0.95–1.05) is the least common type of relative change in the 12 vertebral dimensions (Table 4-3B), occurring only in the anteroposterior breadth of neural spines in cervical 8–caudal 2 and transverse process in cervical 8 (Appendix 4-3). The length of centrum without a posterior ball also changes with isometry in dorsal 15.

Event 1: vertebral ossification (body size: ca. 0.9 m). Ten skeletons are determined to represent individuals that have not yet undergone vertebral ossification based on total body length (< 0.9 m). The remaining 21 individuals are presumed to have ossified vertebrae (body length $\geq$ 0.91 m) (Fig. 4-3). Among the 12 vertebral dimensions, all allometric coefficients have positive allometry before vertebral ossification (Table 4-4; Appendix 4-3). Relatively high allometric coefficients (> the upper limit of a 95% CI: 1.441) occur in the height of neural spine and the length and width of prezygapophysis. After vertebral ossification, positive allometry is still the most common among the 12 vertebral dimensions. However, isometry is found also in the breadth of neural spine

(mean of allometric coefficients = 0.970), and negative allometry occurs in the dimensions of neural canal (k = 0.653 and 0.668 in the height and width, respectively).

In most vertebral dimensions, allometric coefficients are much higher after vertebral ossification rather than before vertebral ossification. The only exception appears in the transverse length of the transverse process, which increases after vertebral ossification. Among the 12 dimensions, the largest degree of shift after vertebral fusion (= -0.602) occurs in the total height of neural canal (Table 4-5). Based on the mean differences in the allometric coefficients from all dimensions (-0.241), significant ontogenetic changes (t-test: $p < 0.05$) occur in the lengths of centrum and neural spine, the width of prezygapophysis and neural canal. Relatively low degree of the mean difference appears in the height of centrum (-0.054) and the length of transverse process (0.079).

The means of the allometric coefficients decrease after vertebral ossification in all vertebrae. The largest degree of shift occurs in dorsal 4 (-0.370) (Table 4-5). The smallest mean difference is found in dorsal 1. Only cervical 3 shows a significant difference in the means of the allometric coefficients (t-test: $p < 0.05$) among all vertebral dimensions.

Event 2: sexual maturity (body size: ca. 1.8 m). Among the 31 skeletons, 20 specimens are determined to be juveniles and 11 are adults based on body size (Table 4-4; Appendix 4-4). Before sexual maturity, positive allometry appears in all dimensions, except for the width of neural canal (1.031) and the breadth of transverse process (1.043), which exhibit isometric change. Relatively

high means of the allometric coefficients (> the upper limit of a 95% CI: 1.285) occur in the height of neural and the diameter of prezygapophysis. After sexual maturity, negative allometric changes are the most common in the height and width of neural canal (0.524 and 0.647). The breadth of neural spine changes with isometry (0.960).

In the seven vertebrae, the allometric coefficients increase in the anteroposterior length of centrum without a posterior ball, the diameter of centrum, the length and breadth of transverse process, the neural spinal height, and the anteroposterior length of prezygapophysis (all positive values in Table 4-5A; Appendix 4-4). Compared to the total mean differences of the allometric coefficients in all dimensions (-0.006), the allometric coefficients significantly increase in the total length of transverse process (*t*-test: $p < 0.05$). After sexual maturity, the allometric coefficients change with a smaller degree in the total length of centrum, the breadth of neural spine, the transverse width of prezygapophysis, and the dimensions of neural canal (Table 4-5A). Among those dimensions, significant changes (*t*-test: $p < 0.05$) occur in the overall length of centrum and the height and the width of neural canal.

Based on the mean differences in the allometric coefficients, cervical 3–dorsal 4 exhibit increased values (Table 4-5B). Only cervical 3 exhibits a significantly increased allometric coefficient (*t*-test: $p < 0.05$). Negative values of the mean differences indicate decreases in the allometric coefficients, which are found in cervical 2, dorsal 10–caudal 2. Only the two caudal vertebrae exhibit a significant degree of shift (*t*-test: $p < 0.05$) after sexual maturity.

Event 3: stoppage of growth (body size: > ca. 2.8 m). Based on body size, the 25 specimens were determined to be fast-growing (i.e., before the stoppage of growth), and six larger individuals represent taxa that have stopped growing (Fig. 4-3). Before the stoppage of growth, all vertebral measurements, except for the neural canal, exhibit a positive allometric change (Table 4-4; Appendix 4-5). Only the diameter of neural canal exhibits negative allometry (0.922 and 0.910 in the height and width, respectively). After the stoppage of growth, positive allometry is found only in the spinal height (1.148) and the transverse length of the transverse process (1.082). Isometric changes occur in the overall length of centrum and the length and width of prezygapophysis.

Among the ten vertebrae, the allometric coefficients of all vertebral dimensions decrease after the stoppage of growth (Table 4-5A). Significant degrees (*t*-test: $p < 0.05$) of change in the allometric coefficients occur in the height of neural canal (mean differences = -0.414) and the diameter of centrum (mean differences = -0.190 in height and -0.184 in width). A relatively large degree of decrease in the allometric coefficients also occurs in the transverse width of neural canal (mean differences = -0.337) and the breadth of neural spine (mean differences = -0.402).

The ten vertebrae also exhibit negative values of the mean difference of the allometric coefficients (Table 4-5B). A significant change occurs only in caudal 2 (*t*-test: $p < 0.05$). The axis and caudal 1 also have a relatively large degree of shifts (-0.391 and -0.325, respectively).

Event 4: neurocentral fusion (body size: 1.32–3.40 m). All vertebrae of the 31 individuals were separated into two groups, before and after neurocentral fusion, for each vertebra. Among the six selected vertebrae from dorsal 4–caudal 2, the specimens were sub-grouped as the following combinations of individuals: 19 vs.10 (caudal 2), 21 vs. eight (caudal 1), 22 vs. eight (sacral 1), 25 vs. five (dorsal 15), 20-two (dorsal 10 and dorsal 4) in unfused and fused neurocentral fusion, respectively. Because all individuals exhibit completely open neurocentral sutures, cervical 2–dorsal 1 cannot be included here. The anteroposterior sequence of neurocentral fusion generally follows the size rank (i.e., smaller to larger body length) of the 31 specimens, except for a few individuals. The individual with 1.35 m in body length already has fused neurocentral sutures in caudal 2 although some smaller individuals still have open sutures in the vertebra (Fig. 4-3; Table 4-1). Two large individuals (body length = 3.20 m and 4.12 m) exhibit fused centra and neural arches in dorsal 4, but a few other specimens, which are larger than 3.20 m, still have open neurocentral sutures in all dorsal vertebrae.

Positive allometry is the most common pattern in the 12 vertebral measurements of the six vertebrae before neurocentral fusion (Appendix 4-6). Isometry is found in the diameter of centrum in sacral 1, the width of neural canal in caudal 1, the length of centrum without a posterior ball in dorsal 15, and the spinal breadth in dorsal 4. Negative allometry occurs in the height and width of neural canal in dorsal 4, dorsal 10, dorsal 15, and sacral 1, but not in the caudal vertebrae. After neurocentral fusion, negative allometry commonly occurs, except

for a few dimensions. Those include the total length of centrum with a posterior ball in all vertebrae, which have positive allometry in the later ontogenetic period. The height of neural spine and the length of transverse process also exhibit positive allometry in most vertebrae, except for transverse process of dorsals 10 and 15.

Table 4-7 shows a summary for the mean differences of the allometric coefficients of the 12 vertebral dimensions from fused to unfused neurocentral fusion. Overall, the degrees of the allometric coefficients decrease in all vertebral dimensions after neurocentral fusion, except for the total length of the centrum with a posterior ball and the anteroposterior length of the prezygapophysis, which exhibits a relatively large degree of shift (> the upper limit of a 95% CI). A significant degree of decrease (*t*-test; $p < 0.05$) is found only in the height of neural canal. A relatively large degree of decrease occurs in the transverse width of prezygapophysis.

The six vertebrae in caudal 2–dorsal 4 exhibit different patterns of relative change among the 12 dimensions (Table 4-7). Negative values of the mean differences, indicating a decrease in the degree of the allometric coefficients, are common in most vertebral dimensions. However, positive values of the mean differences are found in some dimensions of dorsals 4 and 10, such as the dimensions of the centrum, the neural spines (dorsal 4), the prezygapophyseal length (dorsal 4), and the width of the neural canal (dorsal 10). Sacral 1 also has positive values in the mean differences of the allometric coefficients in the

centrum (length without a posterior ball), the prezygapophysis (length), and the neural canal (width).

Ratios of the mean differences of the allometric coefficients are also compared in the six vertebrae (Fig. 4-6; also “ratio” in Table 4-7). Relative to the total mean differences (= 100%), dorsal 4 and dorsal 10 tend to have about the same proportional change among the three vertebral parts: the centrum, neural spine-neural arch, and zygapophysis-neural canal. Dorsal 4 has the largest proportional change (16.3%) in the spinal height after neurocentral fusion, whereas dorsal 10 has considerably large degrees of the mean differences occurring in the width of the prezygapophysis (21%) and the length of the centrum with a posterior ball (18%). In dorsal 15–caudal 2, large degrees of shifts occur primarily in the zygapophysis-neural canal, but relatively small degrees of changes in the centrum, indicating a continuous increase in relative size after neurocentral fusion. Among all measurements, the largest degree of change is found in the width of prezygapophysis (39%) in sacra 1. Because the allometric coefficient is larger after neurocentral fusion, the prezygapophysis must keep increasing in relative size with a larger degree after neurocentral fusion. Caudal 1 and 2 have relatively high percentages of the mean differences in the dimensions of neural canal, due to decreased allometric coefficients after neurocentral fusion.

DISCUSSION

The degrees of allometric change in overall vertebral structure respect to the life history of *Alligator* is of interest in two aspects. First, the relationship between the growth curve and allometric change in vertebrae is discussed. As the growth rate generally slowdowns throughout ontogeny of *Alligator*, decreased degrees of allometric change in vertebral structure are expected to be found in most measurements and most vertebrae. However, there may be some exceptions (i.e., increases in the degree of allometric change in the later ontogenetic periods), which may also provide important information about vertebral growth. Comparisons of the degrees of allometric change in three relative ontogenetic periods (i.e., the cartilage vertebra, intermediate, and slower growth periods; Fig. 4-3) show how the degrees of allometric change shift during postnatal growth. The three ontogenetic periods are defined by the three key ontogenetic events, complete vertebral ossification, sexual maturity, and the stoppage of growth. Those ontogenetic events may give strong impact on vertebral growth. Second, how the developmental origin of the three vertebral parts (centrum, neural spine-transverse process, and zygapophysis-neural canal) reflects allometric change in vertebral structure is discussed. Comparisons of the allometric coefficients of before and after neurocentral fusion provide some information about the relationships among the three vertebral parts.

Allometric Change in Vertebrae during Life History

Event 1: Vertebral ossification. All 12 measurements exhibit larger degree of allometric change before than after vertebral ossification (Table 4-4). Based on the mean of the 12 measurements, the strongest positive allometry occurs while cartilaginous tissues is turning into bone in vertebrae (k = 1.343; Fig. 4-7). The data suggest vertebral growth reflects the growth curve in the cartilage vertebra period of *Alligator*. In particular, relatively high allometric coefficients appear in the neural spines (dorsoventral height = 1.681) and the prezygapophyses (transverse length = 1.481; anteroposterior width = 1.673; Table 4-4). Relative size of the neural canal, which has the strong negative allometry through postnatal ontogeny (Table 4-3), also increases more rapidly with the positive allometry (height = 1.279; width = 1.091) in the cartilage vertebra period than in the later ontogenetic period (after vertebral ossification).

Event 2: Sexual maturity. Sexual maturity often involves various types of changes in physical features for vertebrates. However, this ontogenetic event seems not to have strong impact on allometric growth of vertebrae (Table 4-4). The mean of the allometric coefficients is much lower in this intermediate ontogenetic period (k = 1.084) than in the cartilage vertebra period (i.e., before vertebral ossification). Among the three key ontogenetic events (Fig. 4-7), the degree of shift of the allometric coefficients after sexual maturity is the weakest (-0.086; Table 4-5). Those relatively consistent slopes in most vertebral dimensions indicate that sexual maturity, which is caused by hormone(s)

secreted from the gonads (e.g., Gilbert, 1994), does not strongly influence growth of vertebral structures in *Alligator*.

Event 3: Stoppage of growth. The stoppage of growth usually occurs after *Alligator mississippiensis* reaches 2.80 m in total body length (Fig. 4-3; Wilkinson and Rhodes, 1997). This stoppage of growth is followed by strong negative allometry in most vertebral measures (mean = 0.877; Tables 4-4, 4-5), which exhibit the largest degree of the decrease (-0.268) in the allometric coefficients among the three ontogenetic events (Fig. 4-7).

The mechanism of the stoppage of growth, referred to senescence (Bogin, 2003), is a consequence of changes in hormones, metabolism, and other physiological factors. The only exceptions to the overall pattern of negative allometry appear in the three measurements of centrum: the length with a posterior ball, the height, and the width. The better-developed procoelous articulation in the centra may increase in stability or stiffness of the axial column (Salisbury and Frey, 2000). Thus, this feature is likely advantageous for larger, more mature individuals of *Alligator*.

Allometric Change in Vertebrae after Neurocentral Fusion

Variation in three vertebral parts. Among the three vertebral parts, the zygapophysis-neural canal has the largest difference of allometric change after neurocentral fusion. More than 48% of changes in the allometric coefficients occur in the zygapophysis-neural canal of dorsal 15–caudal 2 (Fig. 4-6). In those vertebrae, the neural canal exhibits the strongest degree of shift in the allometric

coefficients after neurocentral fusion. The most significant decrease in allometric coefficients is in the height of neural canal (mean differences = -0.457; Table 4-6).

In dorsal 15–caudal 2, the four measurements of centrum have the smallest degree of change in the allometric coefficients after neurocentral fusion (≤ 26%; Fig. 4-6). The data indicate the anteroposterior length of centrum increases consistently after neurocentral fusion. In dorsals 4 and 10, the length of centrum, especially with a posterior ball, has a larger degree of allometric change than the other measurements of centrum after neurocentral fusion. The data suggest the centrum is relatively free for increasing size from neurocentral fusion.

The neural spine-transverse process also has a relatively small degree of change in the allometric coefficients (≤ 34%) after neurocentral fusion (Fig. 4-6). The total length of the neural spine consistently increases after neurocentral fusion, but the allometric coefficients of the breadth decrease in dorsal 4, dorsal 10, and sacral 1–caudal 2.

Variation in the vertebral column. The relationships of the degree of shift in the allometric change across the vertebral column are shown in a ternary plot (Fig. 4-8). Notably, dorsals 4 and 10 plot further from the corner of the zygapophysis-neural canal than dorsal 15–caudal 2. This means that the larger degree of allometric change occurs in the zygapophysis-neural canal of dorsal 15–caudal 2 than that of dorsals 4 and 10. Also, dorsal 4 and 10 are relatively closer to the corner of centrum than other vertebrae. Notably, most dimensions of the centrum in dorsals 4 and 10 have positive values of change in the allometric

coefficients (i.e., acceleration of the allometric coefficient) after neurocentral fusion (Fig. 4-6).

So, why do dorsals 4 and 10 differ from other vertebrae? Three possible explanations are suggested here. First, the sample size is too small to interpret the meaning of dorsals 4 and 10, and they may actually have similar patterns of allometric changes as seen in other vertebrae. Second, if dorsals 4 and 10 have different patterns of allometric change as shown in the ternary plot, those patterns may be linked to their unique vertebral morphology along the vertebral column. Among the vertebrae of fully-grown *Alligator*, the mid-dorsal vertebrae tend to have the most elongate centrum, transverse processes, and neural spine (Appendix 4-1). Positive mean differences of the allometric coefficients in the length of centrum (dorsals 4 and 10) and transverse process (dorsal 4) and a relatively consistent degree of allometric change in the length of neural spine (dorsals 4 and 10) may be morphologically linked to the overall structure of the two vertebrae. Third, these anterior and mid-dorsal vertebrae have much later timing of neurocentral fusion than the sacral–caudal vertebrae (Chapter 2) (Fig. 4-8). Delaying neurocentral fusion, which largely occurs in crocodilians, may be advantageous for the increase in size of centrum, neural arch, and/or transverse process in very late ontogenetic periods or continued growth throughout postnatal ontogeny.

Vertebrae of *Alligator* demonstrate timing of neurocentral fusion influences primarily the mid-part of vertebral structure (zygapophysis-neural canal) and the articulation of procoelous centra. The origin of the procoelous centrum remains

uncertain in crocodilian evolution although their ancestry, basal crocodyliforms, have amphiplatyan centrum (Salisbury and Frey, 2000). Thus, better understanding of allometric change in vertebral structure of those archosaurs may allow further investigations of the role of neurocentral fusion in vertebral growth and evolution.

CONCLUSIONS

Relative to the femoral length, allometric change of vertebrae are examined in hatchlings to very mature individuals of *Alligator mississippiensis*. Based on 12 vertebral measurements, the 10 selected vertebrae from the axis–caudal 2 show that the strongest degree of positive allometry occurs before the vertebral fusion (body length < ca. 0.9 m). Sexual maturity (body length = ca. 1.8 m) has the least impact on vertebral growth in *Alligator*. The largest degree of shift (decrease) in the allometric coefficient appears when alligators reach the stoppage of growth (body length > ca. 2.8 m).

The 12 vertebral dimensions exhibit different patterns of allometric change, such as the following.

Centrum: The total length with the posterior ball and the diameter of the posterior surface (centrum height, centrum width) have positive allometric change. Centrum length changes slightly faster than total length of the centrum. The height and length of the posterior ball increase in relative size throughout postnatal ontogeny.

Length of height of neural spine and transverse process: The length of neural spine and transverse process has very strong positive allometry before the vertebral ossification, but the elongation of transverse process and neural spine occur throughout ontogeny.

Breadth of transverse process and neural spine: The breadth of neural spine and transverse process increase with positive allometry before the stoppage of growth, and the degree of the allometric coefficients drastically decreases.

Prezygapophysis: The diameter of prezygapophysis has strong positive allometry until neurocentral fusion occurs.

Neural canal: The dimensions of neural canal change with strong positive allometry until vertebral ossification occurs. Relative size of neural canal and zygapophyses do not change after neurocentral fusion (Tables 4-6, 4-7; Figs. 4-6, 4-8).

Neurocentral fusion primarily influence growth of the mid-part of vertebral structure, zygapophysis-neural canal, but no strong impact to the length of transverse process and the height of neural spine, which tend to keep increasing throughout ontogeny. The length of the centra especially with the posterior ball also increase in the degree of allometric change after neurocentral fusion.

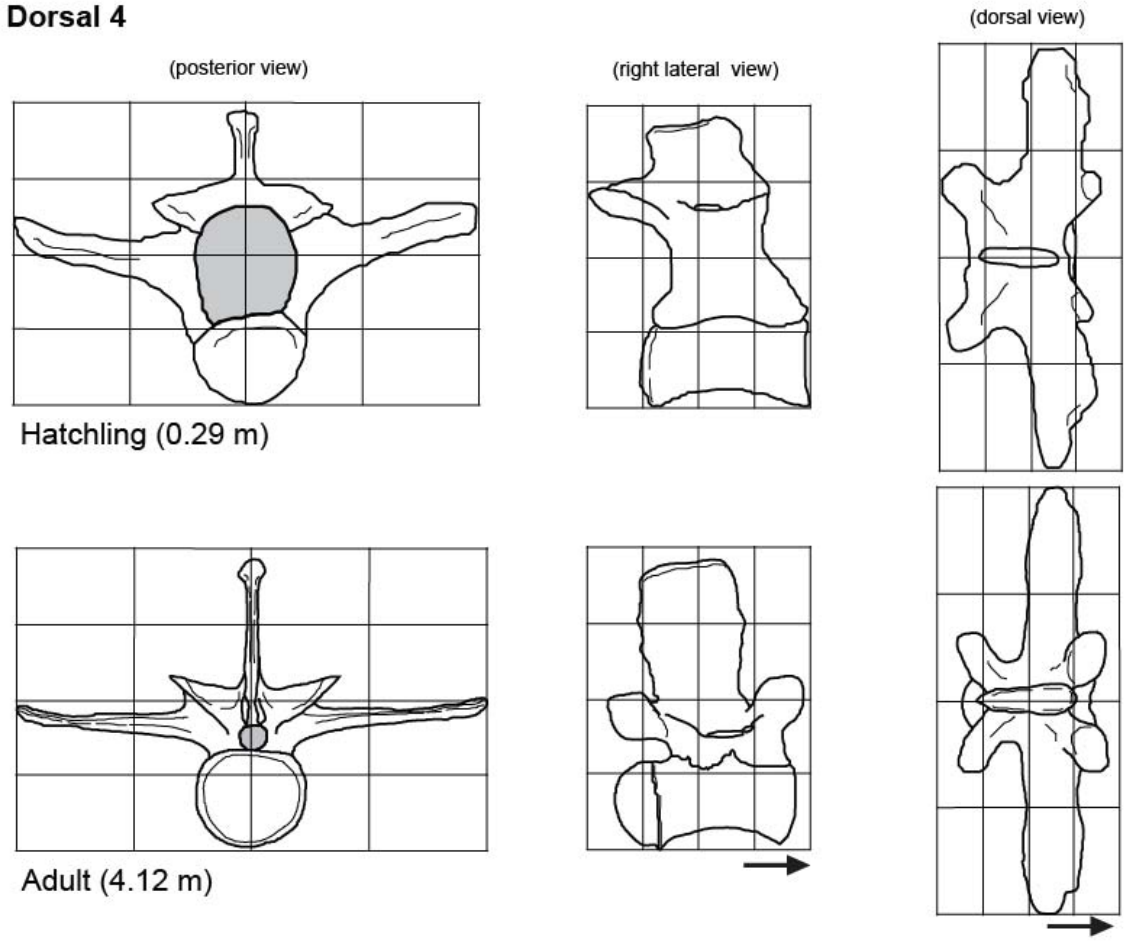

Figure 4-1. Relative proportions of vertebrae in hatchling and very mature *Alligator mississippiensis*. Line drawings of dorsal 4 are shown in posterior, right lateral, and dorsal views. Arrows indicate the anterior direction. The neural canal is filled with gray.

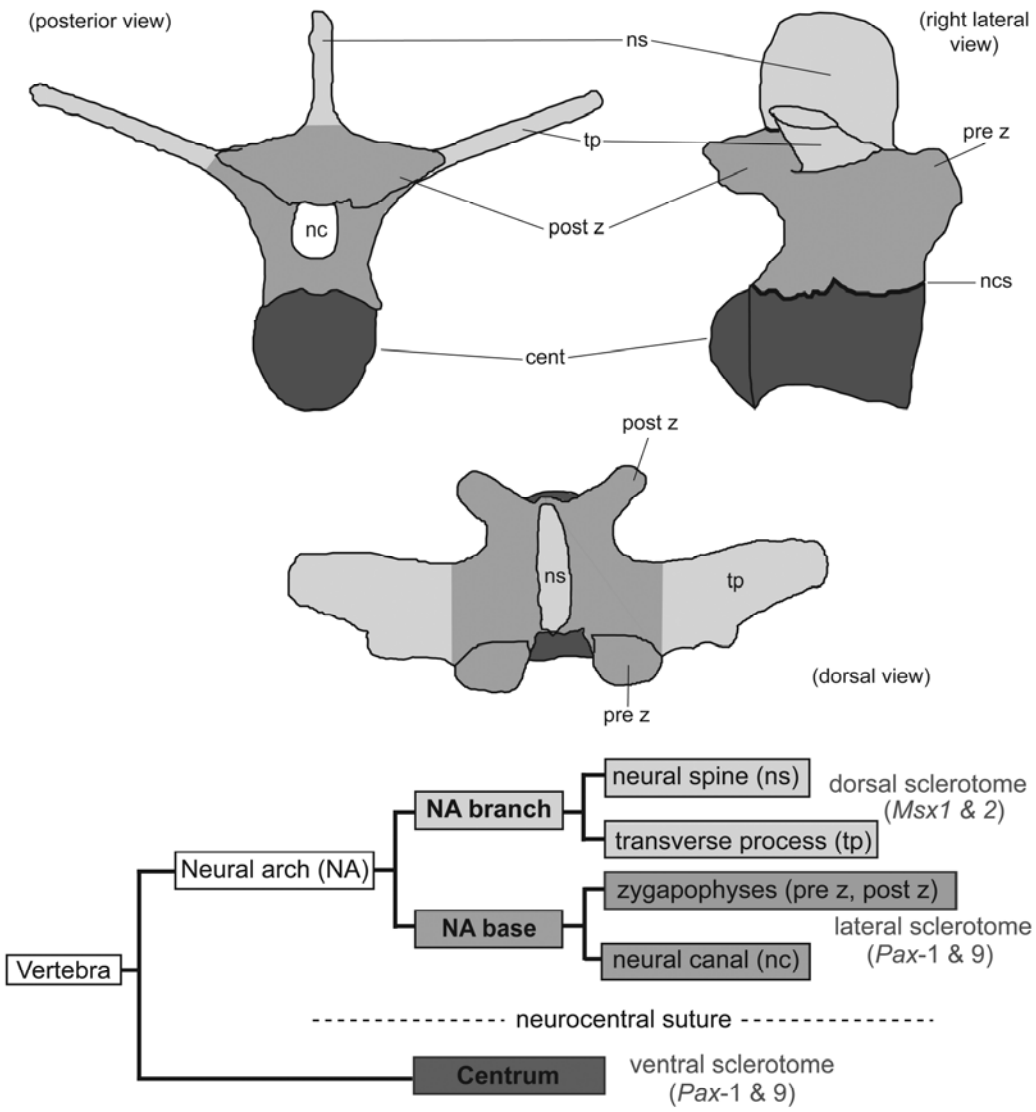

Figure 4-2. Structure of vertebrae in *Alligator*. An anterior dorsal vertebra is shown in posterior, right lateral, and dorsal views. Three main vertebral parts are illustrated and shown in bold letters with grey boxes: (1) centrum, (2) zygapophysis-neural canal; and (3) neural spine-transverse process. The three vertebral parts are defined mainly based on the topological relationship of vertebral structures and the locations for major sclerotome differentiation. Key genes of expressions (suggested by Christ et al., 2000) are also labeled with gray letters. Abbreviations: **cent**, centrum; **ns**, neural spine; **pre z**, prezygapophysis; **post z**, postzygapophysis; **tp**, transverse process.

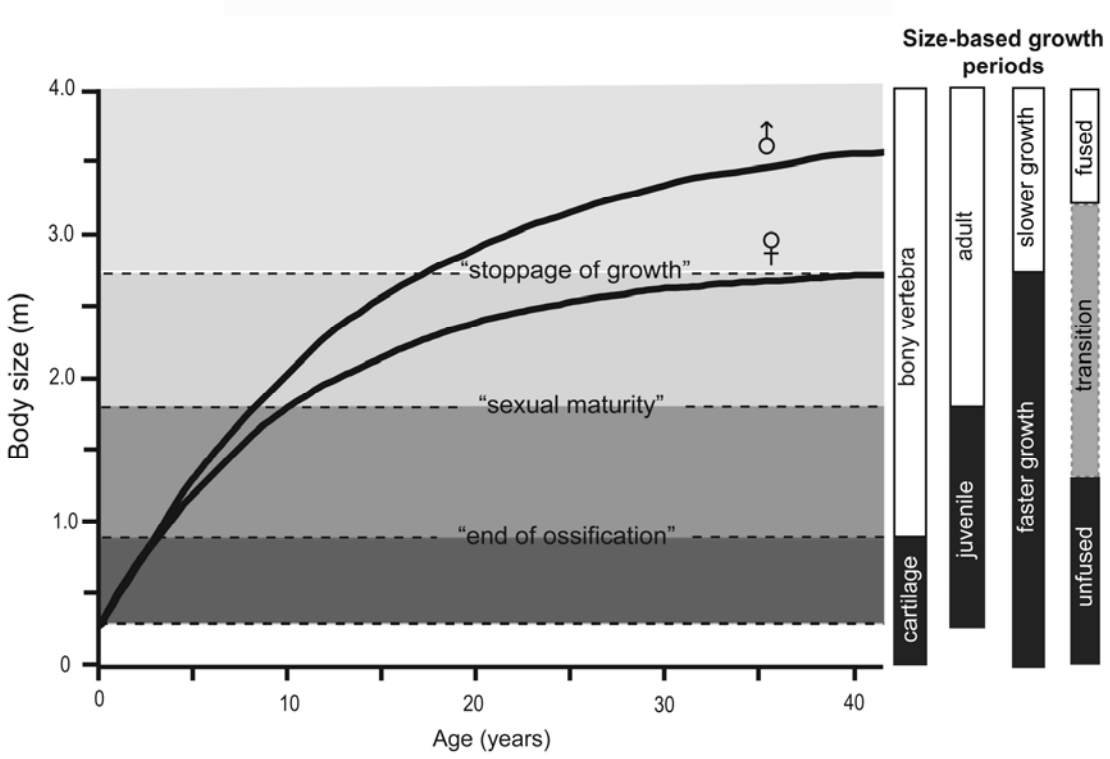

Figure 4-3. Key ontogenetic events in postnatal growth of *Alligator mississippiensis*. Four ontogenetic events, (1) **end of vertebral ossification**, (2) **sexual maturity**, and (3) **the stoppage of growth**, and (4) **neurocentral fusion** are determined by total body size. Neurocentral fusion occurs when animals reach at ca. 1.30 m (in caudal 2) to ca. 3.40 m (in dorsal 4) in body length, as indicated in the right-most bar. The growth curve is modified from Wilkinson and Rhodes (1997).

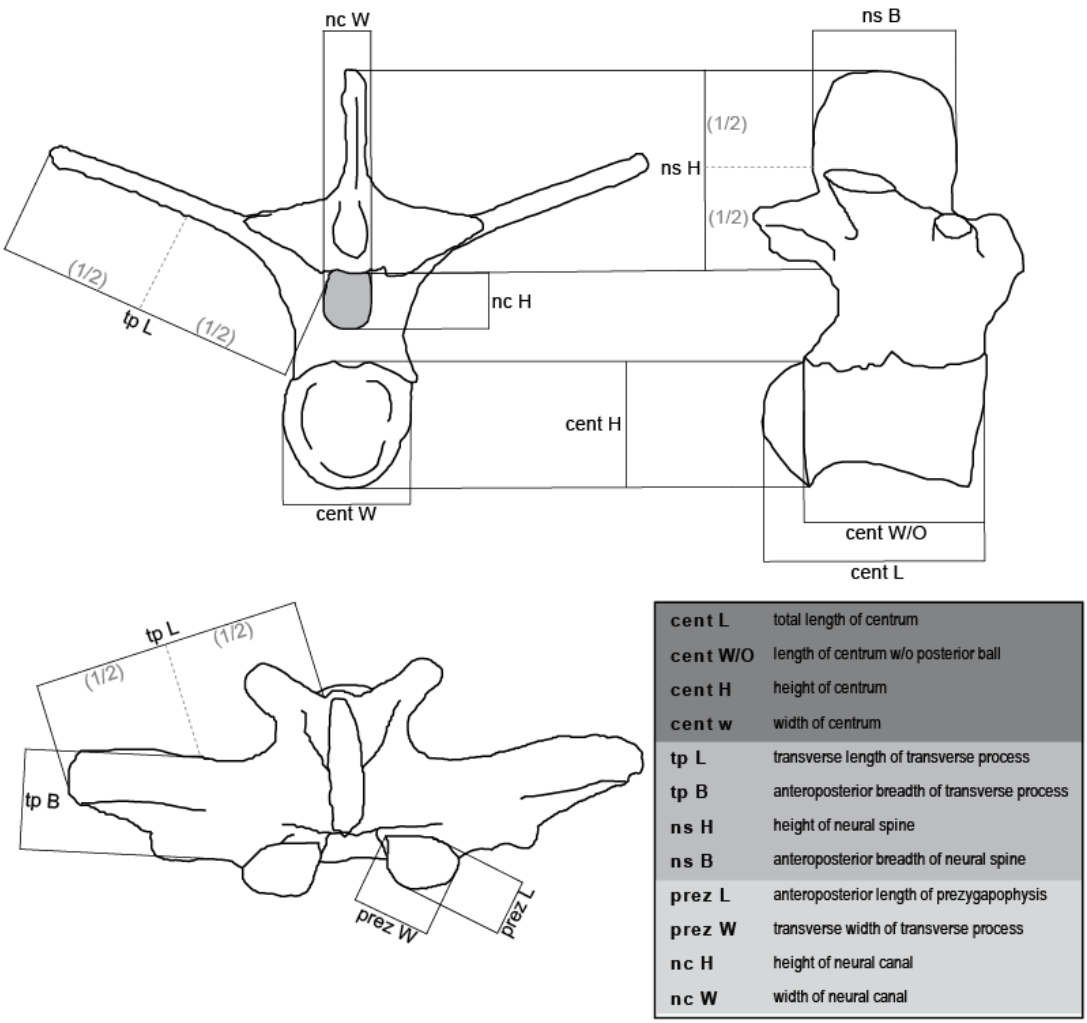

Figure 4-4. Twelve vertebral dimensions of *Alligator mississippiensis*, measured for this study. Illustrations show dorsal 4 in posterior, right lateral, and dorsal views. In the legend, the 12 measurements are separated into the three main vertebral parts (see Fig. 4-2).

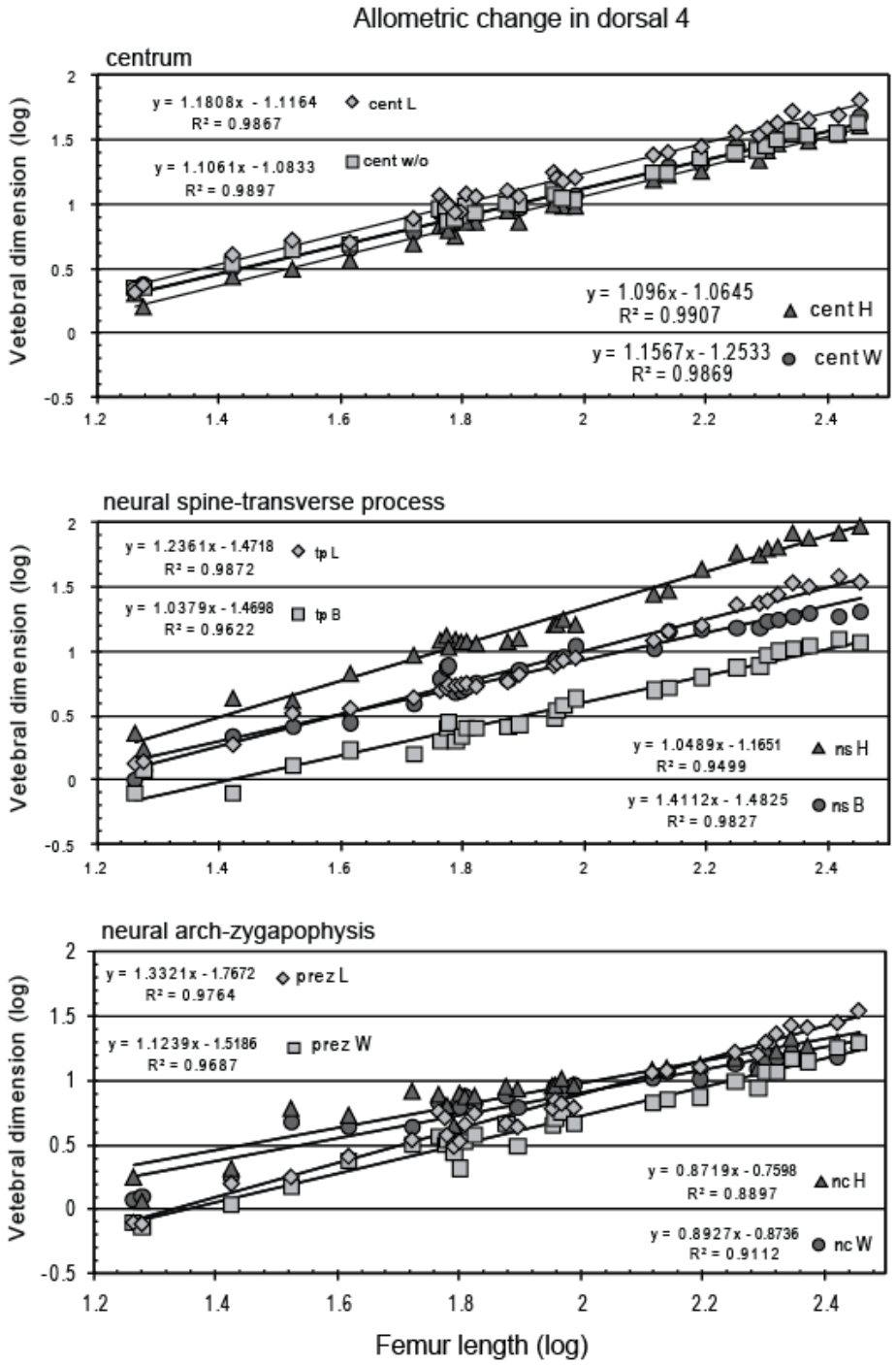

Figure 4-5. Allometric change in dorsal 4 during postnatal ontogeny of *Alligator mississippiensis*. The 31 specimens from hatchlings to very mature individuals show a sample of the allometric coefficients of the 12 vertebral measurements (Y-axis), relative to the femoral length (X-axis). The vertebral measurements are separately shown in the three main vertebral parts (see Figure 4-2). Data of other vertebrae are listed in Appendix 4-2.

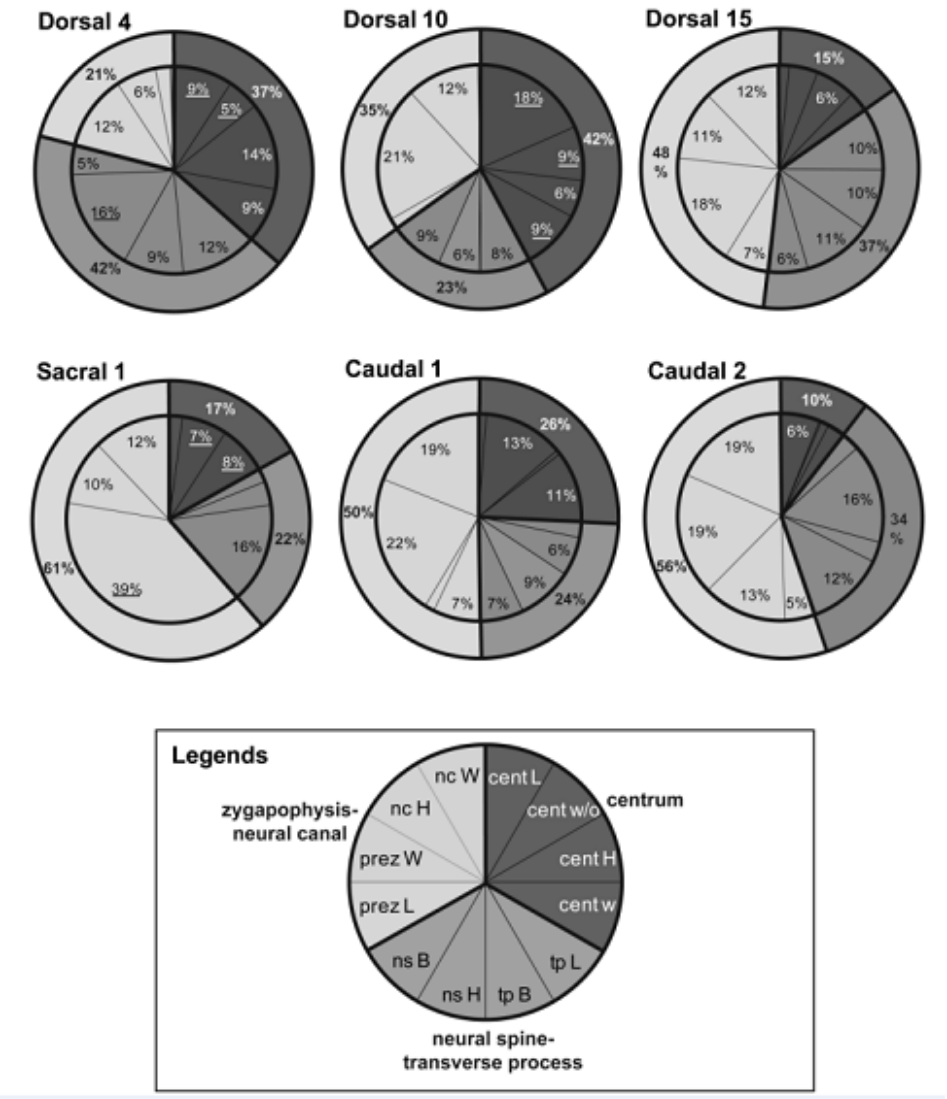

Figure 4-6. Impact of neurocentral fusion to allometric growth of vertebrae in *Alligator mississippiensis*. Based on total changes (100%), degrees of the differences in allometric coefficients after neurocentral fusion are compared in percentage. The same data are also listed in Table 4-7 ('Ratio'). Underlined numbers indicate a positive shift (i.e., increase) of the allometric coefficients after neurocentral fusion. Other numbers indicate decreases in the allometric coefficients after neurocentral fusion. The outer circular zone of each graph represents a subtotal of percentages from each main vertebral part (centrum, neural spine-transverse process, and zygapophysis-neural canal), as established in Figure 4-2.Larger percentages indicate greater degree of shift (either decrease or increase), relative to a total change. Low values indicate allometric growth of vertebral dimension, relatively free from neurocentral fusion (i.e., constantly changing). Percentages lower than 5% are not labeled.

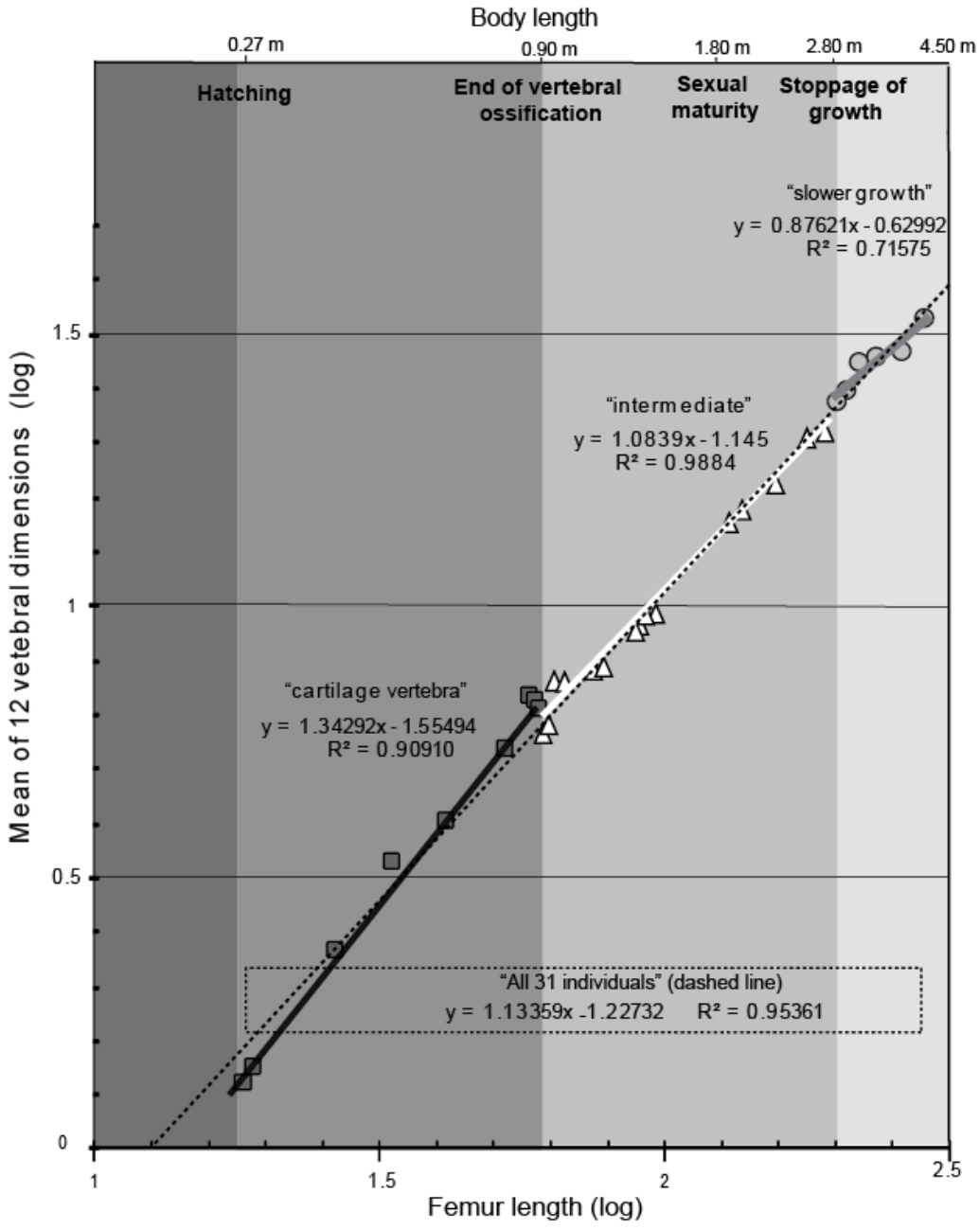

Figure 4-7. Allometric change in vertebrae relative to life history of *Alligator mississippiensis*. The allometric coefficients represent the means of the 12 vertebral dimensions (Y-axis), relative to the femoral length or body length (X-axis), shown separately, based on: (1) between hatching and the end of vertebral ossification (black line); (2) between the end of vertebral ossification and the stoppage of growth (white line); (3) after the stoppage of growth (gray line); and (4) all 31 individuals (dashed line).

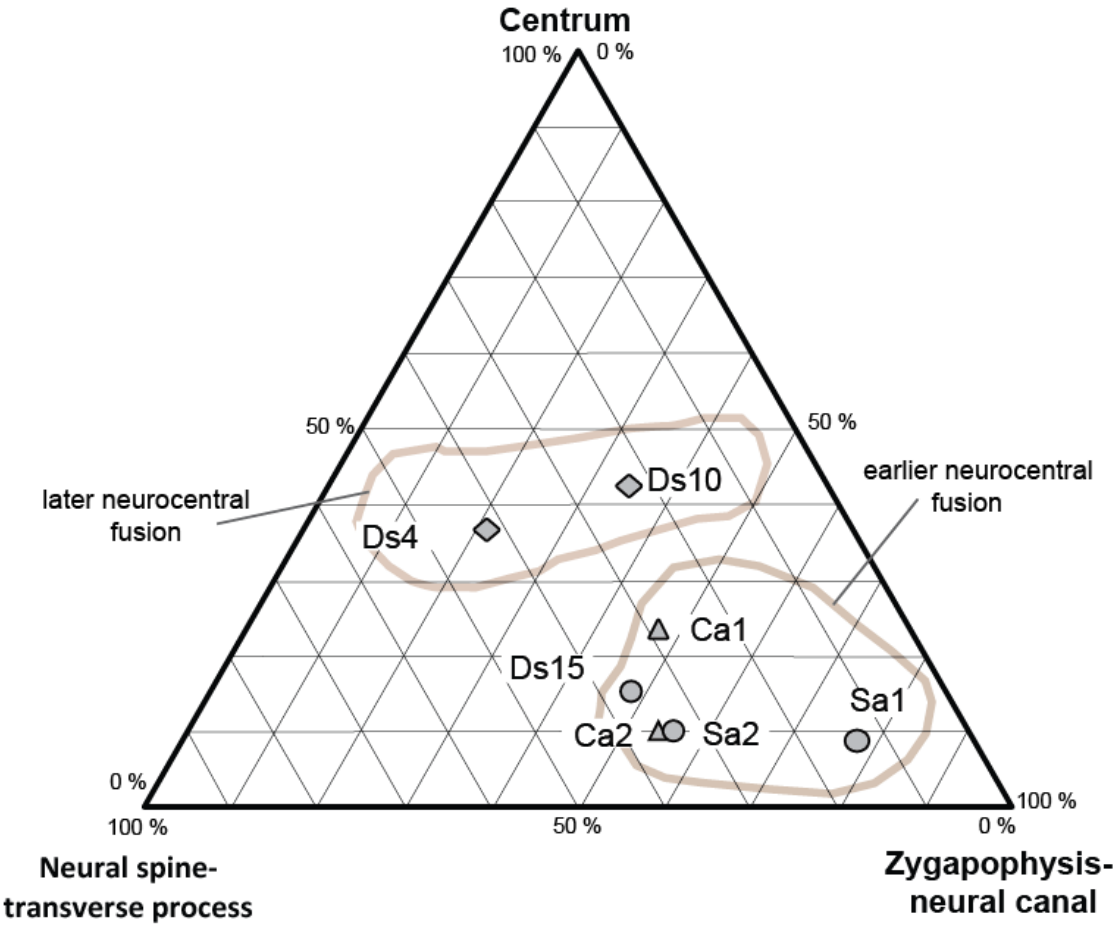

Figure 4-8. Ternary plot showing relationships of vertebral growth and neurocentral fusion in *Alligator mississippiensis*. Degrees of differences of relative changes in growth rates from the post- to the pre-neurocentral fusion periods are calculated in percentages, relative to sum of 12 vertebral dimensions (as shown in Figure 4-6 and Table 4-7). The twelve vertebral dimensions are grouped into three topological parts, as shown in Figure 4-2. The seven vertebrae are circled based on relative timings of neurocentral fusion during ontogeny (see Chapter 2).

TABLE 4-1. Measurements and ontogenetic stages for thirty-one dry skeletons of Alligator mississippiensis *examined for this study. Specimens are listed in order of femoral length.*

Specimens	femur length (mm)	body length (m)*	NCF**	Ontogenetic periods***
6A (UMMZ teaching)	18.3	0.28	Ca 9	Pre-vertebral ossification
UMMZ 238961)	18.9	0.29	Ca?	Pre-vertebral ossification
UF37231	20.8	0.32	Ca9	Pre-vertebral ossification
no # (UMMZ teaching)	26.5	0.40	Ca6	Pre-vertebral ossification
UF 35145	33.2	0.50	Ca5	Pre-vertebral ossification
UMMZ 155216	41.3	0.61	Ca7	Pre-vertebral ossification
UMMZ 238957	52.5	0.78	Ca7	Pre-vertebral ossification
UF39620	58.0	0.86	Ca6	Pre-vertebral ossification
UF 109039	59.4	0.88	Ca5	Pre-vertebral ossification
UF115605	59.9	0.89	Ca 9	Pre-vertebral ossification
UF109040	61.5	0.91	Ca 8	Intermediate 1
UMMZ 238965	62.8	0.92	Ca 4	Intermediate 1
UF 38974	64.1	0.94	Ca3	Intermediate 1
UF40535	66.5	0.98	Ca4	Intermediate 1
UF38972	74.9	1.10	Ca 4	Intermediate 1
UMMZ238959	78.2	1.15	Ca 3	Intermediate 1
UF39622	89.2	1.31	Ca 3	Intermediate 1
UF39621	90.2	1.32	Ca 1	Intermediate 1
UF39623	92.4	1.35	Ca2	Intermediate1
UF 35155	96.8	1.42	Ca 3	Intermediate 1
Ike_006	130.1	1.90	Ca 3	Intermediate 2
UF35153	137.5	2.00	Ca 1	Intermediate 2
AMNH 43316	156.0	2.27	Sa 2	Intermediate 2
UF39106	178.0	2.59	Sa 1	Intermediate 2
AMNH R71621	194.0	2.82	Ds 15	Post-stoppage of growth
UF98341	200.0	2.91	Ds 14	Post-stoppage of growth
AMNH R31563	208.0	3.02	Ds 14	Post-stoppage of growth
UF42548	220.0	3.20	Ds 12	Post-stoppage of growth
UF109411	234.0	3.40	Ds 2	Post-stoppage of growth
UF39618	262.0	3.80	Ds 1	Post-stoppage of growth
UF 134586	284.0	4.12	Ds 2	Post-stoppage of growth

*Body size was estimated by the greatest length of femur using the equation of Farlow et al. (2006).

**NCF (neurocentral fusion) refers to position of the anterior-most vertebra with either completely or partially fused neurocentral junction.

***Ontogenetic periods are established by key ontogenetic events shown in Figure 4-3. The two intermediate periods are separated by sexual maturity.

TABLE 4-2. Key morphological features of vertebrae and neurocentral sutures (NCS) in adult Alligator. Abbreviations: **Ca**, caudal; **Cv**, cervical; **Ds**, dorsal; **Psa**, presacral; **Sa**, sacral. Other anatomical abbreviations are listed in Table 4-2.

Vertebral region	Vertebral position	Vertebrae (top) and NCS (bottom)
Atlas-Axis	Cv 1–2 (Psa 1–2)	First and second presacral vertebrae
Anterior cervical	Cv 3–5 (Psa 3–5)	Short, slender centrum; diapophysis on centrum (convex surface instead of process); diapophysis near or on NCS; low, blade-like neural spine; small hypapophysis; anteroposteriorly elongate parapophysis
Mid-cervical	Cv 6–8 (Psa 6–8)	Blade-like hypapophysis; rod-shaped neural spine; short transverse process extending ventrolaterally; circular-shaped parapophysis
Cervico-dorsal transition	Cv 9–Ds 2 (Psa 9–11)	Shortened centrum, parapophyses on centrum or crossing NCS; hooked hypapophysis; rod-like (circular cross-section) transverse process extending laterally; tall neural spine, slightly blade-shaped
Anterior dorsal	Ds 3–6 (Psa 12–15)	Parapophysis on base of neural arch or on transverse process; hypapohysis reduced or absent; blade-like neural spine; blade-like, very long transverse process
Mid-dorsal	Ds 7–10 (Psa 16–19)	Parapophysis on transverse process; very elongate centrum; bladed neural arch (long anteroposteriorly), flatten top of neural spine
Posterior dorsal	Ds 11–15 (Psa 20–24)	No bony ribs attached to transverse process; short and robust centrum; shortened transverse processes; no trace of rib articular surface
Sacral	Sa 1–2	Large box-shaped ribs; flattened surface on one side of centrum; reduced zygapohyseal articulation between sacral 1 and 2; flattened centrum articulation (between sacral 1 and sacral 2)
Anterior caudal	Ca 1-10	Blade-like neural spine; elongate transverse process (laterally-to-posteriorly)
Mid-caudal	Ca 11–20	Slender neural spine; short transverse process (directing anterolaterally)
Posterior caudal	Ca 21–	Transverse process absent; very short (inclined posteriorly) – lacking neural spine

TABLE 4-3. Statistic summary of allometric coefficients of vertebrae in Alligator mississippiensis *(N = 31).*

A. Basis of vertebrae.

All	Mean ± SD	Min	Max	95% CI	*P*
Axis	1.10452 ± 0.20870	0.73560	1.35676	0.97517–1.23387	0.6543
Cv3	1.08359 ± 0.15496	0.78459	1.29909	0.98755–1.17963	0.3218
Cv8	1.13136 ± 0.14398	0.87775	1.38555	1.04990–1.21282	0.9302
Ds1	1.13239 ± 0.15628	0.87193	1.41124	1.04397–1.22082	0.9546
Ds4	1.17938 ± 0.20549	0.82071	1.52170	1.06312–1.29565	0.4718
Ds10	1.14303 ± 0.23237	0.74504	1.52745	1.01155–1.27450	0.9089
Ds15	1.10919 ± 0.23765	0.73601	1.49070	0.97473–1.24365	0.7130
Sa1	1.17236 ± 0.23058	0.87131	1.49856	1.02944–1.31527	0.6225
Sa2	1.11660 ± 0.19813	0.77473	1.39196	0.99380–1.23940	0.7757
Ca1	1.12256 ± 0.17399	0.83230	1.39829	1.02411–1.22100	0.8087
Ca2	1.16496 ± 0.19466	0.82877	1.46666	1.05482–1.27510	0.6055

B. Basis of vertebral dimensions.

	Mean ± SD	Min	Max	95% CI	*P*
cent L	1.16702 ± 0.03990	1.10833	1.22654	1.14095–1.19309	0.0431*
cent w/o	1.09119 ± 0.05066	0.98299	1.16754	1.05979–1.12259	0.2290
cent H	1.14465 ± 0.06407	1.07576	1.29045	1.10494–1.18436	0.6479
cent w	1.12730 ± 0.05070	1.07478	1.24012	1.09588–1.15872	0.6391
tp L	1.33023 ± 0.08581	1.20828	1.46666	1.27076–1.38969	0.0004*
tp B	1.06087 ± 0.09937	0.84584	1.13533	0.98726–1.13449	0.0956
ns H	1.35353 ± 0.06102	1.20244	1.41124	1.31571–1.39135	0.0001*
ns B	1.06974 ± 0.11485	0.96171	1.35676	0.99856–1.14093	0.1056
prez L	1.28684 ± 0.10976	1.08653	1.48928	1.21881–1.35487	0.0018*
prez W	1.34012 ± 0.15844	1.12393	1.52745	1.24192–1.43833	0.0027*
nc H	0.84207 ± 0.04875	0.74504	0.89103	0.81185–0.87229	0.0001*
nc W	0.82735 ± 0.06973	0.73560	0.92068	0.78413–0.87057	0.0001*

*The asterisk (*) indicates significantly different slopes from the total mean (*t*-test: $p < 0.05$).

C. Total.

	Mean ± SD	Min	Max	95% CI
N = 114	1.13508 ± 0.19066	0.73560	1.52745	1.10008–1.17008

TABLE 4-4. Summary for allometric coefficients of vertebral dimensions in selected ontogenetic periods in Alligator mississippiensis*. Means of ten vertebrae are shown (see results for each vertebra in Appendix 4-5).*

Ontogenetic events	Vertebral ossification		Sexual maturity		Stoppage of growth	
	Before	After	Before	After	Before	After
cent L	1.34563	1.12338	1.23936	1.13078	1.17104	1.01258
cent w/o	1.22766	1.08699	1.11721	1.08204	1.09795	0.89839
cent H	1.22826	1.19077	1.11155	1.19245	1.11268	0.93023
cent w	1.20537	1.17153	1.09410	1.16136	1.11480	0.91607
tp L	1.36242	1.40742	1.28048	1.56006	1.31154	1.08184
tp B	1.14024	1.11340	1.04325	1.17174	1.09159	0.70900
sp H	1.68134	1.31564	1.44560	1.40065	1.32582	1.14798
sp B	1.34322	0.97024	1.24131	0.96044	1.14375	0.69802
prez L	1.48110	1.32651	1.31025	1.40231	1.27222	1.02688
prez W	1.67289	1.28416	1.45541	1.33765	1.30101	1.02356
nc H	1.27884	0.65330	1.10337	0.52419	0.92183	0.51504
nc W	1.09140	0.66810	1.03090	0.64745	0.91028	0.55953
Specimens(N)	10	21	20	11	25	6
Mean	1.34292	1.10382	1.20607	1.13093	1.14438	0.87621
SD	0.18176	0.23137	0.14006	0.29055	0.13337	0.19887
Max	1.68134	1.40742	1.45541	1.56006	1.32582	1.14798
Min	1.09140	0.65330	1.03090	0.52419	0.91028	0.51504
95% CI	0.10284	0.13090	0.07924	0.16439	0.07546	0.11252
Lower limit	1.23536	0.97838	1.12682	0.96654	1.07241	0.76407
upper limit	1.44103	1.24019	1.28531	1.29532	1.22334	0.98911
p	0.0035*	0.7186	0.1209	0.9630	0.7563	0.0012*

*The asterisk (*) indicates significantly different slopes from the total mean (*t*-test: $p < 0.05$).

TABLE4-5. Comparisons for mean differences (mean differ.) of allometric coefficients in vertebrae after three ontogenetic events in Alligator mississippiensis*. The ontogenetic status of each individual relative to three ontogenetic events was determined by body length (BL). More detailed summary is listed in Appendix 4-5.*

A. Vertebral dimensions-basis.

Event (BL)	Vertebral ossification (ca 0.9m)	Sexual maturity (ca 1.8 m)	Stoppage of growth (ca 2.8 m)
	Mean differ. ± SD	Mean differ. ± SD	Mean differ. ± SD
cent L	-0.22225 ± 0.12386*	-0.10859 ± 0.07135*	-0.16517 ± 0.18366
cent w/o	-0.14983 ± 0.15819*	0.07685 ± 0.35842	-0.19033 ± 0.08935*
cent H	-0.05354 ± 0.11205	0.16308 ± 0.34461	-0.18412 ± 0.10389*
cent w	-0.04614 ± 0.11989	0.17566 ± 0.33340	-0.19303 ± 0.11344
tp L	0.07940 ± 0.17707	0.21498 ± 0.18047*	-0.20918 ± 0.09020
tp B	-0.02684 ± 0.50357	0.03193 ± 0.34140	-0.33457 ± 0.16426
ns H	-0.37786 ± 0.28852*	0.22809 ± 0.50001	-0.20714 ± 0.23604
ns B	-0.37039 ± 0.15912*	-0.14987 ± 0.48077	-0.40168 ± 0.21301
prez L	-0.17912 ± 0.23927	0.05991 ± 0.43416	-0.23885 ± 0.44906
prez W	-0.41076 ± 0.26230*	-0.05214 ± 0.50464	-0.31743 ± 0.52549
nc H	-0.60203 ± 0.20743*	-0.35637 ± 0.43199*	-0.41447 ± 0.10644*
nc W	-0.39675 ± 0.22310*	-0.31487 ± 0.42107*	-0.33686 ± 0.17367

B. Vertebrae-basis.

Zone (BL)	Vertebral ossification (ca 0.9m)	Sexual maturity (ca 1.8 m)	Stoppage of growth (ca 2.8 m)
	Mean differ. ± SD	Mean differ. ± SD	Mean differ. ± SD
Cv2	-0.31423 ± 0.21144	-0.22591 ± 0.34417	-0.39088 ± 0.44801
Cv3	-0.17082 ± 0.08232*	0.05400 ± 0.41204	-0.29127 ± 0.28015
Cv8	-0.13940 ± 0.33998	0.01765 ± 0.33138	-0.18184 ± 0.27288
Ds1	-0.08045 ± 0.38685	0.05400 ± 0.33540	-0.18866 ± 0.29437
Ds4	-0.36951 ± 0.34674	0.02287 ± 0.43056	-0.24708 ± 0.27523
Ds10	-0.26163 ± 0.29631	-0.04609 ± 0.23513	-0.23901 ± 0.13354
Ds15	-0.24897 ± 0.20683	-0.10446 ± 0.27692	-0.25947 ± 0.14974
Sa1	-0.29240 ± 0.28704	-0.08129 ± 0.18200	-0.17498 ± 0.30842
Sa2	-0.26677 ± 0.26773	-0.08129 ± 0.18200	-0.24632 ± 0.11514
Ca1	-0.17547 ± 0.30118	-0.20404 ± 0.25760*	-0.32523 ± 0.21415
Ca2	-0.34805 ± 0.26899	-0.26901 ± 0.28332*	-0.39203 ± 0.15021*

C. Total

Zone (BL)	Vertebral ossification (ca 0.9m)	Sexual maturity (ca 1.8 m)	Stoppage of growth (ca 2.8 m)
Mean ± SD	-0.24132 ± 0.28913	-0.08601 ± 0.325524	-0.26640 ± 0.254092

*The asterisk (*) indicates significantly different slopes from the total mean (*t*-test: $p < 0.05$).

TABLE 4-6. Summary of mean differences (mean differ.) of allometric coefficients from six selected vertebrae after neurocentral fusion in Alligator mississippiensis*. The allometric coefficients are listed in Appendix 4-6.*

	Mean differ. ± SD	Max	Min	Lower 95% CI	Upper 95% CI	*P*
cent L	0.18506 ± 0.42699	0.94969	-0.17258	-0.15660	0.52671	0.118
cent w/o	-0.00008 ± 0.29733	0.43734	-0.32638	-0.23799	0.23783	0.173
cent H	-0.20350 ± 0.40606	0.20540	-1.04970	-0.52841	0.12141	0.584
cent w	-0.11466 ± 0.39590	0.48659	-0.74757	-0.43145	0.20212	0.806
tp L	-0.26644 ± 0.32717	0.00000	-0.92648	-0.52823	-0.00465	0.282
tp B	-0.26636 ± 0.25820	0.01669	-0.73223	-0.47295	-0.05976	0.232
ns H	-0.02253 ± 0.54217	1.18526	-0.36397	-0.45635	0.41129	0.579
ns B	-0.08571 ± 0.33118	0.46238	-0.43611	-0.35070	0.17928	0.704
prez L	0.16142 ± 0.57287	1.13804	-0.23863	-0.29696	0.61981	0.214
prez W	-0.41892 ± 0.36800	-0.03910	-1.10328	-0.71338	-0.12447	0.062
nc H	-0.45656 ± 0.15816	-0.18164	-0.59113	-0.58311	-0.33001	0.006*
nc W	-0.25976 ± 0.28219	0.12701	-0.52679	-0.48555	-0.03397	0.476
Total mean ± SD	-0.13038 ± 0.42972					
Total 95% CI	-0.37351–0.11276					

*The asterisk (*) indicates significantly different slopes from the total mean (*t*-test: $p < 0.05$).

TABLE 4-7. Comparisons of mean differences (mean differ.) of allometric coefficients after neurocentral fusion in vertebrae of Alligator mississippiensis*.*

	Dorsal 4		Dorsal 10		Dorsal 15	
	Mean differ.	**Ratio**	**Mean differ.**	**Ratio**	**Mean differ.**	**Ratio**
cent L	0.63040	9.2%	0.94969	18.4%	-0.05079	1.5%
cent w/o	0.31613	5.1%	0.43734	8.5%	-0.15080	4.5%
cent H	-1.04970	13.6%	-0.29944	5.8%	-0.20861	6.2%
cent w	-0.74757	8.7%	0.48659	9.4%	-0.10624	3.2%
tp L	-0.92648	12.0%	-0.39803	7.7%	-0.32706	9.7%
tp B	-0.73223	9.5%	0.01669	0.3%	-0.32258	9.6%
ns H	1.18526	16.3%	-0.32887	6.4%	-0.36397	10.8%
ns B	0.27974	4.6%	-0.43611	8.5%	-0.20689	6.2%
prez L	0.83648	11.8%	-0.08709	1.7%	-0.23863	7.1%
prez W	-0.48393	6.3%	-1.10328	21.4%	-0.60322	18.0%
nc H	-0.18164	2.4%	-0.59113	11.5%	-0.36894	11.0%
nc W	-0.04177	0.5%	0.01967	0.4%	-0.41184	12.3%
Mean	-0.07628		-0.11116		-0.12701	
SD	0.73451		0.54797		0.15148	
Lower 95% CI	-0.39041		-0.23700		0.18372	
Upper 95% CI	0.54296		0.45933		0.18131	

	Sacral 1		Caudal 1		Caudal 2	
	Mean differ.	**Ratio**	**Mean differ.**	**Ratio**	**Mean differ.**	**Ratio**
cent L	na	0.0%	-0.03117	1.2%	-0.17258	6.1%
cent w/o	0.05800	2.0%	-0.32638	12.6%	-0.00848	0.3%
cent H	0.20540	7.1%	-0.01807	0.7%	-0.03604	1.3%
cent w	0.22486	7.7%	-0.29041	11.2%	-0.07945	2.8%
tp L	0.00000	0.0%	-0.06495	2.5%	-0.08362	2.9%
tp B	-0.06143	2.1%	-0.15726	6.1%	-0.45043	15.9%
ns H	-0.10811	3.7%	-0.22572	8.7%	-0.09063	3.2%
ns B	0.46238	15.9%	-0.17309	6.7%	-0.35289	12.4%
prez L	1.13804	39.1%	-0.19296	7.4%	-0.13291	4.7%
prez W	-0.29775	10.2%	-0.03910	1.5%	-0.36607	12.9%
nc H	-0.35227	12.1%	-0.58049	22.4%	-0.54097	19.0%
nc W	0.12701	0.0%	-0.49230	19.0%	-0.52679	18.5%
Mean	0.12701		-0.21599		-0.23674	
SD	0.43101		0.18098		0.19757	
Lower 95% CI	-0.43534		0.10100		0.11121	
Upper 95% CI	0.18131		0.33098		0.36227	

*Ratio is based on the differences in the allometric coefficients of each dimension-to-total.

Appendix 4-1. Twelve vertebral dimensions from the axis–caudal 5 in a very mature individual (body length = 3.02 m) of *Alligator mississippiensis*. Log ratios (based on dorsal 15) for the 12 measurements are divided into three groups of four based on their vertebral region (i.e., centrum, neural spine-transverse process, zygapophyses-neural canal). Abbreviations for measurements are listed in Figure 4-4.

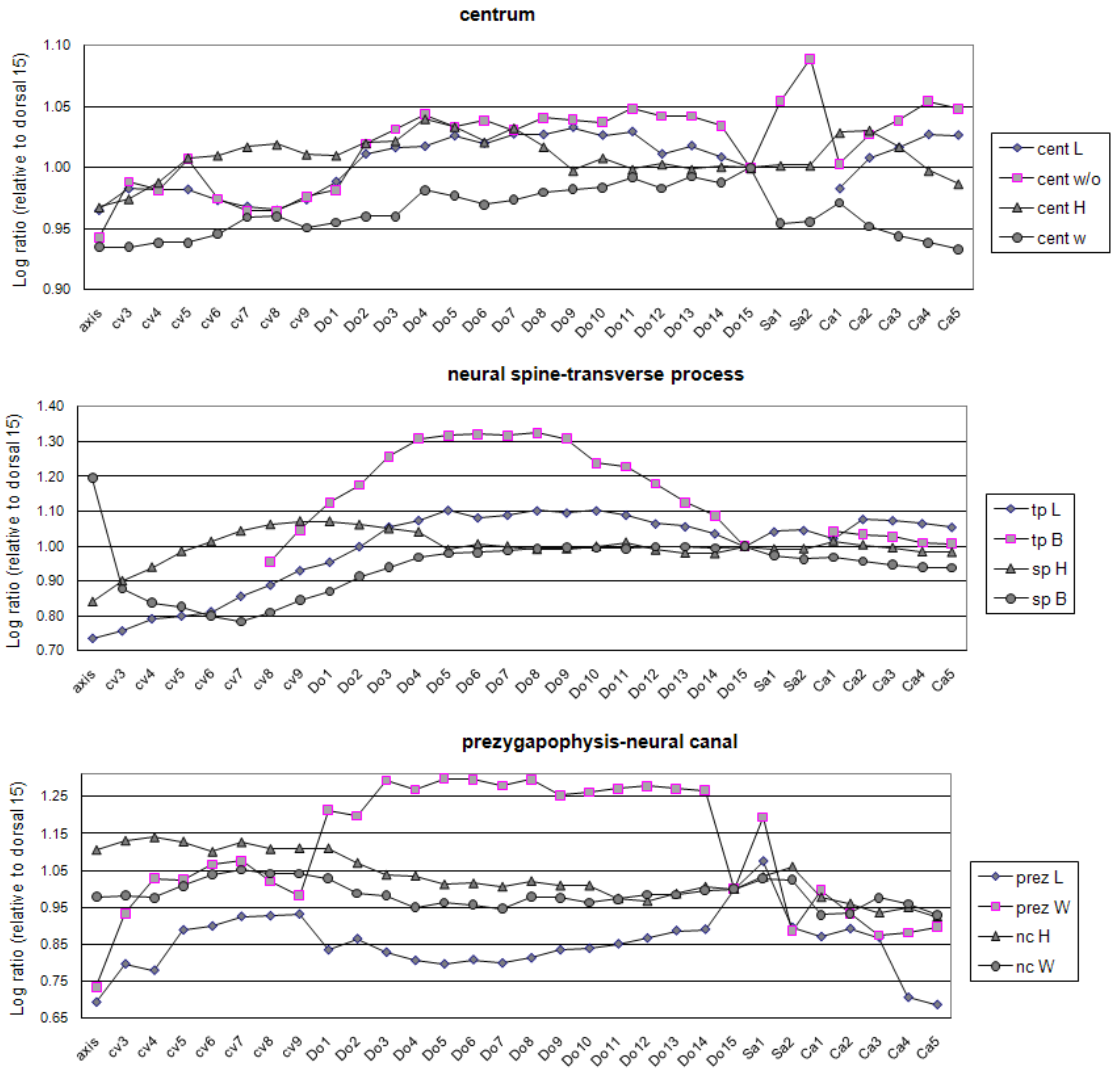

Appendix 4-2. Allometric coefficients of 10 vertebrae in hatchling–very mature *Alligator mississippiensis*. The intercepts and coefficient of determination are also listed in 12 vertebral measurements.

Axis				**Cervical 3**		
	k	***b***	r^2	***k***	***b***	r^2
cent L	1.16166	-1.08110	0.98740	1.18718	-1.12080	0.98322
cent w/o	1.08102	-1.04811	0.98847	1.13435	-1.12275	0.98576
cent H	1.07576	-1.10687	0.98050	1.09597	-1.15216	0.96865
cent w	1.07802	-1.03161	0.97756	1.09118	-1.05788	0.96706
tp L	1.88416	-3.74437	0.62802	1.29787	-2.10022	0.73854
tp B	na	na	na	na	na	na
sp H	1.20244	-1.35875	0.93012	1.29909	-1.47041	0.97368
sp B	1.35676	-1.40293	0.95555	1.16770	-1.45176	0.97577
prez L	1.27790	-1.96217	0.83709	1.08653	-1.45553	0.97528
prez W	1.30112	-2.15352	0.79844	1.14273	-1.64459	0.96420
nc H	0.77492	-0.55221	0.94362	0.84659	-0.69948	0.91600
nc W	0.73560	-0.59481	0.87112	0.78459	-0.71331	0.89929
N (samples)	284			294		
Mean	1.17540	-1.45786	0.89981	1.10307	-1.27172	0.94068
SD	0.30734	0.90327	0.11088	0.16058	0.40932	0.07251
Max	1.88416	-0.55221	0.98847	1.29909	-0.69948	0.98576
Min	0.73560	-3.74437	0.62802	0.78459	-2.10022	0.73854
95% CI	0.03574			0.31473		
Lower limit	1.13965			0.78835		
Upper limit	1.21114			1.41780		

(Appendix 4-2)

Cervical 8

	k	*b*	r^2
cent L	1.19573	-1.15822	0.98601
cent w/o	1.12172	-1.12830	0.98829
cent H	1.17919	-1.29568	0.98964
cent w	1.14718	-1.17219	0.98527
tp L	1.20828	-1.51847	0.98383
tp B	1.03789	-1.46977	0.96224
sp H	1.38555	-1.46344	0.98392
sp B	1.04664	-1.22156	0.96651
prez L	1.25343	-1.64016	0.96063
prez W	1.21282	-1.66436	0.95880
nc H	0.87775	-0.77143	0.86779
nc W	0.91010	-0.89979	0.92398
Samples (N)	360		
Mean	1.13985	-1.26669	0.96315
SD	0.14782	0.28677	0.03724
Max	1.38555	-0.77143	0.98964
Min	0.87775	-1.66436	0.86779
CI	0.01527		
Lower limit	1.12459		
Upper limit	1.15512		

Dorsal 1

	k	*b*	r^2
cent L	1.20229	-1.11643	0.98655
cent w/o	1.10607	-1.08325	0.98971
cent H	1.15669	-1.25327	0.98693
cent w	1.09596	-1.06453	0.99066
tp L	1.23605	-1.47182	0.98722
tp B	1.11081	-1.54979	0.95245
sp H	1.41124	-1.48255	0.98269
sp B	1.04895	-1.16512	0.94995
prez L	1.33210	-1.76723	0.97636
prez W	1.12393	-1.51862	0.96867
nc H	0.87193	-0.75979	0.88973
nc W	0.89271	-0.87358	0.91117
Samples (N)	360		
Mean	1.13436	-1.23238	0.96542
SD	0.16376	0.30146	0.03457
Max	1.41124	-0.75979	0.99066
Min	0.87193	-1.76723	0.88973
CI	0.32096		
Lower limit	0.81340		
Upper limit	1.45531		

Dorsal 4

	k	*b*	r^2
cent L	1.22654	-1.13537	0.96500
cent w/o	1.16754	-1.10437	0.96741
cent H	1.29045	-1.48789	0.96017
cent w	1.24012	-1.34375	0.97270
tp L	1.37330	-1.36442	0.94730
tp B	1.10470	-1.27702	0.91829
sp H	1.35886	-1.41291	0.94716
sp B	0.98004	-0.83143	0.98001
prez L	1.18099	-1.61212	0.93105
prez W	1.52170	-2.09058	0.95534
nc H	0.88763	-0.84865	0.87221
nc W	0.82071	-0.79164	0.93811
Samples (N)	308		
Mean	1.18617	-1.27483	0.94877
SD	0.21410	0.38944	0.02937
Max	1.52170	-0.79164	0.98001
Min	0.82071	-2.09058	0.87221
CI	0.02391		
Lower limit	1.16226		
Upper limit	1.21008		

Dorsal 10

	k	*b*	r^2
cent L	1.11950	-0.87573	0.99001
cent w/o	1.06709	-0.86237	0.99334
cent H	1.15246	-1.21941	0.98758
cent w	1.13885	-1.12069	0.99482
tp L	1.34839	-1.29162	0.99052
tp B	1.13533	-1.31584	0.97091
sp H	1.36912	-1.46641	0.95890
sp B	1.01876	-0.86061	0.98600
prez L	1.32481	-1.86743	0.96049
prez W	1.52745	-2.16727	0.94596
nc H	0.74504	-0.61127	0.86087
nc W	0.76950	-0.66451	0.97157
Samples (N)	264		
Mean	1.14373	-1.18248	0.96728
SD	0.24370	0.49310	0.03895
Max	1.52745	-0.61127	0.99482
Min	0.74504	-2.16727	0.86087
CI	0.47764		
Lower limit	0.66608		
Upper limit	1.62137		

(Appendix 4-2)

Dorsal 15

	k	*b*	r^2
cent L	1.10833	-0.91682	0.99236
cent w/o	0.98299	-0.76618	0.99097
cent H	1.09239	-1.15297	0.97662
cent w	1.17208	-1.12869	0.98293
tp L	1.38909	-1.62996	0.95335
tp B	0.84584	-0.90483	0.96217
sp H	1.36230	-1.45952	0.96615
sp B	1.03884	-0.93021	0.97505
prez L	1.25976	-1.68588	0.96103
prez W	1.49070	-2.04697	0.98956
nc H	0.83193	-0.76311	0.92896
nc W	0.73601	-0.59498	0.90074
Samples (N)	240		
Mean	1.13313	-1.18866	0.96525
SD	0.23358	0.45931	0.02857
Max	1.49070	-0.59498	0.99236
Min	0.73601	-2.04697	0.90074
CI	0.02955		
Lower limit	1.10358		
Upper limit	1.16268		

Sacral 1

k	*b*	r^2
na	na	na
1.09001	-0.89459	0.98201
1.16344	-1.31941	0.98343
1.12749	-1.10289	0.96681
1.27310	-1.24452	0.88527
na	na	na
1.36522	-1.45896	0.93553
0.96171	-0.79372	0.95967
1.48928	-2.09513	0.93586
1.49856	-2.22072	0.92495
0.89103	-0.83415	0.89739
0.87131	-0.81888	0.88541
289		
1.17312	-1.27830	0.93563
0.23027	0.51769	0.03745
1.49856	-0.79372	0.98343
0.87131	-2.22072	0.88527
0.45131		
0.72180		
1.62443		

Caudal 1

	k	*b*	r^2
cent L	1.13564	-0.93778	0.98630
cent w/o	1.05529	-0.93659	0.97246
cent H	1.08211	-1.06656	0.97710
cent w	1.07478	-0.98162	0.97417
tp L	1.34693	-1.42071	0.80101
tp B	1.08893	-1.46639	0.96534
sp H	1.39829	-1.51306	0.96497
sp B	1.05664	-0.99421	0.97710
prez L	1.27411	-1.71344	0.98494
prez W	1.26057	-1.87607	0.97968
nc H	0.86509	-0.83222	0.90548
nc W	0.83230	-0.82561	0.91460
Samples (N)	338		
Mean	1.12561	-1.19071	0.94889
SD	0.18215	0.37254	0.05623
Max	1.39829	-0.82561	0.98630
Min	0.83230	-1.87607	0.80101
CI	0.01942		
Lower limit	1.10620		
Upper limit	1.14503		

Caudal 2

k	*b*	r^2
1.16631	-1.02173	0.98817
1.11344	0.02934	0.98726
1.15804	-1.20993	0.99291
1.10734	-1.06619	0.99274
1.46666	-1.70550	0.95930
1.10260	-1.45936	0.96357
1.38317	-1.48900	0.97988
1.02139	-0.93760	0.96229
1.38949	-1.96308	0.95269
1.32165	-2.00161	0.93309
0.82877	-0.78315	0.88568
0.92068	-1.00959	0.88853
346		
1.17063	-1.19619	0.95660
0.20312	0.58341	0.03921
1.46666	0.02934	0.99291
0.82877	-2.00161	0.88568
0.39811		
0.77252		
1.56874		

Appendix 4-3. Allometric coefficients of 10 vertebrae before and after vertebral ossification in *Alligator mississippiensis*. The intercepts and coefficient of determination are also listed in 12 vertebral dimensions.

Axis	**Before vertebral ossification**			**Before vertebral ossification**		
	k	***b***	r^2	***k***	***b***	r^2
cent L	1.37360	-1.40211	0.97678	1.14075	-1.04284	0.98666
cent w/o	1.22464	-1.25688	0.97229	1.10919	-1.11432	0.98878
cent H	1.16563	-1.22719	0.94979	1.14329	-1.25690	0.97691
cent w	1.27636	-1.32123	0.94206	1.11074	-1.10962	0.98163
tp L	na	na	na	na	na	na
tp B	na	na	na	na	na	na
sp H	1.68480	-2.08135	0.89789	1.18919	-1.34785	0.93332
sp B	1.51234	-1.64635	0.80809	1.30079	-1.28740	0.97666
prez L	1.59196	-2.45332	0.78475	1.16615	-1.73166	0.67356
prez W	1.91930	-3.10187	0.71727	1.17297	-1.89871	0.70296
nc H	1.02883	-0.94759	0.86951	0.69303	-0.38416	0.96583
nc W	1.02611	-1.04855	0.70178	0.63516	-0.38793	0.93072
Mean	1.38036	-1.64865	0.86202	1.06612	-1.15614	0.91170

Cv3	**Before vertebral ossification**			**Before vertebral ossification**		
	k	***b***	r^2	***k***	***b***	r^2
cent L	1.37985	-1.41562	0.97895	1.15723	-1.06134	0.96773
cent w/o	1.30096	-1.37224	0.98055	1.13341	-1.12599	0.97452
cent H	1.20125	-1.29420	0.89530	1.16697	-1.31099	0.96817
cent w	1.22786	-1.25783	0.84759	1.11207	-1.10797	0.98323
tp L	na	na	na	na	na	na
tp B	na	na	na	na	na	na
sp H	1.54682	-1.82282	0.93605	1.38314	-1.66225	0.98287
sp B	1.31089	-1.65967	0.97083	1.20839	-1.51947	0.95198
prez L	1.17815	-1.60314	0.91032	1.03647	-1.34943	0.96731
prez W	1.26840	-1.85246	0.89308	1.04870	-1.44369	0.94635
nc H	1.13241	-1.13761	0.82463	0.79546	-0.59766	0.90191
nc W	0.96084	-0.98257	0.76954	0.75736	-0.65989	0.85428
Mean	1.25074	-1.43982	0.90068	1.07992	-1.18387	0.94984

(Appendix 4-3)

Cv8	Before vertebral ossification			Before vertebral ossification		
	k	***b***	r^2	***k***	***b***	r^2
cent L	1.45940	-1.56113	0.98256	1.15720	-1.08221	0.98391
cent w/o	1.27392	-1.35428	0.97161	1.12971	-1.15064	0.98536
cent H	1.25386	-1.40213	0.96481	1.20342	-1.35112	0.98594
cent w	1.19809	-1.23092	0.96954	1.22719	-1.34904	0.97960
tp L	1.07576	-1.30117	0.99319	1.29555	-1.70537	0.96807
tp B	0.81923	-1.11102	0.77477	1.18275	-1.78004	0.98489
sp H	1.28846	-1.30161	0.93317	1.46148	-1.62664	0.97959
sp B	1.38961	-1.76501	0.94715	0.90776	-0.92831	0.97780
prez L	1.30416	-1.69709	0.90718	1.34042	-1.83227	0.93693
prez W	1.40939	-1.95041	0.93384	1.24980	-1.75161	0.92717
nc H	1.42880	-1.62191	0.90489	0.75861	-0.52804	0.78007
nc W	1.41114	-1.68980	0.92828	0.72511	-0.51060	0.93878
Mean	1.27598	-1.49888	0.93425	1.13658	-1.29966	0.95234

Ds1	Before vertebral ossification			Before vertebral ossification		
	k	***b***	r^2	***k***	***b***	r^2
cent L	1.27493	-1.25560	0.96109	1.18870	-1.13681	0.97894
cent w/o	1.16758	-1.16839	0.97825	1.13772	-1.15454	0.98159
cent H	1.09713	-1.15287	0.95687	1.20843	-1.36468	0.97937
cent w	1.04246	-0.96936	0.96902	1.16531	-1.21471	0.98898
tp L	1.15012	-1.31517	0.97821	1.36484	-1.75113	0.98678
tp B	0.62668	-0.77426	0.91521	1.34540	-2.04813	0.98021
sp H	1.50260	-1.59618	0.96232	1.51697	-1.71699	0.97829
sp B	1.50190	-1.86738	0.94236	0.93646	-0.93317	0.95104
prez L	1.51484	-2.01535	0.96262	1.44821	-2.02733	0.97392
prez W	1.34184	-1.83036	0.98437	1.18961	-1.66939	0.94525
nc H	1.37845	-1.54616	0.84538	0.74129	-0.48979	0.89899
nc W	1.34750	-1.58786	0.89959	0.73773	-0.54864	0.88321
Mean	1.24550	-1.42324	0.94627	1.16505	-1.33794	0.96055

(Appendix 4-3)

Ds4	Before vertebral ossification			Before vertebral ossification		
	k	***b***	r^2	***k***	***b***	r^2
cent L	1.64213	-1.77056	0.95605	1.14322	-0.97016	0.96573
cent w/o	1.55613	-1.70051	0.94715	1.07547	-0.91888	0.98266
cent H	1.46719	-1.74397	0.86670	1.34436	-1.61324	0.96301
cent w	1.36713	-1.53187	0.89918	1.25281	-1.37679	0.97014
tp L	1.65495	-1.77197	0.80564	1.45946	-1.56542	0.98429
tp B	1.06705	-1.16417	0.91683	1.43437	-2.00421	0.91855
sp H	1.80468	-2.09932	0.85450	1.25385	-1.19760	0.97830
sp B	1.17522	-1.14540	0.97034	0.85540	-0.56331	0.97465
prez L	1.50639	-2.08987	0.80024	1.24026	-1.75536	0.96124
prez W	2.16691	-3.07991	0.93424	1.39349	-1.83150	0.97770
nc H	1.54765	-1.89221	0.91178	0.57226	-0.17651	0.92114
nc W	1.11225	-1.26506	0.91700	0.60856	-0.33374	0.93593
Mean	1.50564	-1.77123	0.89830	1.13612	-1.19223	0.96111

Ds10	Before vertebral ossification			Before vertebral ossification		
	k	***b***	r^2	***k***	***b***	r^2
cent L	1.26644	-1.10182	0.98163	1.06621	-0.76199	0.97880
cent w/o	1.15640	-0.99884	0.98538	1.04080	-0.80688	0.98433
cent H	1.28959	-1.40869	0.97812	1.24152	-1.42358	0.98423
cent w	1.10307	-1.05489	0.99350	1.22052	-1.30197	0.99087
tp L	1.37019	-1.30895	0.98008	1.44410	-1.50643	0.98232
tp B	1.44743	-1.76408	0.92555	1.22656	-1.53133	0.99258
sp H	1.90600	-2.30347	0.99354	1.10398	-0.89329	0.91710
sp B	1.21378	-1.16887	0.96346	0.89565	-0.59252	0.99724
prez L	1.71792	-2.46256	0.90135	1.24432	-1.70191	0.95533
prez W	1.84069	-2.64230	0.84376	1.45821	-2.02398	0.91061
nc H	1.24104	-1.38443	0.79922	0.50115	-0.08418	0.90955
nc W	0.74968	-0.64293	0.81423	0.71964	-0.55229	0.98118
Mean	1.35852	-1.52015	0.92998	1.09689	-1.09836	0.96534

(Appendix 4-3)

Ds15	**Before vertebral ossification**			**Before vertebral ossification**		
	k	***b***	r^2	***k***	***b***	r^2
cent L	1.16171	-1.00125	0.98364	1.07035	-0.83335	0.97859
cent w/o	1.09574	-0.93616	0.98594	0.95474	-0.70682	0.97735
cent H	1.25112	-1.36640	0.94442	1.21327	-1.43089	0.97741
cent w	1.40427	-1.46558	0.95962	1.19551	-1.19007	0.98004
tp L	1.43260	-1.66422	0.74563	1.57300	-2.04542	0.99109
tp B	1.05394	-1.23654	0.94185	0.68173	-0.54329	0.93138
sp H	1.86169	-2.20746	0.93672	1.26756	-1.26494	0.97864
sp B	1.42945	-1.51930	0.96715	0.93932	-0.72082	0.99749
prez L	1.62145	-2.19667	0.92470	1.38328	-1.97731	0.96924
prez W	1.69401	-2.35346	0.98126	1.43973	-1.93985	0.97715
nc H	1.09327	-1.17813	0.82565	0.63555	-0.33094	0.92979
nc W	0.74194	-0.64173	0.61655	0.49951	-0.06302	0.95484
Mean	1.32010	-1.48057	0.90109	1.07113	-1.08723	0.97025

Sa1	**Before vertebral ossification**			**Before vertebral ossification**		
	k	***b***	r^2	***k***	***b***	r^2
cent L	na	na	na	na	na	na
cent w/o	1.32190	-1.23586	0.96380	1.00021	-0.68837	0.94776
cent H	1.36397	-1.62358	0.98041	1.13529	-1.26406	0.97081
cent w	1.22267	-1.22655	0.97839	1.19948	-1.26345	0.93417
tp L	1.47509	-1.51251	0.87801	1.40289	-1.53493	0.81162
tp B	na	na	na	na	na	na
sp H	1.89858	-2.25825	0.93193	1.33034	-1.39927	0.90956
sp B	1.31391	-1.35019	0.95540	0.80043	-0.45633	0.97951
prez L	1.49591	-2.03312	0.83088	1.78536	-2.74345	0.95594
prez W	1.95865	-2.92108	0.88068	1.42367	-2.07116	0.88016
nc H	1.28769	-1.46921	0.78957	0.69765	-0.42324	0.95429
nc W	1.06863	-1.15116	0.66890	0.70767	-0.46683	0.90856
Mean	1.44070	-1.67815	0.88580	1.14830	-1.23111	0.92524

(Appendix 4-3)

Ca1	Before vertebral ossification			Before vertebral ossification		
	k	***b***	r^2	***k***	***b***	r^2
cent L	1.25138	-1.12196	0.97831	1.08378	-0.82788	0.97241
cent w/o	1.05468	-0.91484	0.89726	1.14123	-1.12469	0.97225
cent H	0.99669	-0.92820	0.86773	1.13033	-1.16943	0.98151
cent w	1.04969	-0.93043	0.85965	1.13244	-1.10705	0.98185
tp L	1.19390	-1.21447	0.91684	1.27983	-1.26948	0.56372
tp B	1.42301	-1.98389	0.90309	0.97238	-1.21980	0.98649
sp H	1.71314	-1.99554	0.90173	1.33317	-1.38017	0.96642
sp B	1.16676	-1.17485	0.94805	0.98336	-0.83677	0.95845
prez L	1.23615	-1.65293	0.94832	1.29184	-1.75116	0.97409
prez W	1.34487	-1.98968	0.96414	1.30926	-1.98578	0.96268
nc H	1.35763	-1.63068	0.94965	0.57778	-0.21689	0.93193
nc W	1.16181	-1.36720	0.86245	0.60864	-0.34484	0.94004
Mean	1.24581	-1.40872	0.91644	1.07034	-1.10283	0.93265

Ca2	Before vertebral ossification			Before vertebral ossification		
	k	***b***	r^2	***k***	***b***	r^2
cent L	1.30119	-1.23702	0.96271	1.10295	-0.88687	0.98613
cent w/o	1.12461	-1.02520	0.93932	1.14746	-1.09078	0.98572
cent H	1.19617	-1.27484	0.98553	1.12081	-1.12934	0.98425
cent w	1.16212	-1.14993	0.98602	1.09918	-1.05004	0.98378
tp L	1.54673	-1.82986	0.74960	1.43974	-1.64865	0.98471
tp B	1.54434	-2.14620	0.94616	0.95063	-1.13813	0.98232
sp H	1.60659	-1.83751	0.92336	1.31668	-1.35019	0.98566
sp B	1.41837	-1.56282	0.98492	0.87484	-0.62848	0.95090
prez L	1.64407	-2.35703	0.79517	1.32880	-1.83803	0.98440
prez W	1.78486	-2.72998	0.92453	1.15615	-1.65301	0.87249
nc H	1.29265	-1.53417	0.86030	0.56025	-0.20807	0.92185
nc W	1.33404	-1.67879	0.77901	0.68162	-0.49764	0.93580
Mean	1.41298	-1.69695	0.90305	1.06492	-1.09327	0.96317

Appendix 4-4. Allometric coefficients of 10 vertebrae before and after sexual maturity in *Alligator mississippiensis*. The intercepts and coefficient of determination are also listed in 12 vertebral measurements.

Axis	**Before sexual maturity**			**After sexual maturity**		
	k	***b***	r^2	***k***	***b***	r^2
cent L	1.21854	-1.17568	0.96828	1.10121	-0.95099	0.97058
cent w/o	1.08834	-1.06021	0.96805	1.08019	-1.04736	0.95621
cent H	1.01314	-1.00307	0.94501	1.10974	-1.17512	0.92717
cent w	1.09086	-1.05112	0.94190	1.23769	-1.40122	0.93898
tp L	na	na	na	na	na	na
tp B	na	na	na	na	na	na
sp H	1.33345	-1.57501	0.85130	1.20981	-1.39899	0.93993
sp B	1.40456	-1.48138	0.88297	1.40178	-1.51505	0.96539
prez L	1.45576	-2.26198	0.69675	0.70748	-0.68060	0.78310
prez W	1.55790	-2.58392	0.66395	0.70577	-0.82858	0.81753
nc H	0.88269	-0.73354	0.90165	0.46012	0.15336	0.88301
nc W	0.89689	-0.86187	0.79674	0.66924	-0.47071	0.80878
Mean	1.19421	-1.37878	0.86166	0.96830	-0.93153	0.89907

Cervical 3	**Before sexual maturity**			**After sexual maturity**		
	k	***b***	r^2	***k***	***b***	r^2
cent L	1.25554	-1.23407	0.96110	1.16216	-1.07278	0.91879
cent w/o	1.15958	-1.16532	0.96576	1.05681	-0.94731	0.89592
cent H	1.05612	-1.08566	0.90476	1.15191	-1.27563	0.90052
cent w	1.08312	-1.04400	0.89982	1.14140	-1.17268	0.92309
tp L	na	na	na	na	na	na
tp B	na	na	na	na	na	na
sp H	1.26584	-1.41429	0.92141	1.40213	-1.70318	0.93850
sp B	1.23083	-1.55657	0.95020	1.12609	-1.36559	0.84560
prez L	1.14798	-1.55734	0.94518	1.06450	-1.41432	0.87898
prez W	1.23568	-1.79715	0.93408	1.23820	-1.87975	0.82456
nc H	0.97449	-0.91276	0.82890	0.67722	-0.32841	0.92689
nc W	0.89387	-0.89439	0.80641	0.74266	-0.63366	0.72486
Mean	1.13030	-1.26616	0.91176	1.07631	-1.17933	0.87777

(Appendix 4-4)

Cervical 8	**Before sexual maturity**			**After sexual maturity**		
	k	***b***	r^2	***k***	***b***	r^2
cent L	1.28655	-1.30848	0.96962	1.18173	-1.13884	0.95185
cent w/o	1.12772	-1.13740	0.96328	1.19410	-1.29628	0.97846
cent H	1.16823	-1.27673	0.97491	1.25366	-1.46606	0.92880
cent w	1.08217	-1.06422	0.95842	1.19325	-1.26929	0.93244
tp L	1.09196	-1.32239	0.98114	1.55018	-2.29133	0.91061
tp B	0.88158	-1.20896	0.88156	1.25603	-1.95113	0.95496
sp H	1.29104	-1.30380	0.95913	1.69105	-2.15535	0.95333
sp B	1.26611	-1.58718	0.96448	0.79147	-0.66371	0.92899
prez L	1.16850	-1.49940	0.86996	1.28781	-1.70742	0.92849
prez W	1.22404	-1.68177	0.89115	1.31522	-1.90240	0.84698
nc H	1.09178	-1.12805	0.78731	0.62347	-0.21485	0.62126
nc W	1.20574	-1.39013	0.93237	0.75929	-0.59377	0.81146
Mean	1.15712	-1.32571	0.92778	1.17477	-1.38754	0.89564

Dorsal 1	**Before sexual maturity**			**After sexual maturity**		
	k	***b***	r^2	***k***	***b***	r^2
cent L	1.20240	-1.15195	0.96454	1.20156	-1.16753	0.93546
cent w/o	1.07459	-1.03028	0.97060	1.19042	-1.27354	0.95715
cent H	1.08095	-1.12704	0.96662	1.24998	-1.45786	0.93465
cent w	1.01650	-0.93217	0.98059	1.18654	-1.26233	0.94568
tp L	1.09561	-1.23697	0.98426	1.47808	-2.01061	0.93809
tp B	0.78120	-1.00391	0.93061	1.20657	-1.72384	0.88671
sp H	1.29248	-1.28434	0.95357	1.58093	-1.85741	0.93648
sp B	1.28777	-1.56393	0.93952	0.68645	-0.36222	0.84070
prez L	1.26727	-1.65849	0.92611	1.47412	-2.08590	0.94092
prez W	1.14629	-1.55223	0.92043	1.42288	-2.21209	0.93528
nc H	1.11184	-1.15764	0.83960	0.75565	-0.52554	0.77388
nc W	1.14929	-1.29961	0.88643	0.72106	-0.51388	0.79656
Mean	1.12551	-1.24988	0.93857	1.17952	-1.37106	0.90180

(Appendix 4-4)

Dorsal 4	Before sexual maturity			After sexual maturity		
	k	***b***	r^2	***k***	***b***	r^2
cent L	1.38664	-1.39609	0.92685	1.12912	-0.93565	0.95141
cent w/o	1.32593	-1.36073	0.93464	1.21430	-1.23507	0.97186
cent H	1.25662	-1.43186	0.87734	1.39746	-1.72830	0.91236
cent w	1.25675	-1.36742	0.92816	1.54497	-2.04537	0.94257
tp L	1.38311	-1.37767	0.83276	1.58545	-1.85548	0.95321
tp B	0.83872	-0.83738	0.78018	1.71701	-2.65612	0.83915
sp H	1.55935	-1.73725	0.88275	1.45551	-1.66209	0.93660
sp B	1.15147	-1.11108	0.98224	0.87912	-0.62070	0.90192
prez L	1.22894	-1.68614	0.81019	1.48625	-2.32312	0.91748
prez W	1.78554	-2.51748	0.91124	1.64276	-2.40434	0.97024
nc H	1.27859	-1.48985	0.88015	0.38596	0.25874	0.90865
nc W	1.05716	-1.17746	0.92799	0.67315	-0.48170	0.85830
Mean	1.29240	-1.45753	0.88954	1.25926	-1.47410	0.92198

Dorsal 10	Before sexual maturity			After sexual maturity		
	k	***b***	r^2	***k***	***b***	r^2
cent L	1.19442	-0.99538	0.97582	1.07506	-0.78092	0.91989
cent w/o	1.10329	-0.91950	0.98173	1.10661	-0.95815	0.94741
cent H	1.11058	-1.15156	0.95648	1.26283	-1.47094	0.93624
cent w	1.04310	-0.96778	0.99203	1.19480	-1.23988	0.95422
tp L	1.25338	-1.13924	0.97069	1.46312	-1.54735	0.94349
tp B	1.16764	-1.36638	0.89385	1.21175	-1.49684	0.95316
sp H	1.72847	-2.03621	0.94607	1.51933	-1.85515	0.94914
sp B	1.17862	-1.11622	0.97843	0.89504	-0.59122	0.98024
prez L	1.58146	-2.27146	0.93038	1.69366	-2.75228	0.94205
prez W	1.61333	-2.30146	0.85195	1.74156	-2.67388	0.76783
nc H	1.08258	-1.15092	0.83613	0.48952	-0.05574	0.56981
nc W	0.77839	-0.68021	0.89752	0.62896	-0.33924	0.90176
Mean	1.23627	-1.34136	0.93426	1.19019	-1.31347	0.89710

(Appendix 4-4)

Dorsal 15	Before sexual maturity			After sexual maturity		
	k	***b***	r^2	***k***	***b***	r^2
cent L	1.15054	-0.98310	0.98172	1.10458	-0.91221	0.91089
cent w/o	1.03518	-0.84734	0.98414	1.04033	-0.90431	0.89055
cent H	1.04990	-1.08562	0.90736	1.14445	-1.26968	0.89627
cent w	1.22036	-1.20541	0.93919	1.09725	-0.95969	0.92158
tp L	1.24918	-1.40780	0.78832	1.59200	-2.08733	0.96869
tp B	1.06262	-1.24254	0.95179	1.03891	-1.37392	0.94192
sp H	1.60821	-1.84563	0.91971	1.34546	-1.44426	0.94919
sp B	1.26071	-1.27955	0.95709	0.94619	-0.73666	0.98866
prez L	1.32042	-1.77622	0.88098	1.63773	-2.56898	0.89993
prez W	1.54779	-2.13917	0.96123	1.28692	-1.57954	0.97143
nc H	1.09309	-1.17683	0.88570	0.52831	-0.08375	0.82825
nc W	0.90960	-0.87051	0.77816	0.49188	-0.04521	0.77542
Mean	1.20897	-1.32164	0.91128	1.10450	-1.16380	0.91190

Sacral 1	Before sexual maturity			After sexual maturity		
	k	***b***	r^2	***k***	***b***	r^2
cent L	na	na	na	na	na	na
cent w/o	1.22537	-1.09795	0.94767	1.04204	-0.78790	0.91758
cent H	1.19510	-1.37207	0.95934	1.14272	-1.27604	0.90643
cent w	1.02577	-0.93578	0.90356	1.02089	-0.84229	0.85588
tp L	1.13572	-1.00973	0.72260	1.88871	-2.64659	0.73844
tp B	na	na	na	na	na	na
sp H	1.41238	-1.54308	0.84778	0.85936	-0.29749	0.63856
sp B	1.17972	-1.15490	0.96399	0.86952	-0.61772	0.94644
prez L	1.20858	-1.62211	0.83324	2.18729	-3.66716	0.88673
prez W	1.64766	-0.81902	0.85891	2.01245	-3.42858	0.82483
nc H	1.14483	-1.25875	0.86125	0.51810	-0.00900	0.80968
nc W	1.07644	-1.16075	0.81022	0.67795	-0.40147	0.80891
Mean	1.22516	-1.19741	0.87086	1.22190	-1.39742	0.83335

(Appendix 4-4)

Caudal 1	Before sexual maturity			After sexual maturity		
	k	***b***	r^2	***k***	***b***	r^2
cent L	1.21400	-1.06757	0.97135	1.12930	-0.93427	0.94059
cent w/o	0.96449	-0.78838	0.92694	0.87961	-0.51801	0.84204
cent H	1.00612	-0.94061	0.93356	1.09420	-1.08366	0.90777
cent w	1.00610	-0.86910	0.92192	0.97627	-0.74439	0.90658
tp L	1.55176	-1.75473	0.60072	1.45909	-1.70615	0.95297
tp B	1.26132	-1.75034	0.93496	0.96812	-1.20978	0.95312
sp H	1.48756	-1.65918	0.90186	1.45657	-1.65924	0.95634
sp B	1.18242	-1.20363	0.96417	0.85312	-0.54070	0.83519
prez L	1.25256	-1.67891	0.95474	1.20020	-1.54000	0.92422
prez W	1.22277	-1.81655	0.95316	1.04580	-1.37530	0.79866
nc H	1.21549	-1.41444	0.94453	0.39067	0.21752	0.51329
nc W	1.11263	-1.28988	0.91473	0.57581	-0.26990	0.73821
Mean	1.20643	-1.35278	0.91022	1.00240	-0.94699	0.85575

Caudal 2	Before sexual maturity			After sexual maturity		
	k	***b***	r^2	***k***	***b***	r^2
cent L	1.24564	-1.15293	0.97131	1.09226	-0.86126	0.95916
cent w/o	1.06763	-0.94148	0.95813	1.01601	-0.78466	0.95946
cent H	1.17870	-1.24434	0.98538	1.11753	-1.11913	0.92242
cent w	1.11624	-1.08181	0.98686	1.02059	-0.86707	0.90131
tp L	1.48314	-1.73250	0.86973	1.46387	-1.70123	0.95436
tp B	1.30965	-1.80183	0.94544	0.80380	-0.79673	0.91514
sp H	1.47725	-1.64237	0.94757	1.48634	-1.73959	0.95796
sp B	1.27092	-1.34602	0.97508	1.15558	-1.28033	0.89558
prez L	1.47102	-2.09825	0.86341	1.28400	-1.73031	0.94886
prez W	1.57308	-2.41885	0.87087	0.96500	-1.21142	0.90929
nc H	1.15828	-1.32933	0.89542	0.41283	0.13362	0.54958
nc W	1.22896	-1.52056	0.85665	0.53452	-0.15878	0.77935
Mean	1.29838	-1.52586	0.92715	1.02936	-1.00974	0.88771

Appendix 4-5. Allometric coefficients of 10 vertebrae before and after stoppage of growth in *Alligator mississippiensis*. The intercepts and coefficient of determination are also listed in 12 vertebral measurements.

Axis	**Before stoppage of growth**			**After stoppage of growth**		
	k	***b***	r^2	***k***	***b***	r^2
cent L	1.17681	-0.93953	0.97113	0.88005	-0.42260	0.87492
cent w/o	1.07740	-0.97181	0.95887	0.82584	-0.44018	0.76479
cent H	1.04790	-1.15117	0.96063	1.02982	-0.97979	0.75466
cent w	1.05290	-0.92114	0.95539	0.88013	-0.54571	0.80931
tp L	na	na	na	na	na	na
tp B	na	na	na	na	na	na
sp H	1.22787	-1.07965	0.75991	1.43887	-1.94345	0.77785
sp B	1.35798	-1.41301	0.92664	0.83089	-0.14784	0.82474
prez L	1.39826	-1.97562	0.62359	0.25521	0.38591	0.50460
prez W	1.42675	-2.03527	0.62693	0.28761	0.16849	0.65713
nc H	0.82693	-0.44635	0.96308	0.36387	0.38870	0.68861
nc W	0.76259	-0.31491	0.87200	0.65434	-0.42193	0.88245
Mean	1.13554	-1.12485	0.86182	0.74466	-0.39584	0.75391

Cervical 3	**Before stoppage of growth**			**After stoppage of growth**		
	k	***b***	r^2	***k***	***b***	r^2
cent L	1.19250	-0.99757	0.95089	0.74584	-0.07661	0.84209
cent w/o	1.12768	-1.00237	0.95474	0.78566	-0.29189	0.76271
cent H	1.06523	-1.24607	0.95844	1.02226	-0.96069	0.68126
cent w	1.07528	-1.05396	0.98432	0.87494	-0.53627	0.64064
tp L	na	na	na	na	na	na
tp B	na	na	na	na	na	na
sp H	1.29397	-1.36224	0.90817	1.57321	-2.12087	0.86849
sp B	1.17219	-1.52632	0.92560	0.54406	0.03260	0.71152
prez L	1.07854	-1.22102	0.94212	0.44911	0.06956	0.44544
prez W	1.12101	-1.24959	0.91564	0.65167	-0.45984	0.86078
nc H	0.88916	-0.57950	0.84207	0.59040	-0.11546	0.63993
nc W	0.78208	-0.55714	0.75317	0.64774	-0.38538	0.87284
Mean	1.07976	-1.07958	0.91352	0.78849	-0.48448	0.73257

(Appendix 4-5)

Cervical 8	**Before stoppage of growth**			**After stoppage of growth**		
	k	***b***	***r²***	***k***	***b***	***r²***
cent L	1.21247	-1.03052	0.98075	1.05779	-0.83997	0.77562
cent w/o	1.11107	-1.08161	0.98092	0.99390	-0.81928	0.85761
cent H	1.15517	-1.26812	0.98258	0.85919	-0.52353	0.64690
cent w	1.12247	-1.30088	0.97308	1.01160	-0.83720	0.66834
tp L	1.15094	-1.64147	0.95542	0.92357	-0.81206	0.81795
tp B	0.95628	-1.63610	0.96092	0.72461	-0.68246	0.86187
sp H	1.32633	-1.56333	0.96373	1.03993	-0.61148	0.91679
sp B	1.13082	-0.92664	0.96451	0.48448	0.06673	0.89044
prez L	1.22025	-1.80846	0.91162	1.52553	-2.26781	0.87158
prez W	1.19830	-1.61295	0.90946	1.50389	-2.34710	0.55887
nc H	0.93368	-0.50165	0.70432	0.45926	0.19124	0.36140
nc W	0.99530	-0.48898	0.92483	0.74729	-0.55949	0.53655
Mean	1.12609	-1.23839	0.93435	0.94425	-0.83687	0.73033

Dorsal 1	**Before stoppage of growth**			**After stoppage of growth**		
	k	***b***	***r²***	***k***	***b***	***r²***
cent L	1.17453	-1.06393	0.97444	1.09166	-0.90167	0.70740
cent w/o	1.08195	-1.07332	0.97260	0.95090	-0.70210	0.76890
cent H	1.11177	-1.26429	0.97051	0.99231	-0.83905	0.76572
cent w	1.06268	-1.19167	0.98883	1.03579	-0.90381	0.74356
tp L	1.16763	-1.63466	0.98485	0.95111	-0.75888	0.66158
tp B	1.03119	-2.22578	0.98189	0.68889	-0.50582	0.92800
sp H	1.36442	-1.56427	0.95860	1.03881	-0.57370	0.78875
sp B	1.14996	-0.85921	0.88461	0.41193	0.29168	0.69155
prez L	1.27391	-1.81359	0.94314	1.30209	-1.66465	0.86482
prez W	1.07271	-1.39655	0.90736	1.52767	-2.44886	0.93838
nc H	0.92195	-0.48346	0.86538	0.42437	0.27504	0.40513
nc W	0.97078	-0.56043	0.85331	0.70401	-0.46803	0.50724
Mean	1.11529	-1.26093	0.94046	0.92663	-0.76666	0.73092

(Appendix 4-5)

Dorsal 4	Before stoppage of growth			After stoppage of growth		
	k	***b***	r^2	***k***	***b***	r^2
cent L	1.26310	-0.89305	0.95092	1.14788	-0.97684	0.82036
cent w/o	1.18810	-0.77611	0.97214	0.98364	-0.68345	0.86544
cent H	1.25027	-1.42129	0.95553	0.96263	-0.67801	0.69954
cent w	1.19164	-1.13890	0.97175	0.87294	-0.43396	0.76296
tp L	1.34648	-1.20827	0.95256	1.04153	-0.55691	0.65283
tp B	0.99748	-1.69718	0.81849	0.30811	0.68789	0.40749
sp H	1.38791	-0.97353	0.96256	1.05635	-0.70923	0.52358
sp B	1.01765	-0.56264	0.97699	0.93983	-0.75846	0.60822
prez L	1.13302	-1.27824	0.89916	1.57649	-2.52602	0.90688
prez W	1.55797	-1.62303	0.96681	1.11077	-1.13274	0.95221
nc H	1.03410	-0.37049	0.89001	0.56645	-0.17201	0.94318
nc W	0.88074	-0.27866	0.90985	0.71693	-0.58075	0.69974
Mean	1.18737	-1.01845	0.93556	0.94029	-0.71004	0.73687

Dorsal 10	Before stoppage of growth			After stoppage of growth		
	k	***b***	r^2	***k***	***b***	r^2
cent L	1.13343	-0.63872	0.97363	1.15666	-0.97180	0.71980
cent w/o	1.06878	-0.66553	0.98271	0.99800	-0.69854	0.67282
cent H	1.11707	-1.23355	0.97388	0.92593	-0.66035	0.76365
cent w	1.10636	-1.21234	0.98606	0.97266	-0.70704	0.73813
tp L	1.31929	-1.30473	0.96548	1.11274	-0.71419	0.73010
tp B	1.14380	-1.34331	0.95826	0.90023	-0.75978	0.87663
sp H	1.42627	-0.63868	0.88742	1.09125	-0.83437	0.63940
sp B	1.06479	-0.67849	0.99465	0.65453	-0.01670	0.90433
prez L	1.30406	-1.21051	0.89225	1.06165	-1.22886	0.85568
prez W	1.45898	-1.79095	0.87944	1.06992	-1.03977	0.87223
nc H	0.81910	-0.12141	0.85485	0.43297	0.09330	0.82347
nc W	0.77896	-0.70659	0.96864	0.49629	-0.01811	0.61799
Mean	1.14508	-0.96207	0.94311	0.90607	-0.62968	0.76785

(Appendix 4-5)

Dorsal 15	**Before stoppage of growth**			**After stoppage of growth**		
	k	***b***	***r²***	***k***	***b***	***r²***
cent L	1.11128	-0.88953	0.98178	1.07995	-0.85068	0.60725
cent w/o	0.98114	-0.68255	0.97590	0.84800	-0.44333	0.62561
cent H	1.05762	-1.29321	0.95521	0.86810	-0.59999	0.68150
cent w	1.19069	-1.05379	0.96877	1.10559	-0.97987	0.62118
tp L	1.34327	-1.79042	0.96459	1.04185	-0.77806	0.96369
tp B	0.84983	-0.47277	0.91054	0.54250	-0.18359	0.95141
sp H	1.40972	-1.06141	0.95803	1.07097	-0.78963	0.70711
sp B	1.08604	-0.55913	0.97840	0.89816	-0.61941	0.95702
prez L	1.19245	-1.35754	0.90256	0.97546	-0.97281	0.64755
prez W	1.52742	-2.00346	0.97425	0.95370	-0.78569	0.89950
nc H	0.90411	-0.46833	0.90488	0.55193	-0.13317	0.66540
nc W	0.79309	-0.36147	0.85247	0.39681	0.18401	0.85943
Mean	1.12056	-0.99947	0.94395	0.86109	-0.57935	0.76555

Sacral 1	**Before stoppage of growth**			**After stoppage of growth**		
	k	***b***	***r²***	***k***	***b***	***r²***
cent L	na	na	na	na	na	na
cent w/o	1.11062	-0.64829	0.92671	0.98838	-0.65279	0.79524
cent H	1.16687	-1.22562	0.95307	0.82807	-0.52553	0.65003
cent w	1.11634	-1.18358	0.89480	0.96831	-0.71927	0.84971
tp L	1.17287	-1.15694	0.67764	1.15738	-0.91642	0.79553
tp B	na	na	na	na	na	na
sp H	1.42771	-1.24887	0.83501	1.09969	-0.86232	0.77079
sp B	1.02308	-0.42198	0.97075	0.65464	-0.11181	0.60852
prez L	1.29386	-2.36778	0.92261	1.36757	-1.70203	0.79337
prez W	1.42561	-1.58247	0.82131	1.92433	-3.19193	0.56274
nc H	1.00161	-0.50743	0.94151	0.57755	-0.14944	0.54180
nc W	0.94586	-0.54348	0.88741	0.36871	0.33378	0.38177
Mean	1.16844	-1.08864	0.88308	0.99346	-0.84978	0.67495

(Appendix 4-5)

Caudal 1	Before stoppage of growth			After stoppage of growth		
	k	***b***	r^2	***k***	***b***	r^2
cent L	1.15056	-0.74784	0.95994	1.19305	-1.08195	0.86284
cent w/o	1.06892	-1.25550	0.97174	0.82513	-0.39779	0.80055
cent H	1.05385	-1.18938	0.98348	0.91987	-0.66653	0.56221
cent w	1.06331	-1.14469	0.98196	0.68565	-0.05226	0.56174
tp L	1.38167	-1.39983	0.49098	1.23475	-1.17279	0.73460
tp B	1.13822	-1.21083	0.98249	0.93061	-1.11664	0.78472
sp H	1.41335	-1.26337	0.92421	1.05059	-0.69602	0.79688
sp B	1.10179	-0.89625	0.95658	0.88120	-0.60159	0.48222
prez L	1.27097	-1.82178	0.95753	0.84368	-0.69059	0.65280
prez W	1.23722	-1.98673	0.95295	0.53190	-0.13506	0.37040
nc H	0.99698	-0.31033	0.92974	0.42136	0.15154	0.20347
nc W	0.92294	-0.41027	0.90726	0.37927	0.20181	0.19226
Mean	1.14998	-1.13640	0.91657	0.82476	-0.52149	0.58372

Caudal 2	Before stoppage of growth			After stoppage of growth		
	k	***b***	r^2	***k***	***b***	r^2
cent L	1.18510	-0.92364	0.97961	0.76035	-0.06860	0.81532
cent w/o	1.10759	-1.09719	0.98397	0.78443	-0.23197	0.75973
cent H	1.15155	-1.10681	0.98143	0.89412	-0.58035	0.79900
cent w	1.10981	-1.02863	0.98085	0.75306	-0.22698	0.74976
tp L	1.47152	-1.49676	0.97289	1.19181	-1.05603	0.75918
tp B	1.18818	-1.15502	0.98239	0.86806	-0.94844	0.66848
sp H	1.38531	-1.15565	0.97300	1.02016	-0.62892	0.76501
sp B	1.06238	-0.51519	0.94601	0.68051	-0.15062	0.45417
prez L	1.42515	-1.86215	0.94852	0.91195	-0.84905	0.75848
prez W	1.40812	-1.69912	0.82895	0.67412	-0.51122	0.59845
nc H	0.94639	-0.32030	0.84128	0.76220	-0.68754	0.68277
nc W	1.04791	-0.67456	0.88689	0.48388	-0.04075	0.38762
Mean	1.20742	-1.08625	0.94215	0.81539	-0.49837	0.68317

Appendix 4-6. Allometric coefficients of six vertebrae before and after neurocentral fusion in *Alligator mississippiensis*. The intercepts and coefficients of determination are also listed in 12 vertebral dimensions.

Dorsal 4	**Before neurocentral fusion**			**After neurocentral fusion**		
	k	***b***	r^2	***k***	***b***	r^2
cent L	1.27366	-2.70771	0.95845	1.90406	-5.02813	1.00000
cent w/o	1.20752	-2.58719	0.96002	1.52365	-3.76753	1.00000
cent H	1.30276	-3.03600	0.95050	0.25306	0.74985	1.00000
cent w	1.25239	-2.83268	0.96612	0.50481	-0.12938	1.00000
tp L	1.39397	-3.03355	0.93698	0.46749	0.29370	1.00000
tp B	1.10287	-2.56713	0.90458	0.37064	0.12257	1.00000
sp H	1.40143	-3.12709	0.93875	2.58668	-7.42227	1.00000
sp B	0.99534	-2.02375	0.97416	1.27508	-3.01823	1.00000
prez L	1.17938	-2.99145	0.91633	2.01586	-5.91426	1.00000
prez W	1.56293	-3.99218	0.94603	1.07899	-2.30497	1.00000
nc H	0.94528	-2.05383	0.86572	0.76364	-1.53519	1.00000
nc W	0.85269	-1.84504	0.92849	0.81092	-1.74958	1.00000
Mean	1.20585	-2.73313	0.93718	1.12957	-2.47529	1.00000

Dorsal 10	**Before neurocentral fusion**			**After neurocentral fusion**		
	k	***b***	r^2	***k***	***b***	r^2
cent L	1.14056	-2.24814	0.98831	2.09026	-5.64709	1.00000
cent w/o	1.08339	-0.02078	0.99702	1.52073	-3.71486	1.00000
cent H	1.16035	-0.29989	0.98641	0.86092	-1.48376	1.00000
cent w	1.15022	-0.21066	0.98905	1.63682	-4.20013	1.00000
tp L	1.35896	-0.21606	0.98939	0.96093	-1.43705	1.00000
tp B	1.16865	-0.42618	0.95789	1.18534	-2.83932	1.00000
sp H	1.39937	-0.40707	0.96943	1.07050	-2.00054	1.00000
sp B	1.05031	-0.06787	0.98250	0.61420	-0.62479	1.00000
prez L	1.35846	-0.83929	0.96375	1.27138	-3.23421	1.00000
prez W	1.54310	-0.95656	0.93890	0.43982	-0.02287	1.00000
nc H	0.77839	-0.04946	0.86067	0.18727	0.47227	1.00000
nc W	0.78504	-0.05617	0.95903	0.80471	-1.68626	1.00000
Mean	1.16473	-0.48318	0.96520	1.05357	-2.20155	1.00000

(Appendix 4-6)

Dorsal 15	**Before neurocentral fusion**			**After neurocentral fusion**		
	k	***b***	r^2	***k***	***b***	r^2
cent L	1.13590	-2.29525	0.99009	1.08511	-2.12378	0.60735
cent w/o	1.00279	-1.97585	0.98609	0.85199	-1.44281	0.62564
cent H	1.08089	-2.40359	0.95894	0.87228	-1.62348	0.68167
cent w	1.21704	-2.63069	0.97359	1.11081	-2.28298	0.62122
tp L	1.37380	-3.21865	0.91520	1.04674	-2.00594	0.96369
tp B	0.86761	-1.95906	0.93107	0.54503	-0.82292	0.95138
sp H	1.44004	-3.27675	0.94529	1.07608	-2.05211	0.70721
sp B	1.10930	-2.34709	0.96053	0.90241	-1.67806	0.95708
prez L	1.21853	-3.04986	0.93090	0.97991	-2.12198	0.64737
prez W	1.56134	-3.99557	0.98348	0.95811	-1.90947	0.89939
nc H	0.92340	-1.99609	0.90400	0.55446	-0.78342	0.66524
nc W	0.81051	-1.66803	0.85934	0.39867	-0.28365	0.85942
Mean	1.14510	-2.56804	0.94488	0.86513	-1.59422	0.76556

Sacral 1	**Before neurocentral fusion**			**After neurocentral fusion**		
	k	***b***	r^2	***k***	***b***	r^2
cent L	na	na	na	na	na	na
cent w/o	1.16253	-2.35901	0.95277	1.16354	-2.42567	0.82447
cent H	0.99018	-2.81578	0.97193	1.04817	-2.27241	0.71578
cent w	0.97070	-2.50935	0.92399	1.17610	-2.58516	0.84089
tp L	0.95832	-2.42068	0.80444	1.18318	-2.35309	0.83985
tp B	na	na	na	na	na	na
sp H	1.20558	-3.39119	0.93694	1.14416	-2.29851	0.82255
sp B	0.89834	-2.24334	0.95683	0.79023	-1.35235	0.71495
prez L	1.08363	-3.20894	0.87748	1.54601	-3.92716	0.83507
prez W	1.26632	-3.96209	0.88668	2.40435	-7.13924	0.66285
nc H	0.89175	-2.35693	0.85385	0.59400	-0.87910	0.61776
nc W	0.83471	-2.19067	0.78164	0.48244	-0.50010	0.52500
Mean	1.02621	-2.74580	0.89466	1.15322	-2.57328	0.73992

(Appendix 4-6)

Sacral 2	**Before neurocentral fusion**			**After neurocentral fusion**		
	k	***b***	r^2	***k***	***b***	r^2
cent L	na	na	na	na	na	na
cent w/o	1.17953	-2.44060	0.97417	1.07235	-2.10753	0.84244
cent H	1.23379	-2.82918	0.97115	1.31950	-3.17320	0.88468
cent w	1.15658	-2.51094	0.93682	1.19356	-2.62764	0.90257
tp L	1.26426	-2.83753	0.63939	0.85349	-1.24809	0.71703
tp B	na	na	na	na	na	na
sp H	1.39692	-3.17055	0.86027	1.35455	-3.03974	0.87209
sp B	1.15828	-2.52661	0.96103	0.83901	-1.50223	0.90488
prez L	1.25239	-3.18452	0.86822	0.98775	-2.26844	0.69037
prez W	1.25865	-3.29182	0.85882	0.89996	-2.12510	0.69289
nc H	0.92291	-1.96046	0.94169	0.60198	-0.90919	0.65085
nc W	0.83104	-1.70067	0.92737	0.50894	-0.60817	0.71552
Mean	1.16544	-2.64529	0.89389	0.96311	-1.96093	0.78733

Caudal 1	**Before neurocentral fusion**			**After neurocentral fusion**		
	k	***b***	r^2	***k***	***b***	r^2
cent L	1.20198	-2.45866	0.97606	1.17081	-2.39195	0.83941
cent w/o	1.06649	-2.20664	0.94344	0.74011	-1.05138	0.71832
cent H	1.07128	-2.30424	0.95575	1.05322	-2.21145	0.72102
cent w	1.07287	-2.23698	0.94800	0.78246	-1.19541	0.68319
tp L	1.45853	-3.31761	0.65771	1.39358	-3.17132	0.84947
tp B	1.21786	-3.11014	0.94423	1.06060	-2.66098	0.87941
sp H	1.46139	-3.33290	0.92485	1.23568	-2.57470	0.88828
sp B	1.17579	-2.57292	0.97227	1.00270	-2.05846	0.67761
prez L	1.29864	-3.27783	0.97092	1.10568	-2.60032	0.76061
prez W	1.31491	-3.50899	0.96810	1.27581	-3.40067	0.63757
nc H	1.12236	-2.58073	0.93162	0.54187	-0.76806	0.40959
nc W	1.01615	-2.32636	0.90548	0.52385	-0.75502	0.40305
Mean	1.20652	-2.76950	0.92487	0.99053	-2.06998	0.70563

(Appendix 4-6)

Caudal 2	Before neurocentral fusion			After neurocentral fusion		
	k	***b***	r^2	***k***	***b***	r^2
cent L	1.25353	-2.63751	0.97589	1.08095	-2.09098	0.97032
cent w/o	1.12692	-2.35993	0.96834	1.11844	-2.32398	0.97306
cent H	1.21215	-2.72089	0.98901	1.17611	-2.62344	0.94952
cent w	1.14705	-2.47800	0.98892	1.06760	-2.21685	0.93777
tp L	1.51174	-3.55394	0.89567	1.42812	-3.27718	0.96808
tp B	1.29685	-3.30417	0.94957	0.84641	-1.88085	0.94585
sp H	1.45559	-3.31630	0.95095	1.36496	-3.04029	0.96693
sp B	1.16910	-2.55588	0.94735	0.81621	-1.43372	0.80747
prez L	1.48517	-3.86366	0.88672	1.35227	-3.46014	0.96394
prez W	1.57836	-4.27805	0.89211	1.21229	-3.20024	0.94868
nc H	1.13147	-2.61322	0.89842	0.59050	-0.97127	0.87173
nc W	1.18253	-2.83270	0.86002	0.65574	-1.20322	0.85354
Mean	1.29587	-3.04285	0.93358	1.05913	-2.31018	0.92974

LITERATURE CITED

Aichison J. 1990. Relative variation diagrams for describing patterns of compositional variability. Math Geol 22:487–511.

Aichison J, Egozcue JJ. 2005. Compositional data analysis: Where are we and where should we be heading? Math Geol 37:829–850.

Bogin B. 2003. The human pattern of growth and development in paleontological perspective. In: Thompson JL, Krovitz GE, Nelson AJ, editors. Patterns of Growth and Development in the Genus *Homo*. Cambridge, UK: Cambridge University Press. p 15–44.

Brochu CA. 1996. Closure of neurocentral sutures during crocodilian ontogeny: implications for maturity assessment in fossil archosaurs. J Vert Paleontol 16:49–62.

Chiasson RB. 1969. Laboratory Anatomy of the *Alligator*. Dubuque, Iowa: WM. C. Brown Company Publishers. Pp 56.

Christ B, Huang R, Wilting J. 2000. The development of the avian vertebral column. Anat Embryol 202:179–194.

Currie PJ. 2003. Allometric growth in tyrannosaurids (Dinosauria: Theropoda) from the Upper Cretaceous of North America and Asia. Can J Earth Sci 40:651–665.

Farlow A, Hurlburt GR, Elsey RM, Britton ARC, Langston Jr W. 2005. Femoral dimensions and body size of *Alligator mississippiensis*: estimating the size of extinct mesoeucrocodylians. J Vert Paleontol 25:354–369.

Gál JM. 1993. Mammalian spinal biomechanics. J Exp Biol 174:281–297.

Gilbert SF. 1994. Developmental Biology 4th ed. Massachusetts: Sinauer Association Inc. Pp 894 p.

Herring SE. 1993 Epigenetic and functional influences on skull growth. In: Hanken J, Hall BK, editors. The Skull. Volume 1 Development. Chicago: University of Chicago Press. p 153–206.

Hoffstetter R, Gasc JP. 1969. Vertebrae and ribs of modern reptiles. In: Gans C, editor. Biology of the Reptilia, v. 1: Morphology A. New York: Academic Press. p 201–310.

Houck MA, Gauthier JA, Strauss RE. 1990. Allometric scaling in the earliest fossil bird, *Archaeopteryx lithographica*. Science 247:195–198.

McIlhenny EA. 1987. The Alligator's Life History. Berkley: Ten Speed Press. Pp 117.

Mook CC. 1921. Notes on the postcranial skeleton in the Crocodilia. Bulletin of American Museum of Natural History 44:67–100.

Organ CL. 2006. Thoracic epaxial muscles in living archosaurs and ornithopod dinosaurs. Anat Rec 288:782–793.

Pawlowsky-Glahn V, Egozcue JJ, Tolosana-Delgado R. 2006. Lecture Notes on Compositional Data Analysis.

Romer AS. 1956. Osteology or the Reptiles. Chicago: University of Chicago Press. Pp 772.

Salisbury SW, Frey E. 2000. A biomechanical transformation model for the evolution of semi-spherodial articulations between adjoining vertebral bodies in crocodilians. In: Grigg GC, Seebacher F, Franklin CE, editors. Crocodilian Biology and Evolution. Sydney: Surrey Beatty & Sons. p 85–134.
Simpson GG. 1941. Large Pleistocene felines of North America. Am Mus Novit 1136:1–27.
Smith HM. 1960. Evolution of Chordate Structure. An Introduction to Comparative Anatomy. New York: Holt, Reinhard and Winston Inc. Pp 529.
SPSS 17.0 for Windows. Statistical Package for Social Science (SPSS). Release Version 17.0.1. 2008. Chicago: SPSS Incorporation.
Wilkinson PM, Rhodes WE. 1997. Growth rates of American alligators in coastal South Carolina. J Wildlife Management 61:397-402.

Chapter 5

Morphology of Presacral Vertebrae in *Euparkeria capensis* (Diapsida, Archosauriformes) from the Early Triassic of South Africa and the Origin of Delayed Neurocentral Fusion and Complex Neurocentral Suture

ABSTRACT

Presacral vertebrae of the basal archosaur, *Euparkeria capensis* (Diapsida, Archosauriformes) from the Middle Triassic of South Africa, are described. A number of fully-grown individuals show evidence of late neurocentral fusion and relatively complex boundaries between the centrum and neural arch. The two synapomorphic characters for the more derived archosaurs (Pseudosuchia and Ornithodira except for aves) perhaps first occurred in those basal archosauriforms. *Euparkeria* also exhibits evidence of the cervical-to-dorsal sequence of neurocentral fusion, which differs from the dorsal-to-cervical sequence in crocodilians. The phylogenetic distribution of the two sequences suggest the dorsal-to-cervical sequence in crocodilians (and other pseudosuchians) is likely a derived condition in archosaur evolution.

INTRODUCTION

In this chapter, I investigate the evolutionary significance of two features — delayed fusion and complex sutures between the centrum and neural arch — that characterize the neurocentral sutures of crocodilians and many non-avian

archosaurs. First, I explore the origin of the two characters during archosaur evolution. Archosaurs extensively diversified during the Mesozoic, following their earliest appearance in the Upper Permian. The two lineages of the derived archosaurs, Pseudosuchia (crocodile-line) and Ornithodira (dinosaur-line), possess delayed fusion and complex sutures in the presacral vertebrae, suggesting that their common ancestors first gained them during the Triassic. Investigation of the origin of the two characters involves the following questions: (1) how many times did the two characters appear, (2) which character appeared first (if they were independent from each other), (3) did they evolve together (if they appeared together), and (4) what sequence(s) of neurocentral fusion exist in the vertebral column?

Among the basal archosauriforms, *Euparkeria capensis*, from the Lower–Middle Triassic of South Africa, is the basal-most taxon that possesses evidence of delayed fusion and complex sutures. Although relative timing of neurocentral fusion during postnatal ontogeny varies considerably in more derived archosaurs, neurocentral suture complexity clearly increased throughout archosaur evolution (except for birds). Therefore, I hypothesize that the two characters are morphologically linked to each other and had appeared once among archosaurs. To test this hypothesis, detailed morphology of the neurocentral sutures and presacral vertebrae in *Euparkeria* is examined and compared to those of other basal archosaurs and to the ontogenetic series of extant *Alligator*. Data from *Euparkeria* suggest, phylogenetically, the two characters first occurred in those basal archosauriforms during the Lower to Middle Triassic and the dorsal-to-

cervical sequence in crocodilians (and most pseudosuchians) is likely a derived condition in archosaur evolution.

Institutional abbreviations—CM, Carnegie Museum of Natural History, Pittsburg; **DNM**, Dinosaur national Monument, Vernal; **FMNH**, Field Museum of natural History, Chicago; **IVPP**, Institute of Vertebrate Paleontology and Paleoanthropology, Beijing; **MB.R.**, Museum für Naturkunde, Berlin; **MOR**, Museum of the Rockies, Bozeman; **NSM-PV**, National Science Museum in Tokyo; **SAM**, South African Museum, Cape Town; **SMNS**, Staatliches Museum für Naturkunde, Stuttgart; **YPM**, Yale Peabody Museum, New Haven.

Systematic Paleontology

Diapsida Osborn, 1903

Archosauriformes Gauthier et al., 1989

Euparkeria capensis Broom, 1913

Locality and horizon—All known specimens of *Euparkeria* were excavated from the Karoo Basin of South Africa, but detailed information of the fossil locality has been lost. All specimens were perhaps found in the same area (Ewer, 1985). Based on the matrix (medium-sized gray sandstone) and preservation of those skeletons, which are largely articulated and often overlapped each other, at least, some skeletons were excavated from the same quarry (Fig. 5-1). The beds containing *Euparkeria* are considered to be upper

Lower (Scythian) to lower Middle Triassic (Scythian–Anisian boundary) in age (Ewer, 1985; Gower and Weber, 1999).

Materials—Ewer (1985) listed a total of 15 partial skeletons of *Euparkeria*, including 14 at SAM and one at UMZC (formerly, 'D.M.S. Watson collection R527'; Gower and Weber, 1998, p. 371). Well-preserved, articulated vertebrae and other axial skeletons are present in SAM 5867 (holotype), 6047A, 6049, and SAM 8050 (formerly, SAM 7697). The last specimen was not listed in Ewer (1985) and had not been described previously: it consists of at least eight partial skeletons in the single slab (Fig. 5-1).

DESCRIPTION

Most specimens of *Euparkeria* are well preserved. Matrix holds the vertebrae in life position, which allows examinations of their articulation with other bones in the skeleton. Based on the total length of the femur (54.6 mm) and the skull (80.1 mm), the total body length of one of the largest individuals (SAM 5867; Fig. 5-2) is estimated to be ca. 0.5 m. This is considerably smaller than many other, more derived archosaurs (e.g., various non-avian dinosaurs, many pseudosuchians).

Euparkeria has 15 dorsal vertebrae, which are fewer than in basal archosauromorphs (e.g., 17 in *Trilophosaurus*), but greater than in more derived archosaurs (e.g., > 13 in dinosaurs; Müller et al., 2010). The anterior dorsal centra are relatively elongate, which is ca. 90% of the length of the last dorsal

(Fig. 5-2). The centra are amphicoelous, with slightly convex anterior and posterior articular surfaces, but no trace of the notochord exists in any specimens. This morphology contrasts with the platycoelous centrum in *Trilophosaurus* (Gregory, 1945; Romer, 1956). The ventral surface of the dorsal centrum is smooth and rounded, not keeled as seen in more derived archosaurs (e.g., the hypapophysis in crocodilians and extant birds). The length of the transverse process is about the same as the transverse width of the centrum, which indicates *Euparkeria* has more elongate transverse process in the mid-dorsal vertebrae than the basal archosauromorphs. In *Euparkeria*, the transverse process is weakly laminated, consisting of the prezyogodiapophyseal, postzygodiapophyseal, and posterior centrodiapophyseal laminae (terminology and identification of laminae based on Wilson, 1999). The three laminae of the transverse process form a T-shaped cross-section, which resembles the condition in Ornithodira and Pseudosuchia, but differs from the non-laminated, rod-like structure present in basal archosauromorphs (e.g., *Trilophosaurus*). *Euparkeria* has two rib articular facets, the diapophysis and parapophysis, in the cervical and most dorsal vertebrae (e.g., Ewer, 1985, fig. 8).

Among the dozen skeletons of the species, open neurocentral sutures are found in dorsal vertebrae of SAM 6047(A), 6049, 5867, and 8050 (Fig. 5-2). In those specimens, the centra and neural arches are physically separated, with either matrix filling in the spaces between them, or a clear neurocentral suture exposed. In contrast, most cervical vertebrae have completely fused centrum and neural arch. Those articulated specimens indicate that in *Euparkeria* neurocentral

suture closure occurs in the cervical vertebrae first and then the dorsal vertebrae. This cervical-to-dorsal sequence in *Euparkeria* (and various ornithodiran archosaurs; personal observation) differs from the dorsal-to-cervical sequence in crocodilians.

All preserved presacral vertebrae are still imbedded in matrix, and no unfused centra or neural arches have been physically removed for study in *Euparkeria*. Thus, the shape and texture of the articular surfaces between centrum and neural arch cannot be ascertained, but neurocentral sutures are exposed in lateral view in most vertebrae. In the posterior dorsal vertebrae of SAM 5867, interdigitated articulation is absent, but a sharply pointed mid-section, the mid-neurocentral peak is found in the centrum (Fig. 5-2). In contrast to *Alligator*, the posterior neurocentral suture of *Euparkeria* is relatively smooth with gentle curvature. The entire neurocentral suture is weakly corrugated, which is formed by approximately 10 transverse ridges. The mean of the Length Ratio values is 1.033 in dorsal 11–15 of SAM 5867, which is slightly lower than a young *Alligator mississippiensis* (mean = 1.035 with the same vertebrae). In the posterior neurocentral sutures, *Euparkeria* (mean = 1.035) has considerably lower suture complexity than *A. mississippiensis* (mean = 1.083).

DISCUSSION

The vertebrae of basal archosauriforms may display some transitional features between the basal archosauromorphs and the two derived archosaurian

lineages, Ornithodira and Pseudosuchia, in the vertebrae. Below, I discuss how delayed neurocentral fusion and the increase in neurocentral suture complexity have changed through archosaur evolution. Also, the sequences of neurocentral fusion are discussed among archosaurs.

The Origin of Delayed Neurocentral Fusion and Complex Suture

Dilkes (1995) used a character of relative timing of neurocentral fusion (later fusion as more derived state) for his cladistic analysis of the basal archosauromorphs, but vertebral regions (among atlas–posterior caudal vertebrae) and relative timing in ontogeny (i.e., early–late during the life span) were not specified. Based on data from *Alligator mississippiensis* (Chapter 2), very late neurocentral fusion in the presacral vertebrae is here defined as when partially or completely visible neurocentral suture appearing in individuals that have reached sexual maturity or body size ca. 40 % from the upper range in species or taxon. Based on the size of various bones, a number of individuals in *Euparkeria* are determined to be fully-grown and have considerably late neurocentral fusion. More basal archosauriforms, such as *Vancleavea* (Nesbitt et al., 2009, fig. 11) and/or *Erythrosuchus* (Gower 2003: figs. 23–34) may also have late neurocentral fusion. However, more data from other specimens are needed to confirm this with certainty. Also, their phylogenetic positions have been controversial and they may be more derived than *Euparkeria* (e.g., Sereno, 1991; Jull, 1994; Dilkes and Sues, 2009; Trotteyn et al., in press). Thus, *Vancleavea* and *Erythrosuchus* are here suggested not to be included for further discussion.

Compared to those basal archosauriforms, unfused centra and neural arches are rarely found in the basal archosauromorphs (e.g., *Proterosuchus*, *Rhynchosaurus*, *Prolacerta*, *Trilophosaurus*; personal pbseration) and most lepidosauromorphs, indicating they have relatively early neurocentral fusion (Fig. 5-3).

The derived archosaurs, pseudosuchians and non-avian dinosaurs, usually have more complex neurocentral sutures than *Euparkeria* (Fig. 5-4), indicating that the degree of ridged articular surfaces between the centrum and neural arch had increased during archosaur evolution (except for birds), as a similar relation is found during postnatal growth of *Alligator* (Chapters 2, 3). Besides *Euparkeria*, weakly ridged neurocentral articular surfaces are also seen in other basal archosauriforms; e.g., a dorsal vertebra of *Vancleavea* (Nesbitt et al., 2009, fig. 11) (Fig. 5-4). some dorsal vertebrae of *Erythrosuchus* (Gower 2003: figs. 23–24). Thus, relatively delayed neurocentral fusion and complex neurocentral sutures might have appeared together during evolution of basal archosauriforms (Figs. 5-3).

Evolution of the Sequence of Neurocentral Fusion

Multiple specimens of *Euparkeria* (e.g., SAM 6047(A), 6049, 5867, 8050) indicate that neurocentral fusion occurs in the cervical vertebrae first and then in the dorsal vertebrae (Fig. 5-2). The sequences of neurocentral fusion in the vertebral column are largely uncertain in other fossil archosaurs (and even in most vertebrates), primarily due to lack of specimens showing transitional stages

from unfused to fused such as those skeletons of *Euparkeria*. At least, some other taxa allow direct examination of general patterns of sequences of neurocentral fusion, based on specimens exhibiting transitional stages. Those taxa include the basal sauropodomorph *Plateosaurus* (e.g., SMNS 12950), the macronarian sauropod *Camarasaurus* (e.g., YPM 1905; CM 11338), the dicraeosaurid sauropod *Dicraeosaurus* (the mounted skeleton at MB.R), the non-avian theropods *Allosaurus* (e.g., DNM 11541; MOR 693), *Tyrannosaurs* (e.g., FMNH PR 2081), *Dilong* (IVPP V14242, 14243, 11579; Xu et al., 2004; Irmis, 2007), some extant birds (e.g., domestic chickens, ducks, ostriches), and the pterodactyl pterosaur *Anhanguera* (NSM-PV 19892; Kellner and Tomida, 2000). Notably, those ornithodiran archosaurs also have the cervical-to-dorsal sequence, as *Euparkeria* does.

This cervical-to-dorsal sequence differs from the dorsal-to-cervical sequence in extant crocodilians (Chapter 2). Irmis (2007) reported the dorsal-to-cervical sequence also occurs in various aetosaurs (e.g., *Typothorax*, *Desmatosuchus*, *Stagonolepis*) and possibly in the rauisuchians, *Shuvosaurus* and *Effigia*, and the author suggested that the dorsal-to-cervical sequence is commonly appeared among Pseudosuchia, indicating likely a plesiomorphy for Pseudosuchia (Fig. 5-5).

The occurrences of the two different sequences in limited archosaur taxa lead two hypothetical ideas about the polarity of the sequences (Fig. 5-5). First, as Irmis (2007) suggested, the dorsal-to-cervical fusion is a plesiomorphy and the cervical-to-dorsal sequence is an apomorphy for archosaurs. The second idea is

opposite from this: the cervical-to-dorsal fusion is actually a synplesiomorphic character for archosaurs, and the dorsal-to-cervical sequence is a derived character for pseudosuchians. Because the basal archosauromorphs, *Euparkeria*, exhibit the cervical-to-dorsal sequence, the dorsal-to-cervical sequence is here suggested a synapomorphy for the crocodile-lineage (Fig. 5-5).

Neurocentral fusion affects relative growth of overall vertebral structures during postnatal ontogeny of *Alligator* (Chapter 4). Thus, sifting timing of neurocentral fusion and changing the sequence might also gave strong impact to overall vertebral structure during archosaur evolution. Morphological studies of vertebrae in various basal archosaurs must provide important information for further investigations.

CONCLUSIONS

The Middle Triassic archosauriform, *Euparkeria capensis*, exhibit evidence of late neurocentral fusion and slightly complex neurocentral sutures with a mid-neurocentral peak in the presacral vertebrae. *Euparkeria* indicate the two characters first appeared in the basal archosauriforms during archosaur evolution. *Euparkeria* also exhibits the cervical-to-dorsal sequence of neurocentral fusion, which differs from the dorsal-to-cervical sequence in crocodilians. The cervical-to-dorsal sequence in *Euparkeria* suggests that a plesiomorphic character for archosaurs, which is also shared with most ornithodirans and the dorsal-to-cervical sequence is a derived character for pseudosuchians.

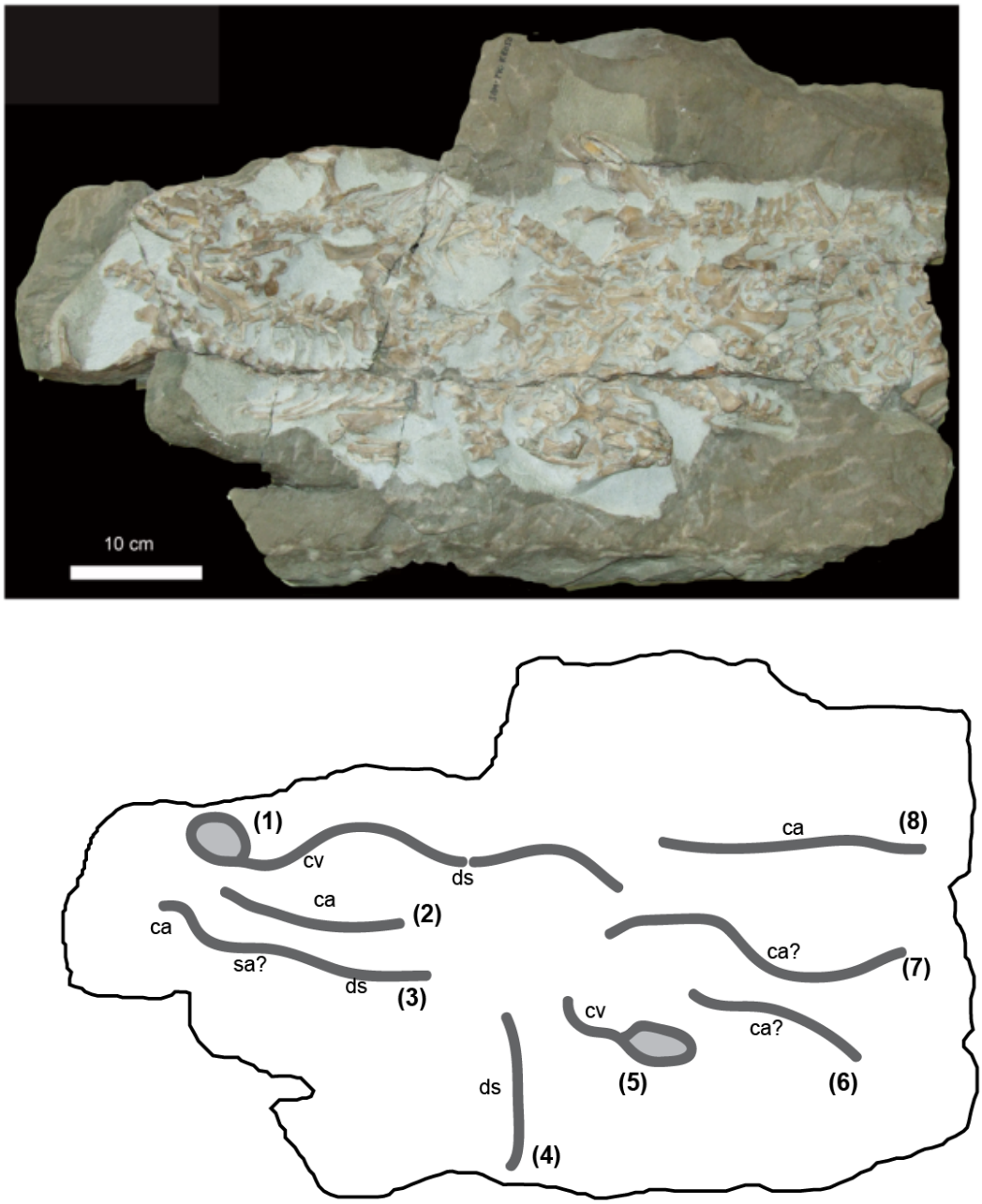

Figure 5-1. Slab with multiple skeletons of *Euparkeria capensis*. At least eight partial skeletons are preserved in this lab. The count of individuals is based on the vertebral column and skulls. The rounded structure of individual 1 and 5 indicates a skull (light grey filled). Vertebral regions are also marked as caudal (ca), cervical (sv), dorsal (ds) and sacral (sa) vertebrae.

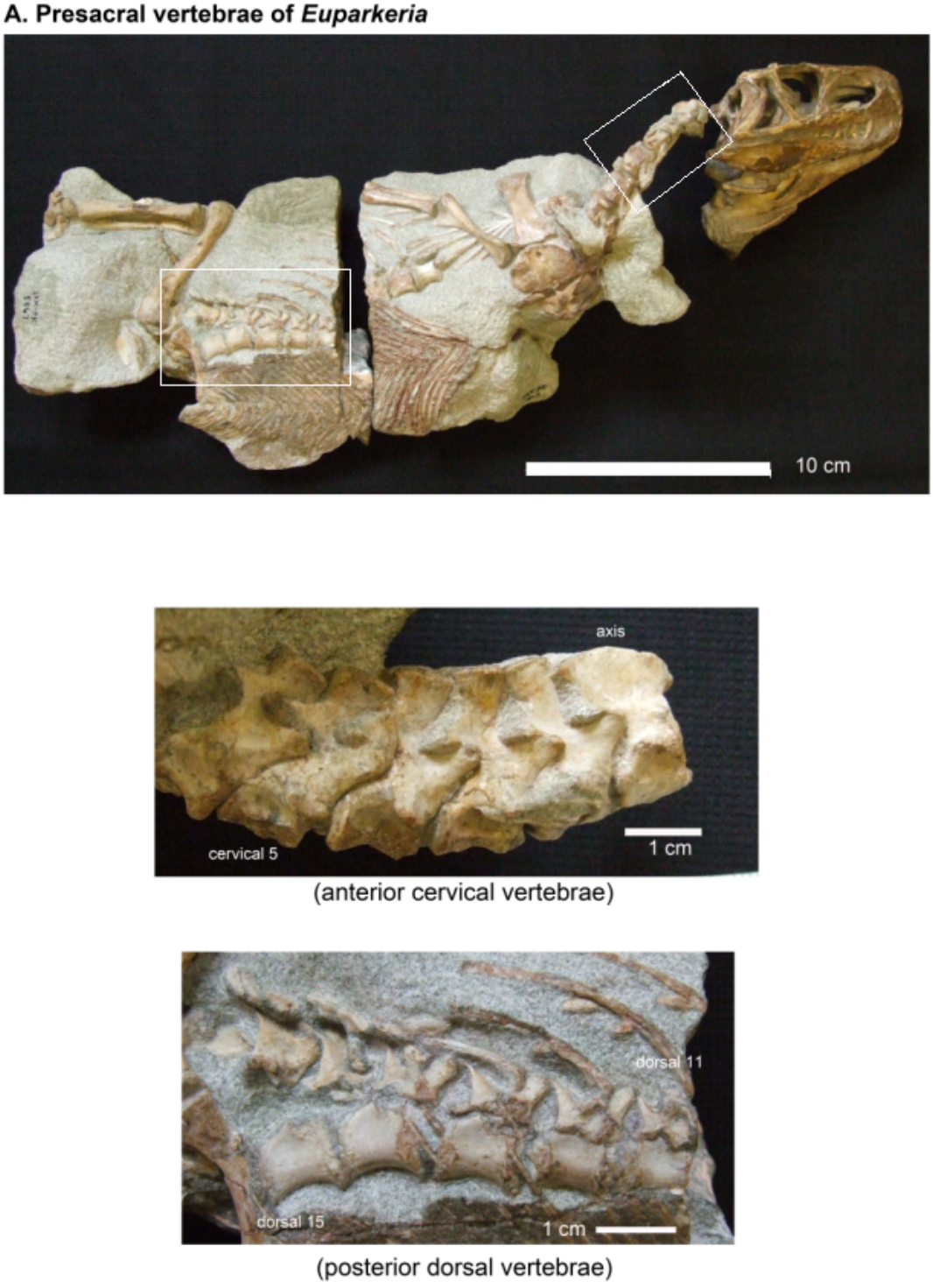

Figure 5-2. Axial skeletons of *Euparkeria capensis*. Articulated presacral vertebrae of the holotype (SAM 5867) (top). Note the neural arches and centra are completely fused in the cervical vertebrae (middle), but only the dorsal vertebrae (bottom) have open neurocentral sutures.

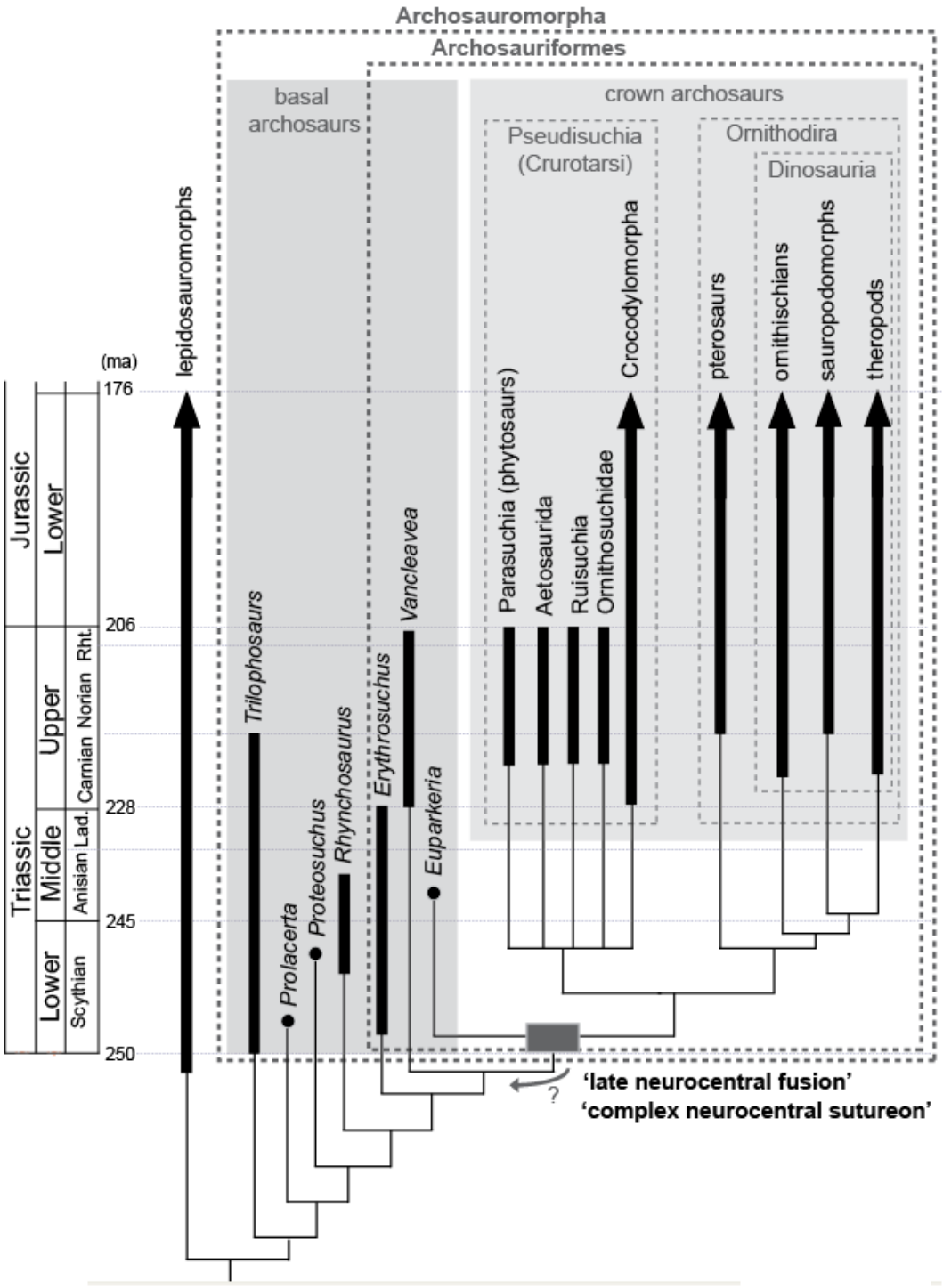

Figure 5-3. The origin of late neurocentral fusion and complex neurocentral suture during basal archosaur evolution. The hypothetical occurrences of the two characters of the neurocentral suture are shown. Phylogenetic relationships and geological distributions are based on Dilkes (1997), Benton (2004), and Nesbitt et al (2010).

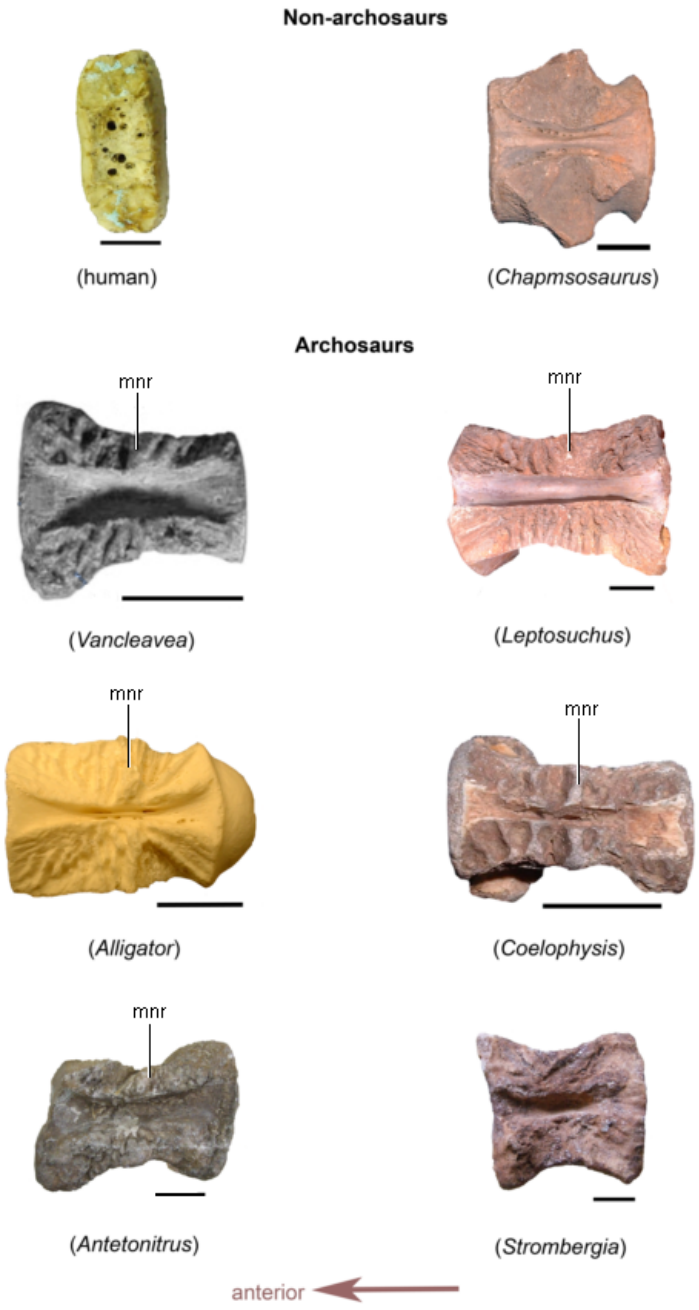

Figure 5-4. Neurocentral articular surfaces in archosaurs and other tetrapods. Centra of anterior or mid-dorsal vertebrae are shown in dorsal view. Note mammal (human) and a basal diapsid *Champsosaurus* have smooth neurocentral articular surfaces. In contrast, archosaurs, including the basal archosauriform (*Vancleavea*) to more derived taxa (others), exhibit transversely ridged, wedged articulations. Mid-neurocentral ridge (**mnr**) is labeled when present. Scale equals to 1 cm except for Antetonitrus (= 10 cm). Image of *Vancleavea* is from Nesbitt et al. (2010).

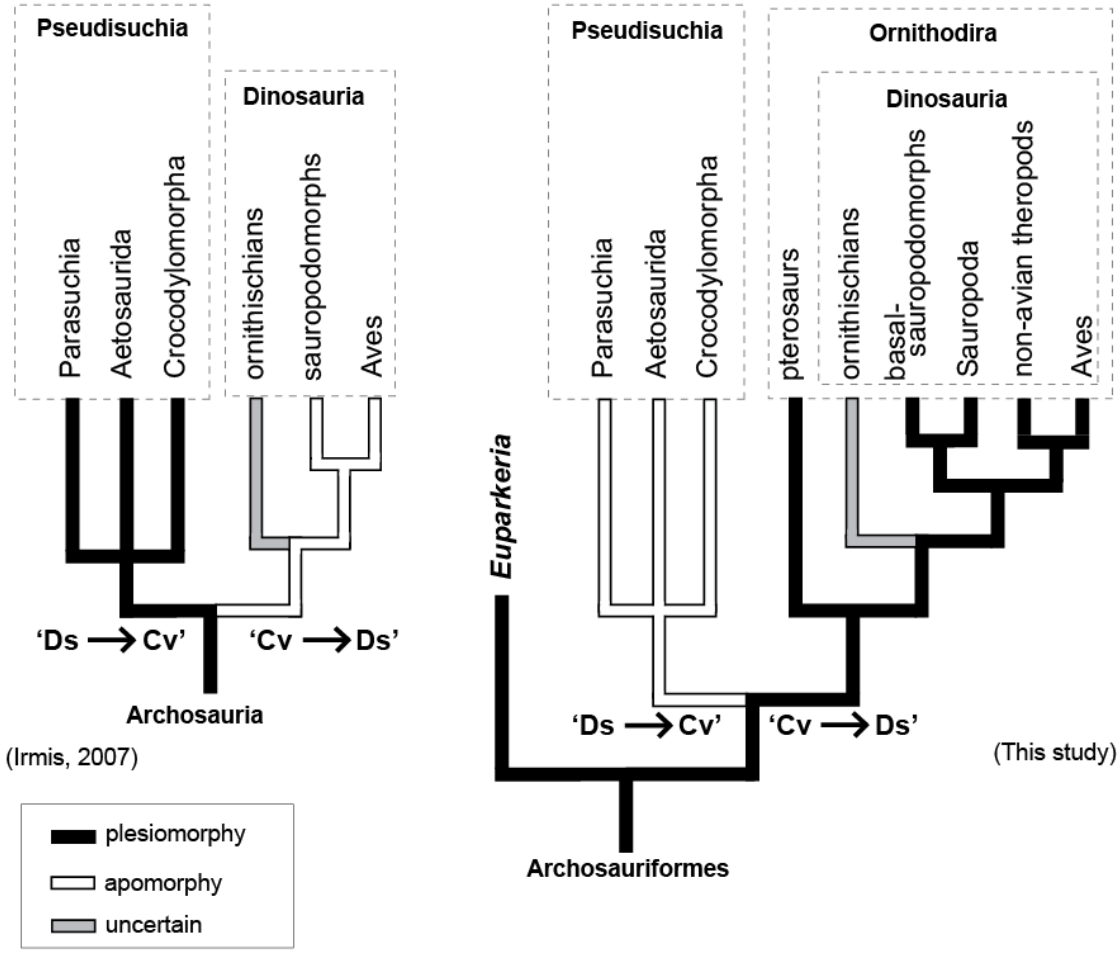

Figure 5-5. Evolution of sequence of neurocentral fusion in archosaurs. Relative timing of neurocentral fusion is compared in cervical (Cv) and dorsal (Ds) vertebrae. **Left**: the hypothesis suggested by Irmis (2007) shows the dorsal to-cervical sequence was suggested as an apomorphy (white line) and the cervical-to-dorsal sequence as a plesiomorphy (black line) for archosaurs. **Right**: A hypothesis proposed in this study shows the opposite combination. The gray line indicates the sequence is uncertain.

LITERATURE CITED

Broom R. 1913. On the South-African Pseudosuchian *Euparkeria* and allied genera. Proc Zool Soc Lond 1913:619-633.

Carrier DR. 1987**.** The evolution of locomotor stamina in tetrapods; circumventing a mechanical constraint. Paleobiology 1987 13:326–341.

Dilkes DW. 1995. The rhynchosaur *Howesia browni* from the Lower Triassic of South Africa. Palaeontol 38:665–685.

Dilkes DW. 1997. The early Triassic rhynchosaur *Mesosuchus browni* and the interrelationships of basal archosauromorph reptiles. Phi Trans R Soc Lond B. 353:501–541.

Dilkes DW, Sues H. 2009. Redescription and phylogeentic relationships of *Doswellia kaltenbachi* (Diapsida: Archosauriformes) from the Upper Triassic of Virginai. J Vert Paleont 29:58–79.

Ewer RF. 1985. The anatomy of the thecodont reptile *Euparkeria capensis* Broom. Phi Trans R Soc Lond 248:379–435.

Gauthier J, Cannatella DCC, de Queiroz K, Kluge AG, Row T. 1989. Tetrapod phylogeny. In: Bremer B, Jornvall H, editors. The hierarchy of life. New York: Elsevier Science Publishers. Pp 337–353.

Gower DJ. 2003. Osteology of the early archosaurian *reptile Erythrosuchus africanus* Broom. Annals South Afr Mus 110:1-84.

Gower DJ, Weber E. 1998. The braincase of *Euparkeria*, and the evolutionary relationships of birds and crocodilians. Biol Rev 73:367–411.

Gregory JT. 1945. Osteology and Relationships of *Trilophosaurus*. Univ Texas Oublic 4401:273–359.

Irmis RB. 2007. Axial skeleton ontogeny in the Parasuchia (Archosauria: Pseudosuchia) and its implications for ontogenetic determination in archosaurs. J Vert Paleontol 27:350–361.

Juul L. 1994. The phylogeny of basal archosaurs. Palaeont Afr 31:1-38.

Kellner AW, Tomida Y. 2000. Description of a new species of *Anhangueridae* (Pterodactyloidea) with comments on the pterosaur fauna from the Santana Formation (Aptian-Albian), Northeastern Brazil. Nat Sci Mus Monog 17:1–135.

Müller, Johannes, Torsten M. Scheyer, Jason J. Head, Paul M. Barrett, Ingmar Werneburg, Per G. P. Ericson, Diego Pol, and Marcelo R. Sánchez-Villagra. 2010. Homeotic effects, somitogenesis and the evolution of vertebral numbers in recent and fossil amniotes. Proc Natl Acad Sci U S A 107: 2118–2123.

Nesbitt S, Stocker MR, Small BJ, Downs A. 2009. The osteology and relationships of *Vancleavea campi* (Reptilia: Archosauriformes). Zool J Linn Soc 157: 814–864.

Organ CL. 2006. Thoracic epaxial muscles in living archosaurs and ornithopod dinosaurs. Anat Rec 288:782-793.

O'Reilly JC, Summers AP, Ritter DA. 2000. The evolution of the functional role of trunk muscles during locomotion in adult amphibians. Am Zool 40: 123–135.

Osborn HF. The reptilian subclasses Diapsida and Synapsida and the early history of the Diaptosauria. Mem Am Mus Nat Hist 1:449-507.
Perry SF. 1988. Functional morphology of the lungs of the Nile crocodile, *Crocodylus niloticus*: Nonrespiratory parameters. J Exp Biol 134:99–147.
Reilly SM, Elias JA. 1998. Locomotion in *Alligator mississippiensis*: Kinematic effects of speed and posture and their relevance to the sprawling-to-erect paradigm. J Exp Biol 201:2259–2574.
Romer AS. 1956. Osteology of the Reptiles. Chicago, University of Chicago Press. Pp 772.
Sereno PC. 1991. Basal archosaurs: Phylogenetic relationships and functional; implications. J. Vert. Paleontol. 11 Supp Mem 2:1-53.
Trotteyn MJ, Haro JA. In press. The braincase of a specimen of *Proterochampsa* Reig (Archosauriformes: Proterochampsidae) from the Late Triassic of Argentina. Paläontol Z.
Wilson JA. 1999. A nomenclature for vertebral laminae in sauropods and other saurischian dinosaurs. J Vert Paleontol 19:639–653.
Xu X, Norell MA, Kuang X, Wang X, Zhao Q, Jia C. 2004. Basal tyrannosaurid from China and evidence for protofeathers in tyrannosaurids. Nature 431:680–684.

Chapter 6

Conclusions

New ways to look into morphology of the neurocentral suture and vertebrae are presented. Histology-based cell and tissue morphology indicates alligators have drastically delayed timing of neurocentral fusion in the presacral vertebrae, primarily due to bipolar cartilaginous cell organization of the neurocentral synchondrosis. The Length Ratio method is useful to examine neurocentral sutures exposed on the external vertebral surfaces between centrum and neural arch, which show suture complexity is significantly high in adult individuals of various species of *Alligator*. Data from the two sources suggest the two morphological features — late neurocentral fusion and complex neurocentral sutures in adult crocodilian — are common in crocodilians and are linked to each other. Delayed neurocentral fusion possibly influences growth of vertebral structure in certain vertebral part(s). The two unique features of neurocentral sutures are deeply nested in the archosaur lineage, which first occurred in some basal archosauriforms during the Early Triassic. The results highlight the importance of neurocentral sutures for understanding morphology, growth, and evolution of vertebrae and axial skeletons. The methods and ideas developed in this work may be useful to investigate morphology of neurocentral sutures and vertebrae in other vertebrates. A summary of each chapter is listed below.

In Chapter 2, histology of alligator vertebrae shows neurocentral fusion is the result of endochondral ossification of the neurocentral synchondrosis. The neurocentral synchondrosis seems to be secondary cartilage in *Alligator*, which has not been repeated previously in any other reptiles. Presacral vertebrae have considerably delayed neurocentral fusion (i.e., body length < 2.5 m or often patent throughout ontogeny). This late fusion is linked to bipolar organization of the three types of cartilaginous cells. It is still uncertain if the same kind of synchondroid cartilage is homologous to other reptiles or other vertebrates.

In Chapter 3, neurocentral sutures exposed the external vertebral surfaces show that suture complexity significantly increases in most presacral vertebrae during postnatal ontogeny of alligators. In fully-grown *Alligator mississippiensis*, the posterior cervical–anterior dorsal vertebrae generally have the highest degree of suture complexity. Similar patterns of the intracolumnar distribution of highly complex neurocentral sutures also occur in other species of *Alligator* and other genera, indicating complex neurocentral sutures are a synapomorphy for crocodilians. Because suture complexity keeps increasing in presacral vertebrae during postnatal ontogeny, this feature may be linked to patency of neurocentral fusion through the life span.

Chapter 4 shows the patterns of allometric changes in vertebrae, which have not been fully studied in other vertebrates, in *Alligator mississippiensis*. Alligator vertebrae exhibit strong positive allometry in the size of the centrum, neural spine-transverse process, and zygapophyses, but negative allometry occurs in the diameter of neural canal during postnatal ontogeny. Degrees of

allometric changes, however, drastically shift (i.e., mostly, decrease) after the completion of vertebral ossification (body length = ca. 0.9 m) and during the stoppage of growth (body length > 2.8 m). After neurocentral fusion, overall size of the neural canal and zygapophysis tends to stop increasing, but centra (especially, the posterior ball), neural spines, and transverse processes consistently increase in the length. The method presented here can be useful for comparisons of other vertebrates.

Study of alligator vertebrae suggests that delayed neurocentral sutures and complex sutures in dorsal vertebrae are unique among terrestrial tetrapods (except for turtles). Those synapomorphic features for crocodilians further extend to various non-avian archosaurs (Chapter 5). The origin of the two features is, perhaps, in basal archosauriforms, such as *Euparkeria*, from the Early Triassic.